Growth rate dependent impact of oscillating glucose conditions on *Escherichia coli* physiology

Vorgelegt von
Dipl.-Ing. Eva Brand
aus Gera

Von der Fakultät III – Prozesswissenschaften
der Technischen Universität Berlin
zur Erlangung des akademischen Doktorgrades

Doktor der Ingenieurwissenschaften
- Dr. Ing. –

genehmigte Dissertation

Promotionsausschuss:

Vorsitzender:	Prof. Dr. Jens Kurreck
Gutachter:	Prof. Dr. Peter Neubauer
Gutachter:	Prof. Dr. Juri Rappsilber
Gutachter:	Prof. Dr. Thomas Schweder

Tag der wissenschaftlichen Aussprache: 21. September 2017

Berlin 2018

Die Untersuchungen zur vorliegenden Arbeit wurden vom Oktober 2010 bis November 2013 am Institut für Biotechnologie, Fachbereich Bioverfahrenstechnik, Technische Universität Berlin unter der Leitung von Prof. Dr. Peter Neubauer durchgeführt.

Proteom und Transkriptomanalysen wurden in der Zeit vom 11. April bis 8. Juni am Center of Food and Fermentation Technologies in der Arbeitsgruppe von Prof. Raivo Vilu unter Mithilfe von Karl Peebo durchgeführt.

For my family -

at the end of the day my most valuable treasure, greatest challenge and joyful proudness.

Abstract

Escherichia coli is the most used microorganism for biotechnological production processes due to its outstanding cultivation robustness and genetic and metabolic engineering possibilities. The established production process is a high cell density cultivation starting with a batch cultivation and followed by a fed-batch feeding strategy to avoid acetate accumulation and anaerobic conditions. The scale-up of a high cell density cultivation for increased productivity is accompanied with the appearance of heterogeneities in the cultivation broth especially regarding the substrate and oxygen distribution due to insufficient mixing when the cultivation mode changes from batch to fed-batch mode. These heterogeneities generally lead to a reduction in the specific production performance. To study the effect of heterogeneities on the *Escherichia coli* metabolism a scale-down reactor comprised of a stirred tank reactor in loop with a plug flow reactor was successfully established. The effect of heterogeneities, especially of oscillating glucose conditions, on the *Escherichia coli* metabolism are well studied for cultivations, where the cells are adapted to high glucose availability at batch phase and the growth rate decreases during transition to fed-batch strategy.

In the present study the focus lies on the effect of oscillating glucose conditions on the *Escherichia coli* metabolism, when the cells are primarily adapted to low glucose availability and reduced growth rate. Therefore, a cultivation process was established with an internal, enzyme-based fed-batch before the start of oscillating glucose conditions (referred to as mechanical feeding). This cultivation process was compared in terms of cell growth, general cultivation parameters and accumulation of organic and amino acids to reference cultivation process without oscillating glucose conditions and to a cultivation with initial batch mode. Additionally, the proteome and selected transcriptome was analyzed for the newly established cultivation process and its reference cultivation.

The growth rate and glucose availability before the onset of oscillating glucose conditions was found to have an immediate effect on the accumulation of organic acids and amino acids in the stirred tank of the scale-down reactor. Though organic

acids accumulated along the plug flow reactor at oscillating glucose conditions for cells adapted to high and low growth rate, the re-assimilation was found to be reduced for the latter. 5 h of oscillating glucose conditions were not sufficient to synchronize the accumulation pattern of both cultivations. Proteome data show, that the increase in growth rate during transition from enzyme based fed-batch to mechanical fed-batch with oscillating glucose condition leads to a level decrease of protein involved in biosynthesis pathways. The increased growth rate caused more level changes of proteins of the central carbon metabolism and synthesis pathways for amino acids and nucleotide precursors than oscillating glucose conditions. In fact, the adaptation to oscillating glucose conditions for the newly established cultivation process compared to its reference stirred tank reactor cultivation on the proteome level was mainly found in the activation of the glyoxylate shunt and increase in two of four respiration complexes.

This study shows, that the physiological status of the *Escherichia coli* cell before the change of cultivation parameter can have an important effect on its central metabolism and performance due to prolonged adaptation processes.

Zusammenfassung

Escherichia coli ist aufgrund seiner herausragenden Kultivierungseigenschaften sowie den weitreichenden Möglichkeiten der genetischen und metabolischen Anpassung das am häufigsten verwendete Bakterium für biotechnologische Produktionsprozesse. Dabei ist der etablierte Produktionsprozess eine Hochzelldichtekultivierung, die mit einem Batch-Ansatz startet. In der Folge wird eine Fed-Batch Fütterungsstrategie angewendet, um die Akkumulation von Azetat und anaerobe Bedingungen zu vermeiden. Die maßstabsgerechte Vergrößerung einer Hochzelldichtekultivierung für erhöhte Produktivität führt zu der Entstehung von Heterogenitäten in der Kultivierungsbrühe. Diese betreffen speziell die Substrat- und Sauerstoffverteilung aufgrund unzureichender Durchmischung, wenn von einer Batch Kultivierung auf eine Fed-batch Kultivierung umgestellt wird. Heterogenitäten führen generell zu einer verringerten spezifischen Produktionsleistung. Um den Effekt von Heterogenitäten auf den *Escherichia coli* Stoffwechsel zu untersuchen, wurde ein Scale-Down Reaktor, bestehend aus einem Rührtankreaktor verbunden mit einem Pfropfenstromreaktor, erfolgreich etabliert. Der Effekt von Heterogenitäten, speziell von oszillierenden Glucosepulsen, auf den *Escherichia coli* Stoffwechsel, ist bereits gut für Kultivierungen untersucht, in denen die Zellen an hohe Glukosekonzentration der Batchphase angepasst sind, und die Wachstumsrate während des Übergangs zum Fed-batch sank.

In dieser Studie liegt der Fokus auf dem Effekt von oszillierenden Glukosepulsen auf den *Escherichia coli* Stoffwechsel, wenn die Zellen zuvor an eine geringe Glukosekonzentration und reduzierte Wachstumsrate angepasst sind. Dazu wurde ein Kultivierungsprozess mit einem enzymbasierten Fed-batch vor dem Beginn der oszillierenden Glukosepulse etabliert (gleichbedeutend mit mechanischer Fütterung). Dieser Kultivierungsprozess wurde in Bezug auf Zellwachstum, allgemeine Kultivierungsparameter und Akkumulation organischer Säuren und Aminosäuren mit einer Referenzkultivierung ohne oszillierende Glukosepulse und mit einer Kultivierung mit anfänglicher Batch Kultivierung verglichen. Zusätzlich

wurde das Proteom und ausgewählte Teile des Transkriptoms im neu etablierten Kultivierungsprozesses und der Referenzkultivierung untersucht.

Die Wachstumsrate und Glukoseverfügbarkeit vor dem Start der oszillierenden Glukosepulse haben einen unmittelbaren Effekt auf die Akkumulation organischer Säuren und Aminosäuren im Rührkessel Reaktor des Scale-Down Reaktors. Obwohl organische Säuren entlang des Pfropfenstromreaktors sowohl in den Kulturen, die an hohe oder geringe Wachstumsrate präadaptiert wurden, akkumulierten, war die Reassimilation bei letzteren geringer. Fünf Stunden oszillierende Glukosepulse waren nicht ausreichend, um das Akkumulationsmuster beider Kultivierung anzugleichen. Weiterhin zeigen Proteomdaten, dass die Erhöhung der Wachstumsrate während des Übergangs von enzymbasiertem Fed-batch zum mechanischen Fed-batch mit oszillierenden Glukosepulsen zu einer Verringerung der Menge an Proteinen führt, die an zentralen Biosynthesewegen beteiligt sind. Die Erhöhung der Wachstumsrate verursachte wesentlich mehr Konzentrationsänderungen von Proteine des zentralen Kohlenstoffwechsels und der Synthesewege für Aminosäuren und Nukleotidvorläufern als oszillierende Glukosepulse. Tatsächlich beruht die Anpassung an oszillierende Glukosepulse für den neu etablierten Kultivierungsprozess verglichen mit der Rührtankreaktor Kultivierung als Referenz bezüglich des Proteoms hauptsächlich in der Aktivierung des Glyoxylatzyklus und der Erhöhung von zwei von vier Atmungs-Komplexen.

Diese Studie zeigt, dass der physiologische Status von *Escherichia coli* Zellen in der initialen Kultivierungsphase aufgrund langer Anpassungsprozesse einen bedeutenden Effekt auf den zentralen Kohlenstoffwechsel und Leistungsfähigkeit in der folgenden Fed-batch Phase haben kann.

Acknowledgements

So many people contributed not only in a scientific way to this thesis. And I am happy to have the opportunity to express my gratitude.

Prof. Peter Neubauer I want to thank in the first place for all his support and providing the possibility of this thesis. During my participation at the department of bioprocess engineering I experienced how he built it up not only with scientific knowledge, but also with kindness and fairness for the people around. I appreciated the productive and collegial atmosphere at the department he contributed to a lot.

I also want to thank Dr.-Ing. Stefan Junne for supervising the project. He taught me a lot and helped me especially in the beginning with the reactor cultivations. Without his support the execution of the experiments had been hardly possible.

Furthermore, I want to thank the Deutsche Forschungsgemeinschaft (DFG) for the financial support of the project (project nr. 10034161). It was the basic requirement and I am happy that the project was chosen to be supported.

Also I want to thank Prof. Raivo Vilu of the “Center of Food and Fermentation Technology” in Tallinn, Estonia, for welcoming me in his lab and introducing me to Karl Peebo, who was such a great help and appreciated host to me. I want to thank Indrek Koppel for his help for real-time PCR realization and evaluation. And I also want to thank Prof. Dr. Reinhard Guthke and Dipl.-Ing. Wolfgang Schmidt-Heck (AG Systembiologie / Bioinformatik, Leibniz-Institut für Naturstoff-Forschung und Infektionsbiologie - Hans-Knöll-Institut, Jena) for the clustering of the proteome data, classification to the KEGG-pathways and supporting me understanding of the method.

It is also my wish, to thank all those who participated in experimental work during the project, either by preparing their own diploma thesis, as student assistant or learning cultivation for their own PhD thesis. These are Iren Czisar, Dennis Runge, Julia Geyer, Sergej Trippel, Robert Spann, Anna Maria Marba, Basant El Kady, Ping Lu, and Christoph Klaue.

I further want to thank the members of the department team during my scientific work. They all together made this special time to a happy memory I am very grateful for. I especially want to thank Mirja Krause for being a good friend who gave so many appropriate advices, Julia Glazyrina, Sergej Trippel and Robert Spann for their positive spirits, Anna Maria Marba, Ping Lu and Basant El Kady for their kindness and Iren, Julia and Christoph for being patient with me. Especially I want to thank Dirk Itzeck for introducing me into the practical part of bioreactor cultivations, Brigitte Burckhardt for caring and running the HPLC and preparing the samples with, and Irmgard Maue-Mohn for providing and keeping a running lab system.

Though many more people contributed to the success of this work, I want to express my special gratitude to my family. Particularly my beloved life partner and devoted father to our children, Mathias, I want to thank from the bottom of my heart for being always supportive, patient and the best friend to me.

Contributions

Besides the author (Eva Brand), several scientists contributed to this work.

Dr. Lu Ping, Basant El Kady, Anna Maria Marba, Sergej Trippel, Robert Spann, Iren Csizar and Christoph Klaue contributed to the bioreactor cultivations, sampling and sample analysis.

Prof. Raivo Vilu and Karl Peebo (Center of Food and Fermentation Technology, Tallinn, Estonia) contributed substantially to the sample preparation for proteome and transcriptome analysis. Indrek Koppel contributed to successful real-time PCR performances and evaluation.

The clustering of the proteome data and classification to KEGG-pathways was kindly contributed by Prof. Dr. Reinhard Guthke and Dipl.-Ing. Wolfgang Schmidt-Heck (AG Systembiologie / Bioinformatik, Leibniz-Institut für Naturstoff-Forschung und Infektionsbiologie - Hans-Knöll-Institut, Jena).

Table of contents

Abbreviations

ATP	adenosine triphosphate
cAMP	cyclic adenosine monophosphate
CoA	coenzyme A
CPR	carbon dioxide production rate
CRP	cAMP receptor protein
DCW	dried cell weight
DNA	deoxyribonucleic acid
DOT	dissolved oxygen tension
E. coli	*Escherichia coli*
et al.	*et alii*
FB	fed-batch
FNR	fumarate and nitrate reductase regulatory protein
GDP	guanosine diphosphate
GTP	guanosine triphosphate
HCDC	high cell density cultivation
$k_L a$	oxygen mass transfer coefficient
Lrp	leucine responsive protein
NADH	nicotinamide adenine dinucleotide
NADPH	nicotinamide adenine dinucleotide phosphate
OD	optical density
OUR	oxygen uptake rate
PCR	polymerase chain reaction
PFR	plug flow reactor
ppGpp	guanosine 3’-diphosphate 5’-diphosphate
PPP	pentose phosphate pathway

PTS	phosphotransferases system
q_{Omax}	maximal oxygen uptake rate
q_{Scap}	glucose uptake capacity
q_{Smax}	maximal substrate uptake rate
rpm	rounds per minute
SDS	sodium dodecyl sulfate
STR	stirred tank reactor
TCA	tricarboxylic acid
TCR / Two-CR	two-compartment reactor

1. Introduction

1.1 Escherichia coli as workhorse for large scale production

The model organism *Escherichia coli* (*E. coli*) is known to be a workhorse for studies regarding general metabolism and physiology, genetics and genetic engineering, synthesis of different products and the corresponding cultivation processes. In the 1930 basic studies on its general physiology were published (Hershey, 1939; Huntington and Winslow, 1937; Martin, 1932) and especially in the 1940s already several studies on *E. coli* genetics (Lederberg, 1947). The reason for the success of *E. coli* are its growth on a wide variaty of substrates, its easy and fast growing cultivation and its facultative anaerobiosis, so it can grow at aerobic and anaerobic cultivation conditions. With further enhanced genetic tools (Wood, 1983), genetic engineering of *E. coli* started in the late 1980s to gain different types of products (Brinkmann *et al.*, 1989; Hanahan, 1983; Ingram *et al.*, 1987). Nowadays, *E. coli* is used for a wide range of applications including the production of recombinant proteins, plasmid DNA, peptides, metabolites and microdiesel production (Brand *et al.*, 2012; Ferreira *et al.*, 2000; Grunzel *et al.*, 2014; Jantama *et al.*, 2008; Kalscheuer *et al.*, 2006; Meagher *et al.*, 1977; Song *et al.*, 2006; Swartz, 2001; Watanabe *et al.*, 2006; Yu *et al.*, 2011). Depending on the product, requirements like bulk production, high quality or high product yields are in focus of the cultivation result. At most production processes the overall yield increases with increasing biomass. Therefore, for several applications a fed-batch high cell density cultivation (HCDC) in large scale vessels is the preferred cultivation technique (Babu *et al.*, 2000; Choi *et al.*, 2006; Lin *et al.*, 2005; Liu *et al.*, 2012).

Several studies showed, that the scale up of *E. coli* cultivations has a tremendious impact on cellular metabolism and production performance. In this literature review, the most relevant factors regarding the impact of cultivation size and

process parameters on *E. coli* physiology and central carbon metabolism will be named.

1.2 Influence of large scale cultivation conditions on *E. coli* metabolism

1.2.1 Criteria and challenges of process scale-up

High cost and time input lies in the nature of large scale processes. Therefore, a screening of suitable *E. coli* strains for the production of the desired product usually takes place at bench scale conditions. Nevertheless, it may happen that the strain that showed best results at bench scale is a suboptimal producer at large scale cultivation (Williams *et al.*, 2009; Yau *et al.*, 2008). This can happen especially when the screening was performed in batch cultures while the production process is a HCDC with fed-batch regime. An inappropriate selection of the production strain can be circumvent by the application of fed-batch small scale cultivation for screening purposes (Šiurkus *et al.*, 2010). Another reason with high impact are changes in the cultivation environment due to scale-up with its criteria and challenges.

The biggest issue regarding scale-up is the mixing of the cultivation broth, reviewed by Villardsen *et al.* (Villadsen *et al.*, 2011). With appropriate mixing, the transfer of heat, oxygen, carbon dioxide, glucose and pH agent can be set at optimal cultivation conditions. When a stirred tank reactor (STR) cultivation is scaled up, the mixing time increases due to limited power input of the impeller (Evangelista *et al.*, 1969). While the impact of mechanical stress is more relevant for mycelial cultivations than for *E. coli*, the effect of increasing mixing times has a measurable impact on production performance (Nienow and Flickinger, 2009). The reason is the emergence of heterogeneities. To minimize the effect, the dominant scale-up criteria are the power-to-volume ratio and the oxygen mass transfer coefficient ($k_L a$) (Sweere *et al.*, 1987).

Nevertheless, at large scale cultivations of several m^3, it is not possible to meet the compliance of the scale-up criteria anymore. Especially the high metabolic activity of *E. coli*, one of the reasons for its preferred usage as production organism, complicates the prevention of metabolically relevant heterogeneities. Several studies show, that *E. coli* reacts within 30 s with activated transcription profiles to changing environmental conditions, while the activation for transcription is supposed to be triggered even earlier (Löffler *et al.*, 2016; Schweder *et al.*, 1999; Taymaz-Nikerel *et al.*, 2013). Even faster is the secretion of acetate and formate after a glucose pulse into the medium, which was measurable after 2 s of exposure to an altered environment (Lara *et al.*, 2009). Therefore, the understanding of mixing limitations and presence of heterogeneities in large scale cultivations is very important for understanding *E. coli* metabolism at large scale conditions.

1.2.2 Mixing limitations and presence of heterogeneities in larges *E. coli* cultivations

As mentioned earlier, the typical cultivation process for production with *E. coli* is a HCDC with fed-batch strategy. The substrate, usually glucose, is applied by continuous addition at the top of the fermenter. With the supply of substrate the growth and metabolic activity / oxygen demand of *E. coli* can be directly influenced. Hence, the most important control parameter at a HCDC is the feed rate (Neubauer and Junne, 2010). Further components which are added are oxygen, pH regulation and heat, while the produced carbon dioxide is dissipated. The oxygen is supplied by an air sparger at the bottom of the cultivation vessel, pH regulation and substrate solution are added from the top. This setup and process performance influences the degree of heterogeneities during the cultivation process.

Substrate distribution: The substrate in an *E. coli* large scale cultivation is usually a highly concentrated glucose solution (600 – 850 g L^{-1}), which is applied at the top of the cultivation vessel. Reason for this highly concentrated solution is the volume of the glucose solution (Enfors *et al.*, 2001). The lower the concentration is the more

volume has to be added during the cultivation. For K-12 strain W 3110 0.57 g biomass per g glucose were gained in a batch cultivation (Luli and Strohl, 1990). In a HCD fed-batch cultivation with a final biomass yield of 150 g L^{-1}, the feed volume of a 600 g L^{-1} glucose solution is approx. one half of the final volume. The drawback of the highly concentrated glucose solution is its high viscosity compared to water (Nikam *et al.*, 2000).

Oxygen distribution: The supply of sufficient oxygen to keep a large scale *E. coli* cultivation aerobic is very challenging (Steel and Maxon, 1966). One mole of pure oxygen possesses a volume of approx. 22.4 L. Additionally, the oxygen has to cross over from the gaseous phase into the liquid phase, which depends on the concentration gradient and the $k_L a$ value. Since the cultivation is kept at a minimum DOT, e. g. 30%, the maximal possible concentration gradient will not be reached. The $k_L a$ value of low-viscosity fluids is dependent on the energy put in for dissipation and the ratio of cultivation broth and X-sectional area of the bioreactor. It is further dependent on the transfer area of the air bubbles and hence on medium composition and, more important with increasing cultivation time, on fluid viscosity. During cultivation most parameters of the oxygen transfer rate are given, so that the stirrer speed is the only parameter adjustable for sufficient oxygen supply (Oosterhuis and Kossen, 1984). Nevertheless, the maximal stirrer speed bears limitations due to mechanical forces. Hewitt and Nienow published a comprising summary on mixing limitations in 2007 (Hewitt and Nienow, 2007). Manfredini *et al.* (1983) performed a mapping of DOT along the radial axis and height in a 112 m^3 cultivation vessel with four Rushton turbine of a *Streptomyces aurofacies* cultivation which represents a non-Newtonian fluid. The radial DOT varied up to 10%, while the axial DOT varied more than 30%. Though these results are not applicable to *E. coli* cultivations, they show the importance of DOT gradients.

The limited mixing capabilities at large scale conditions lead to a feeding zone at the top of the cultivation vessel. This feeding zone is characterized by a high glucose concentration due to the prolonged mixing time of the viscous feed solution (Bylund *et al.*, 1998; Larsson *et al.*, 1996), like shown schematically in figure 1. The cells in this area take up glucose to their maximal rate. As a consequence of the fast metabolism of *E. coli*, the oxygen supply becomes limiting in this area and the cells experience an environment with glucose excess and oxygen depletion (Enfors *et al.*, 2001). On the other hand, the cells at the bottom of the cultivation vessel experience sufficient oxygen supply, but glucose limitation. Consequently, the cells oscillate between both zones. These oscillations in the environmental conditions effect the growth and metabolic activity of the cells, which was the focus of several studies. Bylund *et al.* (1998) measured the glucose distribution in a 12 m^3 *E. coli* bioreactor cultivation with three Rushton turbines. The cells grew to a density of 30 g L^{-1} biomass. Glucose concentration was measured at the bottom, in the middle and at the top of the cultivation broth. When the feed was applied at an inappropriate mixed zone, the glucose concentration was 400 times higher in the feed zone than the mean value. This led to acetate formation, an increased metabolic maintenance and consequently 20% decreased biomass.

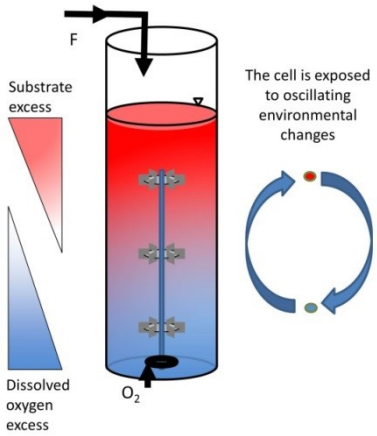

Figure 1: Schematical glucose and oxygen distribution in a large scale *E. coli* fed-batch high cell density cultivation process. When the feed (F) is applied from the top and the air / oxygen (O_2) from the bottom the cells oscillate between both zones due to insufficient mixing.

In the study of Enfors *et al.* (2001) substrate oscillations were determined in a large scale *E. coli* cultivation. But the appearance of gradients are not restricted to very large reactors, but also can be estimated in smaller scales. A substrate concentration of 4 g L^{-1} close to the feeding point and 0 - 0.02 g L^{-1} at the bottom quarter of a stirred tank bioreactor was simulated for a liquid volume of 900 L and a substrate concentration of 600 g L^{-1} glucose in the feed, when the stirrer rate of six blade impellers was set to 400 rpm (Lapin *et al.*, 2006). Hence, the effect of oscillating substrate concentrations can also be present in pilot scale cultivations. To study the effect of oscillating conditions, several scale-down approaches were developed in the past.

1.2.3 The development of Two-compartment scale-down reactors

Several scale-down approaches were performed to simulate large scale cultivations in lab scale. Generally, scale-down reactors are composed of different compartments to simulate the different zones. The parameters to be considered are the fractions of the zones and the residence times the cells are in these zones. The compartment representing the bulk zone is usually a STR, while the other zone can be either simulated with a STR or a plug flow reactor (PFR).

The main interest by applying a scale-down reactor is to study the reasons of altered physiology of production strains compared to lab scale cultivations. One of the first two-compartment scale-down concepts were used by Oosterhuis *et al.* for optimization studies on the production of gluconic acid by *Gluconobacter oxydans* (Oosterhuis *et al.*, 1985). In the study two STRs were interconnected and the cells were exposed to oxygen gradients. The same concept was also used for more recent studies by Sandoval-Basurto (2005). The effect of repeated oxygen depletion on the performance of a recombinant *E. coli* strain was studied. This system was further used to determine the transcriptional and metabolic response to oxygen oscillations (Lara *et al.*, 2006). The drawback of this setup is the mixed residence

time in the compartment which does not represent the bulk zone. While in the STR-PFR system the residence time of the cells in the simulated condition is within a small variation, only a mean residence time for the STR-STR system can be determined. A very recent study compared the scale-down performances of a STR-STR concept to a STR-PFR concept. Interestingly, both concepts were found to simulate large scale conditions with a similar performance (Limberg *et al.*, 2016). Nevertheless, for studies of time resolved metabolic response to changing environmental conditions undefined residence times are disadvantageous.

Hence, a STR-PFR system was already used by George *et al.* for ethanol production studies on baker's yeast (George *et al.*, 1993). The PFR was fitted with static mixers to enable gassing and ensure plug flow behavior. Two years later this setup was used by Neubauer *et al.* to simulate oscillating glucose pulses on an *E. coli* cultivation (Neubauer *et al.*, 1995b). The advantage of this setup is the defined residence time of the cells exposed to conditions different to the bulk zone, so that samples can be taken after exposures to the oscillating condition. Later on, this setup was used for several scale-down experiments also for *Bacillus subtilis* and *Corynebacterium glutamicum* studies (Junne *et al.*, 2011; Käß *et al.*, 2014; Lemoine *et al.*, 2015) (figure 2).

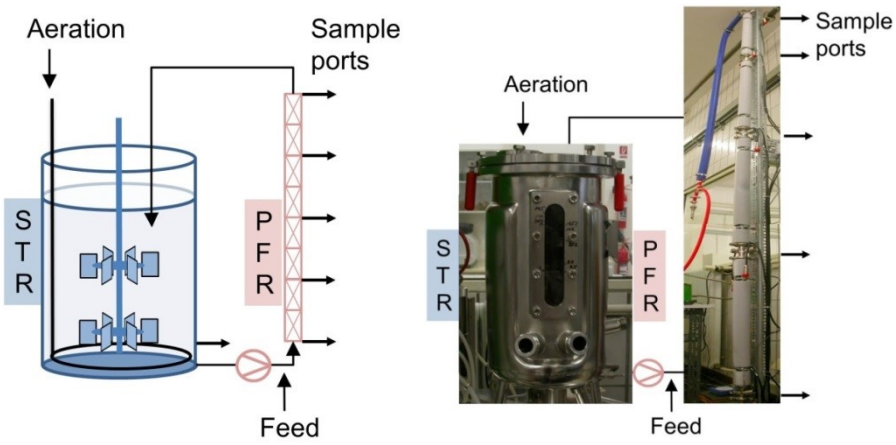

Figure 2: Schematic and actual setup of a STR-PFR scale-down reactor to investigate oscillating glucose conditions.

A very recent approach for scale-down studies is the use of a three compartment reactor (Lemoine *et al.*, 2015). The system consists basically of a STR-PFR system where a second PFR is connected to the STR. With this setup additionally to the bulk

zone and the feeding zone also the starvation zone at the bottom of a large scale cultivation vessel can be simulated.

1.2.4 The influence of heterogeneities on large scale and scale-down *E. coli* cultivations

One of the earliest application of the STR-PFR scale-down system for *E. coli* physiology studies was performed by Neubauer *et al.* in 1995 to simulate oscillating glucose pulses (Neubauer *et al.*, 1995b). In the study, the glucose pulses were generated at the entrance of an aerated PFR. Though acetate accumulated in the PFR part, it was re-assimilated in the STR. Growth reduction was found, when anaerobic conditions were generated by the high glucose concentration. Neubauer *et al.* also studied the effect of oscillating glucose starvation on the cells resulting in the synthesis of guanosine 3'-diphosphate 5'-diphosphate (ppGpp), which triggers a starvation response in *E. coli* (Neubauer *et al.*, 1995a). They found, that a peak in ppGpp accumulation was achieved in the PFR already in less than 1 min after exposure to starvation.

Schweder *et al.* published a study on stress response genes activated at high glucose concentrations simulated in a STR-PFR scale-down reactor (Schweder *et al.*, 1999). Compared to the former study of Neubauer, the PFR was not aerated, so that oxygen limitation can be assumed when the feed was applied at the entrance of the PFR. The glucose concentration at the inlet of the feed was approx. 1 g L^{-1}. The mRNA levels of *proU*, *ackA*, *dnaK*, *clpB*, *pfl* and *frd* along the PFR were measured at 13.5 and 17.5 h after start of fed-batch phase. It was found, that they increased along the PFR more than twice for at least one measurement. These results were compared to a 20 m^3 large scale fed-batch cultivation, where elevated levels of some of these mRNAs were also found in the middle and top part of the cultivation vessel. Also Xu *et al.* used this type of scale-down reactor setup to compare an *E. coli* cultivation with a 20 m^3 large scale cultivation in terms of reduced biomass and synthesis of mixed acid fermentation products (Xu *et al.*, 1999). They described the accumulation of mixed acid fermentation compounds in the PFR and the re-assimilation in the STR with formate being less re-assimilated than the other acids. Hence, an accumulation of formate was observed. They also found a reduced

biomass of 12%, which was the same for the large scale cultivation. The volume fractions they used were 90% in the STR and 10% in the PFR. This fraction is supposed to represent the bulk zone and the feeding zone in a large scale cultivation, respectively.

Enfors *et al.* compared *E. coli* W 3110 cultivations with different reactor scales and types (Enfors *et al.*, 2001). The three reactors compared were a 30 m^2 large scale reactor with 21 - 22 m^3 working volume, a conventional stirred tank reactor and a scale-down reactor. The scale-down reactor was composed of a STR and a PFR to represent the bulk zone and the feeding zone. The volume of the PFR was 10% of total broth volume when aerated or 15% when not aerated. The residence time was 54 s and the feed was applied at the entrance of the PFR resulting in a concentration of about 1 g L^{-1} glucose. Glucose concentrations were analyzed in the large scale cultivation near the feeding point and found to be partly several times higher than the mean glucose concentration, so the cells experience these glucose peaks. The mean glucose concentration in the top was twice the concentration at the bottom. The DOT was 53% at the bottom and 25% at the middle sampling port. At a biomass concentration of 30 g L^{-1} formate started to accumulate in the culture. This accumulation was assumed to appear due to anaerobic compartments in the reactor, very likely in the feeding zone with high glucose concentration. Nevertheless, the accumulation of acetate as a product of mixed acid fermentation could not be observed. They further concluded, that the mixed acid fermentation of the cells is not inhibited by the intervals when aerobic conditions are present, though the FNR protein is supposed to be inactivated at aerobic conditions. When the data were compared with those of the scale-down reactor, they also found that acetate, lactate and formate accumulate at anaerobic conditions and presence of glucose in the PFR, but the re-assimilation rate of the first two metabolites in the aerobic STR is higher (reported before by Xu *et al.* 1999). Consequently, in the STR the accumulation only of formate was observed, comparable to the large scale

cultivation. The analysis of transcription profiles of stress response related genes along the PFR and in the large scale reactor also showed, that the cells frequently put extra energy to transcription each time they pass the feeding zone.

These studies show the partly tremendous effect of insufficient mixing on the *E. coli* metabolism. They furthermore show, that a STR-PFR setup is a powerful device for scale-down studies with defined residence times in the PFR part for sample analysis.

1.3 The interplay of central carbon metabolism and global regulation systems of *E. coli*

E. coli's natural habitat is the intestine of creatures. Its success as production strain for industrial applications is based on its wide variety of cultivation possibilities. As facultative anaerobic bacterium it can grow at aerobic and anaerobic conditions, though better growth performance is achieved at the presence of oxygen. Furthermore, it is capable of utilizing a wide variety of substrates and electron acceptors for respiration. Additionally, it is very robust to changing environmental conditions regarding pH, temperature and osmotic stress (Shimizu, 2013). In this chapter the point of focus is the influence of global regulation systems, triggered by environmental changes and conditions, on the central carbon metabolism of *E. coli*.

1.3.1 Regulation points of central carbon metabolism

The central carbon metabolism consists of the interplay between glycolysis, glyconeogenesis, pentose phosphate pathway (PPP) and tricarboxylic acid (TCA) cycle (Holms, 1996). While glycolysis, glyconeogenesis and PPP are directly linked, the link between glycolysis and TCA cycle is mediated by the acetate node (Valgepea *et al.*, 2010). In the following the use of glucose as substrate by exclusively *E. coli* forms the focus of metabolic regulation.

The glycolysis describes the conversion from one molecule glucose to two pyruvate coupled with the generation of two adenosine triphosphate (ATP) and two nicotinamide adenine dinucleotide (NADH) with ten enzymatic steps (Romano and

Conway, 1996). The first step when *E. coli* utilizes glucose is its transport across the membrane and conversion to glucose-6-phosphate via the glucose PTS permease. The activity of this permease system is regulated by several factors since its activity determines the glucose mediated carbon flow into the cell at fed-batch cultivations of *E. coli*. Glucose-6-phosphate can either be utilized for further glycolysis reaction or as precursor for PPP. The PPP is crucial for the generation of anabolic compounds and can also be fed via gluconeogenesis when glucose-6-phosphate is directly not available. Basically, glycolysis and gluconeogenesis share the same set of enzymes with two exceptions which function as regulatory switches, depending on the substrate availability and cellular demand for reaction compounds. These two regulatory points are the conversion from fructose-6-phosphate to fructose-1,6-bisphosphate (phosphofructokinase at glycolysis and fructose-1,6-bisphosphatase at gluconeogenesis) and the conversion from phosphoenolpyruvate to pyruvate (pyruvatekinase for glycolysis and pyruvatecarboxylase / phosphoenolpyruvate-carboxykinase for gluconeogenesis). The bottlenecks of glycolysis were reported to be the enzymes fructose-1,6-bisphosphatase aldolase, which breaks down the six carbon backbone of glucose to two three carbon compounds, dihydroxyacetone-phosphate and glycerinealdehyde-3-phosphate, and the following triosephosphate-isomerase, which converts both three carbon compounds into each other (Hollinshead *et al.*, 2016).

For the PPP the regulatory step is the conversion of glucose-6-phosphate to ribulose-5-phosphate, commonly named oxidative part of the PPP that generates nicotinamide adenine dinucleotide phosphate (NADPH) (Hollinshead *et al.*, 2016). The following reactions of the non-oxidative part are all reversible and the flux is determined by the pool size of the compounds.

The TCA cycle is special since it combines catabolism of carbohydrates, fatty acids and amino acids. The basic reaction is the degradation of acetyl-Coenzyme A (CoA), which derives from several catabolic pathways, to carbon dioxide by stepwise shortening of a 6 carbon backbone, citrate, to a 4 carbon backbone, oxaloacetate. Oxaloacetate fuses again with acetyl-CoA to citrate by the enzyme citrate-synthase. The TCA cycle is the most complex part of the central metabolism and its fluxes are

determined by the compounds fed in and extracted. Therefore, also the regulation pattern is more complex and will be described in connection to the general effect of the corresponding global regulator described below.

1.3.2 Global regulators of *E. coli* most crucial for central carbon metabolism and carbon fluxes

In *E. coli*, the expression of about one half of all genes is modulated by only seven global regulators (Martinez-Antonio and Collado-Vides, 2003). These are CRP, FNR, ArcA, Fis, Ihf, Lrp and NarL. Of these seven global regulators the first three can directly influence the fluxes of the central carbon metabolism by altering the expression of according genes (Perrenoud and Sauer, 2005).

1.3.2.1 CRP: CRP stands for cyclic adenosine monophosphate (cAMP) receptor protein (Deutscher, 2008). Its function as global regulator starts with the binding to cAMP. cAMP is the product of adenylate cyclase (*cyaA*) and increases at glucose concentrations below 3 mM (Notley-McRobb *et al.*, 1997), but without a striking shift in glucose assimilation or growth rate at this threshold value. When active, cAMP-CRP activates the transcription of 321 genes (176 operons) and represses the transcription of 46 genes (16 operons) (Khankal *et al.*, 2009; Zheng *et al.*, 2004). Generally, the transcription of transporters and enzymes involved in substrate utilization other than glucose are up-regulated at the presence of cAMP-CRP (Shimada *et al.*, 2011), e.g. the lac-Operon for lactate utilization. In a recent study it was shown, that cAMP-CRP regulation does not exclusively prefer the uptake of only glucose prior to other substrates, but it controls the overall carbon uptake rate (Hermsen *et al.*, 2015).

Shimada *et al.* (2011) screened the *E. coli* genome for further cAMP-CRP binding sites and found even 183 novel regulation target sites, which were examined positively by using a *lacZ* reporter assay. They concluded, that "*CRP plays a key regulatory role in the whole processes from the selective transport of carbon sources, the glycolysis-gluconeogenesis switching to the metabolisms downstream of glycolysis, including tricarboxylic acid (TCA) cycle, pyruvate dehydrogenase (PDH) pathway and aerobic respiration*". This study enables a deepened understanding of

how cAMP-CRP regulates the central carbon metabolism. In the following, only the findings directly related to glucose utilization are summarized. Though the increased transcription of the *pts* operon by positive regulation of cAMP-CRP was known before (Postma *et al.*, 1993), in this study they found almost all genes for the transport of carbon sources to be regulated by cAMP-CRP. Additionally, all ABC family transporters were found to be regulated by cAMP-CRP. From this, the authors concluded that cAMP-CRP sorts the transport of carbon sources as one of its major roles. Among the genes involved in glycolysis underlying cAMP-CRP regulation is *fbaA*, which encodes for fructose-1,6-bisphosphate aldolase. This enzyme was mentioned above as bottleneck of glycolysis since it catalyzes the reversible cleavage of the six carbon backbone of fructose-1,6-bisphosphate. Further genes are *gapA* (glyceraldehyde-3-phosphate dehydrogenase) and *pgk* (phosphoglycerate kinase). They further found indications that *glk* (glucokinase, glycogendegradation), *yggF* (type II fructose-1,6-bisphosphatase, gluconeogenesis), *ppsA* (phosphoenolpyruvate synthase, gluconeogenesis), *talA* (transaldolase, link between glycolysis and PPP) and *tktB* (transketolase II, link between glycolysis and PPP) are under the control of activator cAMP-CRP. Additionally, *pgi* (glucosephosphate isomerase) and *gpm*M (phosphoglycero mutase III) promoters can be activated by CRP while the *fbaB* (class-I fructose-bisphosphate aldolase) promoter can be repressed.

As mentioned above, the PPP derives from glucose-6-phosphate, so that it shares the substrate with glycolysis. Shimada *et al.* (2011) found with Genomix SELEX method, that the expression of the enzymes catalyzing the last steps of PPP, encoded by *tktAB* and *talAB*, is positively regulated by cAMP-CRP. With this study the overall regulation of gene expression of key enzymes involved in glucose uptake, glycolysis, gluconeogenesis and PPP by cAMP-CRP became more evident.

Since cAMP-CRP regulates the expression of the majority of key genes regarding glucose uptake and metabolism, it is not surprising that it also regulates parts of the central carbon metabolism downstream of glycolysis and respiration. The study by Shimada *et al.* (2011) showed, that CRP also regulates the genes encoding for the pyruvate dehydrogenase complex, most of the TCA cycle enzymes and NADH–

ubiquinone oxidoreductase I (*nuoABCDEFGHIJKLMN*), NADH-ubiquinone oxidoreductase II (*ndh*) and cytochrome bo terminal oxidase (*cyoABCDE*).

1.3.2.2 FNR: FNR stands for "fumarate and nitrate reduction" (Lambden and Guest, 1976) because mutants of this gene were found to be unable to use fumarate and nitrate as electron receptor. FNR belongs like CRP to the CRP/FNR superfamily of transcription factors (Körner *et al.*, 2003) and is the global regulator for the transition to anaerobic metabolism in *E. coli*. The cellular concentration is similar at aerobic and anaerobic growth (Sutton *et al.*, 2004), but FNR requires a [4Fe-4S] cluster to be active. At the presence of oxygen, this cluster is oxidized to [2Fe-2S] cluster. After prolonged exposure to oxygen this cluster is destroyed completely. At absence of oxygen FNR is activated.

Active FNR protein activates transcription of genes of anaerobic metabolism and represses transcription of aerobic metabolism related genes (Kang *et al.*, 2005; Salmon *et al.*, 2003). These activated genes belong to anaerobic oxidation of carbon sources, anaerobic reduction of terminal electron receptors and the transport of both, while the repression targets genes of respiratory enzymes like NADH dehydrogenase II and cytochrome oxidases. Unden *et al.* published in 1991 a summary of FNR regulated genes (Unden and Trageser, 1991). Those positively regulated and directly involved in central carbon metabolism are *frdABCD* (fumarate reductase), *fumB* (fumarase B) and *pfl* (pyruvate-formate lyase), while *fnr* itself and *cyoABCDE* (cytochrome o complex) are negatively regulated.

Kang *et al.* (2005) found altogether 184 operons with 465 genes to be regulated by FNR and/or oxygen. Of these, 297 showed at least 3-fold change in gene expression between aerobiosis and oxygen depletion. They found a repression of genes involved in aerobic respiration and TCA cycle activity, while those involved in anaerobic respiration and fermentation were activated. In contrary to previous studies they found that the *Ppdh* promotor of the *pdh* operon was not strongly regulated by FNR. Interestingly, the also found *talA* and *tktB* being repressed by FNR. Among the genes with decreased expression at oxygen depletion and depression partly FNR dependent are many of the aerobic metabolism. Those of the TCA cycle are *gltA*, *acnB*, *icdA*, *sucABCD*, *sdhCDAB*, *fumA*, *mdh* and glyoxylate shunt

aceA. Interestingly, *gltA*, *acnB* and *mdh* have been reported before to be negatively regulated by ArcA (see chapter 1.3.2.3) and not FNR (Cunningham et al., 1997; Park et al., 1994, 1995), indicating some overlapping of ArcA and FNR regulation. Also genes of glycolysis were found to be repressed by FNR like *pgi*, *pfkB* and *fbaB*. But these genes did not show any oxygen dependent gene expression.

1.3.2.3 ArcAB two-component system: The ArcAB (anoxic redox control) is comprised of a membrane associated redox kinase and phosphatase (ArcB) and a cytosolic transcription factor (ArcA) (Alvarez and Georgellis, 2010). Generally, this two-component system senses the redox state of the cell (Iuchi *et al.*, 1990; Iuchi and Lin, 1993). A recent study showed, that the three quinones ubiquinone, demethyl-menaquinone and menaquinone, can activate or deactivate the sensor ArcB (van Beilen and Hellingwerf, 2016). During transition from aerobic to anaerobic growth the activity of ArcB increases, which activates ArcA. Activated ArcA is known to repress genes related to aerobic growth, especially the genes of TCA cycle and glyoxylate shunt genes (Liu *et al.*, 2016). These are *gltA, acnA*, *icdA*, *sucABCD*, *sdhCDAB*, *fumAC*, *mdh* and *aceBAK*. ArcA is also supposed to activate the transcription of the *cydAB* operon at microaerophilic conditions (Tseng *et al.*, 1996). The knockout of ArcA can increase recombinant protein production due to increased TCA cycle activity (Vemuri *et al.*, 2006). While the activity of FNR at exclusively anaerobic conditions represents rather a switch point, the ArcAB two-component system reacts in a broader spectrum between aerobic and anaerobic conditions (Lynch and Lin, 1996), so that the transcriptional regulation of both systems overlaps in some cases like mentioned above.

1.4 Growth rate related physiology of *E. coli*

In industrial *E. coli* fed-batch cultivations the glucose supply is the growth rate limiting factor. The example of the cAMP-CRP regulation shows, how the availability of glucose influences the central carbon metabolism of *E. coli*. Consequently, also the growth rate effects the central carbon metabolism, though the effect is not only limited to cAMP-CRP activation. Generally, rapid growing cells primarily rely on glycolytic acitivity (Molenaar *et al.*, 2009; You *et al.*, 2013). By using parallel

catabolic pathways, the co-utilization of at least two substrates even increases the growth rate compared to single substrate utilization. This was brought into a formular for growth by Hermsen *et al.* (2015). Since the PPP is the source for anabolic reaction intermediates, the first enzyme of the pathway, glucose-6-phosphate dehydrogenase (encoded by *zwf*), is the key entrance enzyme and subject to regulatory mechanisms regarding pentose-phosphate pathway activity and its expression rate was found to be growth rate related (Rowley *et al.*, 1992). These are few examples, how the growth rate influences the central carbon metabolism. Nevertheless, most effects can be deduced to the glucose uptake and respiration capacities of the cell, its overflow metabolism and the proteomic composition. These topics are the content of the following chapters.

1.4.1 Growth rate related glucose uptake and respiration rate

In an *E. coli* fed-batch cultivation the growth rate is directly coupled to the glucose supply, but the way the glucose is metabolized depends on further conditions. The accumulation of acetate is supposed to appear due to limiting steps either in the respiratory chain or in the TCA cycle (El-Mansi and Holms, 1989; Holms, 1986; Majewski and Domach, 1990). Both activities are controlled by global regulators as mentioned above. Therefore, the determination of the maximal glucose uptake capacity (q_{Smax}) is a helpful indicator for the metabolic state of the cell. Several studies of the late 70's showed, that q_{Smax} depends on the growth rate by variation of the glucose:phosphoenolpyruvate phosphotransferase system content of the cell (Hunter and Kornberg, 1979; Neijssel *et al.*, 1977, 1980). Hunter and Kornberg (1979) also showed, that glucose pulses stimulate the respiratory chain, indicating an interaction between glucose uptake and oxygen consumption. Lin *et al.* (2001) studied the relation between growth rate, q_{Smax} and maximal oxygen uptake rate (q_{Omax}). Therefore, they performed a batch cultivation of a recombinant *E. coli* W3110 with a subsequent fed-batch feeding strategy. Here, the feeding rate was kept constant and unsaturating glucose pulses at aerobic conditions were added. They found, that q_{Smax} and q_{Omax} decrease proportionally with decreasing growth rate, though the proportion for both parameters to the growth rate is quite different. A direct proportional correlation for q_{Smax} was observed for a growth rate

from 0.02 h^{-1} to 0.15 h^{-1} with an increase from 0.06 mmol g^{-1} h^{-1} to 1.45 mmol g^{-1} h^{-1}. The linear regression fit was q_{Smax} = 5.54 x μ + 0.53 with a coefficient of determination of 0.91. For q_{Omax} a direct proportional correlation was found for growth rates from 0.02 h^{-1} to 0.25 h^{-1} with an increase from 5 mmol g^{-1} h^{-1} to 20 mmol g^{-1} h^{-1}. Here, the linear regression fit was q_{Omax} = 59.22 x μ + 4.59 with a coefficient of determination of 0.92. These two formulas reveal the limitation of maximal glucose uptake with increasing growth rate before the limitation of maximal oxygen uptake rate. Furthermore, a second, even more important conclusion can be drawn: the proportional parameter of both formulas differs by a factor of 10. The oxidation of one mole glucose consumes 6 moles of oxygen ($C_6H_{12}O_6$ + 6 O_2 -> 6 CO_2 + 6 H_2O), so q_{Smax} and q_{Omax}, though proportional to the growth rate, are not proportional to each other. This means, with decreasing growth rate q_{Omax} decreases faster than q_{Smax}. Lin *et al.* (2001) assumed, that the changes of q_{Smax} and q_{Omax} with growth rate is mediated by changes of the amounts of the responsible enzymes. This assumption is in accordance with the finding of a drastic decrease of q_{Smax} and q_{Omax} due to a strong recombinant protein expression (Neubauer *et al.*, 2003).

In the same study Lin *et al.* (2001) also added an acetate pulse on top of a glucose pulse. From the reaction of the cultivation broth they could further conclude, that the accumulation of acetate is the result of limitations in the TCA cycle and not in the respiratory chain.

1.4.2 Growth rate related overflow metabolism

In the former mentioned study of Lin *et al.* (2001) it was found, that acetate accumulates due to lower substrate uptake of the TCA cycle compared to the pyruvate generation of glycolysis. This phenomenon is called overflow metabolism (Farmer and Liao, 1997; Kleman and Strohl, 1994). It is of special interest, since the accumulation of 2 g L^{-1} (~ 30 mM) acetate leads to growth inhibition (Phue *et al.*, 2010; Shiloach and Fass, 2005), at special circumstances already at 8 mM (Roe *et al.*, 2002). Additionally, recombinant protein production can be affected negatively (Jensen and Carlsen, 1990). Many studies were performed to understand the

mechanism behind it. Valgepea *et al.* (2010) used accelerostat cultivations for acetate accumulation studies, where the growth rate constantly increased during cultivation (Paalme *et al.*, 1997). They found, that the acetate node breaks at a growth rate of 0.27 h^{-1}. This growth rate is slightly higher than the maximal growth rate, at which the q_{Omax} is still proportional to the growth rate determined by Lin *et al.* (2001). Valgepea *et al.* (2010) used proteome, transcriptome and metabolome analysis for a wide range of growth rate (0.1 h^{-1} – 0.5 h^{-1}). The level of cAMP increased at growth rate of 0.1 h^{-1} until 0.3 h^{-1} and a carbon catabolite repression was observed before acetate accumulation. Though the acetate synthesizing enzymes were found down-regulated on the transcriptome and proteome level at μ = 0.2 h^{-1}, also the acetate consuming enzyme level decreased, while the TCA cycle genes expression and protein levels were not reduced until a growth rate of 0.4 h^{-1} was reached. From the obtained results they concluded, that acetate accumulation is caused by down-regulation of the acetate consuming assimilating acetyl-CoA synthetase mediated by carbon catabolite repression.

1.4.3 Growth rate related proteome and transcriptome studies on *E. coli* cultivations

The analysis of physiological status of *E. coli* became more global with more advanced technologies. While in former days the changes in metabolome was the most applied analysis technology regarding the metabolic network, in the first years of the new millennium many studies regarding transcriptome analysis, for example by microarray detection, were published. The transcriptome describes the pool of activated and repressed genes by analyzing the change in the corresponding mRNA copy numbers. Since *E. coli* possesses also a post-transcriptional regulation, the analysis of the metabolic network of *E. coli* by transcriptome analysis is often enhanced by proteome analysis, which describes the presence and amount of proteins in the cell (reviewed by Han and Vogel (Han and Lee, 2006; Vogel and Marcotte, 2012)).

Many proteome studies exist for *E. coli* when exposed to special stress situations. Among the first proteomics studies was the analysis of heat shock response (Lemaux *et al.*, 1978; Neidhardt and VanBogelen, 1981). Further stress responses

analyzed by proteomic studies are those to pH changes (Blankenhorn *et al.*, 1999; Yohannes *et al.*, 2004), organic solvents (Yan *et al.*, 2002) and temperature (Herendeen *et al.*, 1979; VanBogelen and Neidhardt, 1990). But also stress responses closer to HCDC issues were analyzed, like those to cell density (Franzén *et al.*, 1999; Yoon *et al.*, 2003), nutrient starvation (VanBogelen *et al.*, 1996; Wick *et al.*, 2001) and anaerobic conditions (Smith and Neidhardt, 1983).

Several studies were performed with batch cultivations and sudden extreme shifts to stimulate the proteomic change in the cells to a very high degree, while only a limited number exist on a HCDC like performed for most production processes or in relation to growth rate. Among these studies are those of Yoon *et al.*, who analyzed the proteome profile during a HCDC (Yoon *et al.*, 2003), and Valgepea *et al.* (2013), who analyzed changes in transcriptome, proteome and metabolic flux during an accelerostat cultivation with increasing growth rate (Valgepea *et al.*, 2013).

Yoon *et al.* (2003) used the *E. coli* strain W 3110 for their study. The cultivation was started as batch with 10 g L^{-1} in a mineral salt medium. After nearly all glucose was consumed they applied a fed-batch with a feeding solution of 700 g L^{-1} and an exponential increase so the specific growth rate was 0.14 h^{-1}. Generally, two changing points in the proteome data were observed. The first shift was the transition from batch to fed-batch, the second was towards the end of cultivation, when the cell density led to stress responses.

They found, that the expression of most TCA cycle genes was up-regulated after transition from batch to fed-batch and again decreased towards the end of cultivation (final biomass concentration: 74 g DCW L^{-1}). In a similar way behaved the expression levels of NADH dehydrogenase and ATPase. This observation was also in accordance to several proteome patterns. Additionally, an increase in glyoxylate shunt enzymes was observed during the exponential growth. From these data they concluded, that the TCA cycle is highly active during exponential growth also to provide the cells with precursors for amino acid synthesis. The increased proteome profile for genes involved in glycolysis and PPP towards the end of cultivation they explained with the reduced energy generation by the TCA cycle. Regarding the proteome of ribosomes and enzymes involved in amino acid and nucleotide

precursor synthesis they further observed a decrease when the cultivation mode switched from batch to fed-batch and a further decrease at the end of cultivation.

Valgepea *et al.* presented a study with proteome data related to changing growth rates (Valgepea *et al.*, 2013). In this study, they performed three accelerostat cultivations with *E. coli* K-12 MG1655. For the growth rate range of 0.11 h^{-1} to 0.49 h^{-1} they analyzed the metabolome, transcriptome and proteome of *E. coli*. Furthermore, metabolic flux analysis was applied on the received data. Thereby it was possible to evaluate the metabolic regulation on the transcriptional, post-transcriptional, translational and post-translational level. The genome-wide absolute quantitative transcription data were generated for μ = 0.11; 0.21; 0.31; 0.40; 0.48 h^{-1}, those for protein abundances at μ = 0.20; 0.30; 0.40; 0.49 h^{-1}. For the growth rates of 0.11 h^{-1} and 0.49 h^{-1} they found an increase in mRNA and protein concentration per cell by 4.2-fold and 2-fold, respectively, showing higher increase of mRNA compared to protein. When the increase of cell size is taken into account, the mRNA molecules per fL increased 1.8-fold, while the protein molecules per fL decreased 1.2-fold. Most of the protein concentrations is controlled at the post-transcriptional level, while the protein-per-mRNA ratio decreased from 100 – 10.000 at low growth rate to 50 – 4.000 at high growth rate, where abundant proteins always show about 100-fold higher protein-per-mRNA ratios than low abundant proteins regardless of the growth rate.

Regarding the regulation levels, only 25% of the 1112 analyzed genes showed transcriptional regulation. Nevertheless, the fraction of transcriptional regulation was high for genes involved in glyoxylate shunt, NADH metabolism and various degradation pathways. The protein concentration of most genes (56%) was found to be regulated at a post-transcriptional level with high fractions for genes of cell cycle, translation, amino acid metabolism and amino acid synthesis. Also the high flux pathways glycolysis and TCA cycle showed post-translational regulation for >60% of the genes. On top of these findings, the metabolic flux is mainly regulated by post-translational regulation for 81% of the genes. The highest post-translational regulation was found for genes of energy production and conversion, translation and TCA cycle and glycolysis. The next level regarded the enzymatic kinetics of

proteins of central carbon metabolism. Interestingly, the average protein concentrations of glycolysis, TCA cycle, PPP and acetate synthesis were kept at a constant level or even decreased when the growth rate and consequently the fluxes increased. The apparent catalytic rates were found slightly higher for TCA cycle than for glycolysis and 12-fold higher for the PPP at low growth rates. Also, the apparent catalytic rates of ribosomes increased, since the ribosomal protein concentration increased only 1.5-fold at five times faster growth.

These studies show the influence of growth rate on the central carbon metabolism.

2. Materials and Methods

2.1 Chemicals

All chemicals were purchased from Carl Roth (Karlsruhe, Germany) or Sigma-Aldrich (St. Louis, USA), if not stated otherwise. A list of all chemicals can be found in the Appendix (Chapter 8.1)

2.2 Strain and medium composition

2.2.1 Escherichia coli strain

The strain used in this study was *Escherichia coli* K-12 W3110 [F^- λ^- IN(*rrnD-rrnE*)1] (Bachmann, 1972; Hayashi *et al.*, 2006). The stocks were generated from cultures in the exponential growth phase grown on Luria-Bertani plates and stored in 25% glycerol solution at – 80 °C.

2.2.2 Media and buffer composition

The components of the Luria-Bertani medium were dissolved in water and autoclaved. For the EnBase medium, different stocks were dissolved in water and autoclaved separately to avoid precipitation and chemical interaction. The carbon source of the EnBase medium was autoclaved separately. The trace elements stock contained selenium, molybdenum and nickel according to Soini *et al.* (Soini *et al.*, 2008*)*. The medium was mixed from stocks freshly each time before use. For bioreactor cultivation the medium was prepared like described in chapter 2.3.2.

Luria-Bertani medium

Tryptone	10 g L^{-1}
Yeast extract	5 g L^{-1}
NaCl	10 g L^{-1}
Agar (for plates)	15 g L^{-1}
pH7	

EnBase Medium without substrate

Na_2SO_4	2 g L^{-1}	10x Macro Elements autoclaved pH 7
$(NH_4)_2SO_4$	6.12 g L^{-1}	
NH_4Cl	0.5 g L^{-1}	
K_2HPO_4	14.6 g L^{-1}	
NaH_2PO_4 H_2O	3.6 g L^{-1}	
$(NH_4)_2$-H-citrate	1 g L^{-1}	
Antifoam	0.1 g L^{-1}	
Thiamine	0.1 g L^{-1}	500x sterile filtered
$MgSO_4$ $7H_2O$	0.74 g L^{-1}	500x autoclaved separately
$CaCl_2$ $2H_2O$	1 mg L^{-1}	500x Trace Elements solution
$ZnSO_4$ $7H_2O$	0.36 mg L^{-1}	
$MnSO_4$ H_2O	0.2 mg L^{-1}	
Na_2-EDTA	40.2 mg L^{-1}	
$FeCl_3$ H_2O	33.4 mg L^{-1}	
$CuSO_4$ $5H_2O$	0.32 mg L^{-1}	
$CoCl_2$ $6H_2O$	0.36 mg L^{-1}	
Na_2SeO_3 $5H_2O$	0.264 mg L^{-1}	
Na_2MoO_4 $2H_2O$	0.24 mg L^{-1}	
$Ni(NO_3)_2$ $6H_2O$	1.45 mg L^{-1}	

PBS-Buffer (used for proteome sample preparation)

NaCl	8 g L^{-1}
KCl	0.2 g L^{-1}
Na_2HPO_4	1.44 g L^{-1}
KH_2PO_4	0.24 g L^{-1}

2.3 Cultivation Conditions

2.3.1 Shake Flask Cultivations

50 µL of stock solution (chapter 2.2.1) were transferred into 10 mL Luria-Bertani medium in a 100 mL Erlenmeyer flask. The flask was sealed with a membrane permeable to air (AerOtop enhanced seal) and shaken at 200 rpm and 37 °C for about 2 hours to an OD_{600} = 1.

From this Luria-Bertani preculture, 5 mL were transferred to 250 mL of EnBase medium containing 2 g L^{-1} glucose. The culture was shaken in a 2.5 L Ultra yield

flask™ (Thomson instrument company, USA) and covered with AerOtop Seal to ensure a continuous aerobic cultivation at 200 rpm and 37 °C until it reached an optical density of OD_{600}=0.3.

For one experiment with a batch phase prior to mechanical feed start, 5 mL of cells in Luria-Bertani medium with OD_{600}=1 were transferred to 250 mL of EnBase Medium containing 10 g L^{-1} dextrin and 0.6 U L^{-1} α-amylase. The cells grew in 12 h to an OD_{600} = 10 before they were used for reactor inoculation.

2.3.2 Bioreactor cultivations

Before sterilization of the bioreactor, water, dextrin, macro elements and trace elements were filled into it. Thiamine and $MgSO_4$ were added after sterilization and the working temperature of 37 °C was reached.

The cultivation process in the fermenter can be divided into two parts: Phase 1 to reach a working cell density and Phase 2, the experimental part, with the mechanical feeding phase.

Phase 1 with fed-batch condition: The complete 250 mL EnBase shake flask culture was transferred to the bioreactor (15 L Biostat E, Sartorius SA, Göttingen, Germany) filled with 9.75 L EnBase medium. This medium contained additionally 20 g L^{-1} dextrin (Krause *et al.*, 2010). After addition of 100 U L^{-1} of α-amylase (BioSilta Ltd., Cambridge, UK) for initiating a constant rate of glucose release of about 1 g L^{-1} h^{-1} the culture was grown for 15 h at 37 °C. The aeration was set to 0.5 vvm and the DOT was controlled by stirrer regulation for at least 30% and the pH 7 by addition of 25% ammonium hydroxide. The cells grew exponentially until the released glucose became limiting. The cells were in fed-batch mode for about 3 hours before the mechanical feeding started. The overall cultivation time for the biomass gaining phase was about 14 h.

Phase 1 with batch condition: 250 mL of cell grown in EnBase medium with dextrin instead of glucose were transferred to the bioreactor with 9.75 L EnBase medium, which contained 15 g L^{-1} glucose instead of the glucose polymer. The DOT increase at the end of the batch phase (after acetate consumption) was the signal to start the mechanical feeding applied at the entrance of the PFR.

Phase 2: After connection of the PFR, the exponential feed (e = 0.2) was applied with a predetermined feed rate of 0.6 g glucose g^{-1} DCW h^{-1} and a glucose solution of 400 g L^{-1}. The feed solution contained EnBase medium to avoid dilution of the fermentation broth. The exponential feed phase was continued for up to 8 h. When OD_{600} = 20 was reached, 1.8486 g L^{-1} MgSO4 was added additionally to the fermentation broth and repeated each increase by OD_{600} = 20.

2.4 Online Measurement

The online sensors at the STR comprise pt-100 temperature sensor, a pH sensor (65/90VT) and a DOT sensor (both Mettler-Toledo Deutschland GmbH, Gießen, Germany). In the PFR the DOT sensor (Visiferm DO ARC 120; Hamilton Inc., Bonaduz, Switzerland) and the pH sensor (Polilyte Plus ARC 120; Hamilton Inc., Bonaduz, Switzerland) were placed on the height of each sample port. The pH sensors were calibrated with commercial pH 7 and pH 4 buffers. The DOT sensor in the STR was calibrated to 0% during sterilization and to 100% shortly before inoculation. The DOT sensors of the PFR were calibrated against air and with nitrogen sparged water.

Exhaust gas was analyzed with an O_2 and CO_2 sensor (Bluesense Gassensor GmbH, Herten, Germany).

2.5 Sampling, sample preparation and analysis of metabolites

2.5.1 Sampling

Samples were taken from a port at the bottom of the STR and five ports along the PFR. For maximal reduced contamination, needles and adapters of the Monovette® system (Sarstedt AG, Nümbrecht, Germany) were used. The supernatant was prepared directly at sampling by using a hydrophilic nitrocellulose filter (Millipore Inc., Schwalbach, Germany).

2.5.2 Cell growth

The cell growth was monitored by OD_{600} measurements (Novaspec III by Amersham Biosciences, UK). For dried cell weight determination 2 mL suspension were pipetted into a dried and weighted 2 mL tube. The cells were centrifuged for 5 min at 21,500 x g. The supernatant was discarded and the cells were washed with 1 mL 0.9% NaCl solution. After a repeated step of centrifugation and supernatant discard the tube with its content was dried at 75 °C. The tube was weighted again and with the difference in weight the CDW was calculated.

2.5.3 Sample Preparation and Analysis of Metabolites

High Performance Liquid Chromatography (HPLC) was performed using Agilent 1200 Series HPLC System (Agilent Technologies, Waldbronn, Germany)

2.5.3.1 Short chain fatty acids: For sampling of the extracellular short chain fatty acids the cultivation broth was filtered directly when taking the sample. The supernatant was transferred to 1.5 mL tubes and immediately stored in -80 °C freezer. To determine the concentration of short chain fatty acids of the whole suspension the samples were treated like described by Hardiman for nucleotide quenching (Hardiman, 2009). Therefore, 5 mL syringes were filled with 2 mL of

perchloric acid (70%) without the presence of air bubbles. The syringes were stored at -80°C. For sampling, the cultivation broth was transferred directly at the port with the Monovette® system into the syringe until it reached a volume of 5 mL. The samples were immediately shaken on ice for 15 min with a turnaround after 5 min. Afterwards, the samples were transferred into prechilled 50 mL Falcon tubes and 845 µL of a prechilled, 5M K_2CO_3 was added carefully due to foam formation. After short mixing by hand, the tubes were centrifuged at -2 °C for 10 min at 5,200 rpm. After centrifugation, 2 mL of supernatant were transferred into prechilled Eppendorf tubes and stored at -80°C in a steel block. **Quantitative analysis with High Performance Liquid:** HPLC analysis was performed like described by Glazyrina *et al.* (2010). The samples were thawed on ice and centrifuged once more (4 °C, 15,000 x g, 10 min). The supernatant was transferred into HPLC vials (Fisherbrand™) with 200 µL inlets, while the gas phase above the liquid was kept as small as possible to avoid evaporation. The vials were closed with caps (Thermo Fisher Scientific GmbH, Schwerte, Germany) with 8 mm silicone septums (VWR GmbH, Germany). HPLC analysis was performed with HyperRez XP Carbohydrate H^+ column, 300 × 7.7 mm, particle size 8 µm (Thermo Fisher Scientific, GmbH, Schwerte, Germany) in combination with a refractive index detector. As eluents HPLC grade water (purified with an RF ultrapure water system, Wilhelm Werner GmbH, Leverkusen, Germany) and 5 mM H_2SO_4. The injection volume was 20 µL, the isocratic pump rate set to 0.5 mL min^{-1} at 15 °C and the draw and injections speed of the injection needle to 200 µL min^{-1}.

2.5.3.2 Amino acids: The same supernatant taken for short chain fatty acid sampling was also used to analyze the free amino acids with HPLC. Therefore, it was thawed on ice and centrifuged (4 °C, 15,000 x g, 10 min). 250 µL of the sample were pipetted into the HPLC vial and mixed with 250 of a 225 µM α-aminobutyric acid solution as internal standard. To determine the amino acid concentration of the whole suspension, 5 mL syringes were filled with 2 mL methanol. Air bubbles inside

the syringe were eliminated and the syringe closed with a Monovette® adapter before storage at -80 °C. Samples were quenched directly by adding 3 mL of suspension with the syringe system. For HPLC analysis, the quenched suspension was thawed on ice, diluted with prechilled 0.9% NaCl to OD_{600} = 1 and 0.5 mL were homogenized with ultrasound. The homogenization was performed on ice with a special ultrasound device (UP200, Dr. Hielscher GmbH, Teltow, Germany) on ice 5 times for 30 sec (30 sec off) with an amplitude of 50% and with a sonotrode of 1 mm diameter. Afterwards, the samples were centrifuged (4 °C, 15,000 x g, 10 min) and 100 µL of the supernatant transferred to an Eppendorf tube with 100 µL internal standard. After mixing by pipetting the sample was transferred to HPLC vials with inlets. **HPLC**: The analysis with HPLC was performed like described by Krömer (2006). A GEMINI® column (5 µm, 100 Å, 150 x 4.6 mm) with a Security Guard pre-column (GEMINI C18) was used (both by Phenomenex, Aschaffenburg, Germany) in combination with a fluorescence detector. The injection volume was 10 µL, the draw speed set to 200 µL min^{-1}, the injection speed to 600 µL min^{-1} and the column heated to 40 °C. As solvent buffer A (40 mM NaH_2PO_4) and buffer B (45% acetonitrile, 45% methanol and 10% H_2O) were used with a flow rate of 1 mL min^{-1} at a procedure described in table 2.1

Table 2.1: HPLC gradient operation for amino acid analysis

Time (min)	Buffer A (%)	Buffer B (%)
0	100	0
40.5	59.5	40.5
41	39	61
44	18	82
44.5	0	100
61	100	0

The amino acids measured and evaluated were all canonical amino acids except arginine, proline and tyrosine. Additionally, norvaline was measured.

2.5.3.3 Glucose and dextrin: The supernatant taken like described was thawed on ice. Of a 10% KOH solution12 µL were pipetted in prepared Eppendorf tubes on ice. 188 µL of sample were added and mixed to inactivate the amylase. After centrifugation, the supernatant was transferred into HPLC vials with inlets. **HPLC**: A HiPlex-Ca column from Agilent was used in combination with a refractive index detector. The solvent was ultrapure water. The injection volume was 20 µL, the draw speed and the injection speed set to 200 µL min^{-1}. The maximal pressure was set to 60 bar. A flow program according to table 2.2 was applied.

Table 2.3: Flow profile for HPLC-analysis of glucose and dextrin

Time (min)	Flow (mL min^{-1})
0	0.25
30	0.25
32	0.5
55	0.5
55.5	1
59.5	1
601	0.25

2.6 Sampling, sample analysis and data processing for proteome data

2.6.1 Sampling

Samples for proteome analysis were taken from a STR and a TCR cultivation for comparison. For each cultivation the samples were taken from the STR shortly before mechanical feed start and 1 h, 2 h, 4 h and 6 h after mechanical feed start. Therefore, 1 mL of suspension was transferred into an Eppendorf tube, centrifuged (4 °C, maximal speed, 1 min) and washed once with ice-cold phosphate buffered saline (PBS-buffer). After a second centrifugation as much as possible of the supernatant was discarded without affecting the pellet, and the samples were frozen in liquid nitrogen and stored at -80 °C before further processing.

2.6.2 Sample preparation

The samples were sent to Karl Peebo (group of Prof. Raivo Vilu, Center of Food and Fermentation Technology, Tallinn, Estonia) on dried ice before further processing. All further preparation and analysis was performed at the Center of Food and Fermentation Technology, Tallinn.

An important part of the sample preparation is the mixing of sample biomass 1:1 with special SILAC-labeled E. coli biomass according to Ong *et al.* (2002). The labeled biomass acts as reference for quantitative analysis and aliquots with 100 µg were kindly provided by Karl Peebo.

In the first step, the samples were diluted in ice-cold TE-buffer (1M Tris HCl, pH 7.65) in a way to be able to pipette 100 µg of biomass to the SILAC-labeled biomass aliquots. Finally, the sample and the SILAC labeled biomass were mixed, centrifuged (14,000 x g, 1 min, 4 °C), the supernatant discarded and frozen at -80 °C.

For proteome analysis the samples were sent in to Proteomics Core Facility at University of Tartu.

2.6.3 Sample analysis and data evaluation

The sample analysis was performed like described by Peebo *et al.* (2014). The raw data was further analyzed with MaxQuant software. Three technical replicates were run. The standard deviation was calculated to be maximal 6%. The received data displayed the ratio of heavy to light proteins for each protein. The ratio of samples after the mechanical feed start to the sample before mechanical feed start was calculated by assuming the heavy proteins to be constant. The changes in ratio were further clustered by Dipl-Ing. Schmidt-Heck (AG Systembiologie / Bioinformatik, Leibniz-Institut für Naturstoff-Forschung und Infektionsbiologie - Hans-Knöll-Institut, Jena) with the Fuzzy-C-means clustering method (Bezdek and Hathaway, 1992). For clustering all proteins were considered, which showed in at least one cultivation a change of more than 1.5-fold of concentration.

2.7 Sampling, sample analysis and data processing for transcriptome data

2.7.1 Sampling

The same samples taken for proteome analysis were also taken for transcriptome analysis. Additionally, samples were also taken 3 h, 5 h, 7 h and 8 h after mechanical feed start, so that samples every hour were taken. At 1 h, 2 h, 4 h, 6 h and 8 h samples were also taken along the PFR. Therefore, 1 mL cultivation broth was mixed immediately after sampling with 1 mL RNAlater (Qiagen), incubated for 5 min at room temperature and centrifuged for 10 min at 8,000 rpm. The supernatant was discarded and the pellet stored at -80 °C.

2.7.2 Sample preparation

The samples were sent to Karl Peebo (group of Prof. Raivo Vilu, Center of Food and Fermentation Technology, Tallinn, Estonia) on dried ice before further processing. All further preparation and analysis was performed at the Center of Food and Fermentation Technology, Tallinn.

Before transcriptome analysis can be performed, the mRNA of the samples has to be extracted and the quality checked with an SDS-gel. Afterwards, the mRNA has to be transcribed to cDNA and the original mRNA hydrolyzed. After purification of cDNA and its concentration measurement a quantitative DNA analysis with gene specific primers by real-time PCR can be performed eventually.

Extraction of mRNA: The samples were diluted in an appropriate amount of PBS-buffer to transfer 0.5 mg to an Eppendorf tube. After centrifugation (14,000 x g, 1 min, 4 °C) and discarding the supernatant the total RNA was extracted with RNeasy Mini Kit (Qiagen, Hilden, Germany) according to the manual. Only for cell lysis, a lysozyme solution (2 mg mL^{-1}) was used.

cDNA synthesis: cDNA was synthesized with Superscript III enzyme kit (Invitrogen) from 15 µg of total RNA at 46°C overnight. The following reagents per reaction were used: 1 µg $µl^{-1}$ of Random Decamers (Invitrogen, Carlsbad, CA), 6 µl 5x first-strand buffer (Invitrogen), 3 µl 0.1 M DTT (Invitrogen), 0.9 µl dNTPs (Invitrogen, final concentrations: dATP, dCTP, dGTP 0.5 mM and dTTP 0.3 mM, aminoalyl-dUTP 0.2 mM), 1 µl Rnase Inhibitor (Bioron, Ludwigshafen, Germany), 2 µl Superscript III (Invitrogen).

RNA hydrolysis: RNA strands were hydrolyzed by adding 3 µl 0.2 M EDTA pH 8.0 and 4.5 µl 1 M NaOH. After 15 min 70°C incubation, the samples were neutralized with 4.5 µl 1 M HCl. The produced cDNA was purified with GeneJET^{TM} PCR Purification Kit (Fermentas) according to its manual

2.7.3 Sample analysis and data evaluation

Real-time PCR: Real-time PCR reactions were carried out using a Roche LightCycler 2.0 (Basel, Switzerland) and 5x HOT FIREPol EvaGreen qPCR Mix Plus (no ROX) (Solis BioDyne, Tartu, Estonia). PCR reactions were carried out in 10 µl reactions with 20 ng cDNA. The primers had a concentration of 200 nm and are listed in table 2.2. They were kindly provided by Karl Peebo (group of Prof. Raivo Vilu, Center of Food and Fermentation Technology, Tallinn, Estonia). Each sample was run in triplicates.

Table 2.2: Primer sequences for real-time quantitative PCR

Gene	Left Primer	Right Primer
aceA	CCTGTTCTGGTGTGAAACCT	CCACATGCTGTGGATACC
aceE	CGATCGAATCGGTCATCC	AGCTGAACGAATACGGCG
ackA	AAGTGACCAGCGACTGCC	CCGATGTATTTCGCCAGG
acs	CGGGCGCATTATTGATTC	CCGCCAGTACGCTTCAGT
frdA	TCTCAGGCCTTCTGGCAC	CGTACGCTTTCGCCAGTT
fumA	CCTTGGCAGTATCGGTGG	GCCGGGAAATCTTCCACT
fumB	TGCGCAAATCGACCTGTA	AGGGCTTTGGTTTCCTGG
gltB	CGCATGTTATGTCGCTCG	GCGTATCTGCGCGGTAGT
ilvB	AAAATCAAGCAGCCGCAC	ACGCTGCAAATCCGCTAC
ilvI	CAGGCGGTGATCGAGACT	CACCGGAATTGATCCAGC
leuA	GCGCACCAGCCAGTTAGT	TTTTCGCGGTTTTTCAGC
mdh	CGCCCGTTTCTTCTCTCA	GCCCAGGGGCGATATCTTT
pflB	AAGAAATGGCTGCGAAATAC	GCTTCTTGTTCGGTGATCTT
pflD	AGTGGGCTGTGTGGAATTAT	AGGGTGATGTAGTGGCTGAT
poxB	CGCCTATTGTTCATGCCC	AATTGCGTGCCGAGTAGC
sucA	CCAGCCATCGGTGAAATC	TATGCGGGAACGGGTAGA
sucC	TTTATGGCCTCCACCGAA	GTCCCTGATACGGCATCG

After qPCR reaction, the same threshold value at approximately half height of the light intensity curve was applied to all runs. The average and standard deviation of each triplicate was calculated. With this it was possible to determine the cycles the qPCR of each sample took to reach the same intensity. As reference, the samples before mechanical feed start were taken and the samples of the same cultivation were set in relation to it with the formula Ratio (sample/reference) = 2^(copy number sample / copy number reference). With this, the change of transcriptome concentration during cultivation was calculated.

3. Results

3.1 Establishment of scale-down cultivations

The experimental part of this dissertation started with the establishment of scale-down cultivations with an EnBase mediated phase 1 cultivation before experimental phase 2 cultivation with mechanical feed.

3.1.1 Phase 1 cultivation – biomass gaining phase

The aim of the experimental setup for phase 1 cultivation was to create reproducible metabolic conditions for the experimental part of the cultivation. Therefore, an EnBase cultivation was performed, where a soluble glucose polymer, dextrin, was degraded with a constant glucose release rate. 9.75 L cultivation volume was inoculated with 250 mL preculture with the same medium composition but initial 2 g L^{-1} glucose. The DOT was measured online and increased by increasing stirrer speed when it dropped below 30%. The pH was measured online and kept at 7 with ammonia.

Figure 3.1.1 shows the cultivation parameters for phase 1 cultivation. The DCW increased to 5.6 g L^{-1} after 14 h of cultivation. The growth rate of fitted DCW values shows a constant value of 0.55 h^{-1} until 10.3 h of cultivation, afterwards it dropped to 0.04 h^{-1} at 14 h of cultivation. The DOT kept at 100% until 5h and dropped continuously until 9 h. When the DOT dropped below 30%, it further went down to 20% due to a delay before the stirrer speed regulation led to increased DOT. The stirrer speed regulation was active 1.5 h until 10.5 h. At the time the glucose became limiting, the DOT increased to 70% at 11 h and further increased to 80% at 13 h of cultivation. In 14 h the dextrin concentration decreased from 20 g L^{-1} to 11 g L^{-1}, resulting in an average glucose release of 0.64 g L^{-1} h^{-1}. Until approx. 7 h of cultivation the glucose release was higher than the glucose consumption by the cells, so the glucose concentration increased to 4.2 g L^{-1}. Afterwards, it dropped to 0.16 at 11h. The acetate concentration increased continuously until 9h to 1.6 mM with the strongest increase between 5h and 9 h. Afterwards, it dropped like glucose

until 11 h to 0.2 mM. The specific oxygen uptake rate (OUR) shows strong oscillations until approx. 6.5 h due to oscillations in the measured values which were intensified by the low biomass concentration. When the glucose concentration dropped, also the specific OUR dropped from around 18 g g^{-1} h^{-1} to 1.8 g g^{-1} h^{-1} at 10.5 h of cultivation time. At the end of cultivation, the value for the specific OUR was 0.7 g g^{-1} h^{-1}. The specific carbon dioxide production rate (CPR) was around 13.3 g g^{-1} h^{-1} at 5 h of cultivation and slightly increased to 14 g g^{-1} h^{-1} at the same time the glucose release rate became less than the glucose consumption rate (at 7 h). Finally, it dropped at the same time like the oxygen uptake rate to 1.6 g g^{-1} h^{-1} and decreased to 0.55 g g^{-1} h^{-1} towards the end of phase 1 cultivation. The respiratory quotient stayed around 0.8 with the exception at the time of rapid decrease of qO^2 and qCO^2 around 10.5 h. This peak is very likely produced by a delay of the oxygen sensor compared to the carbon dioxide sensor in combination with the rapid decrease.

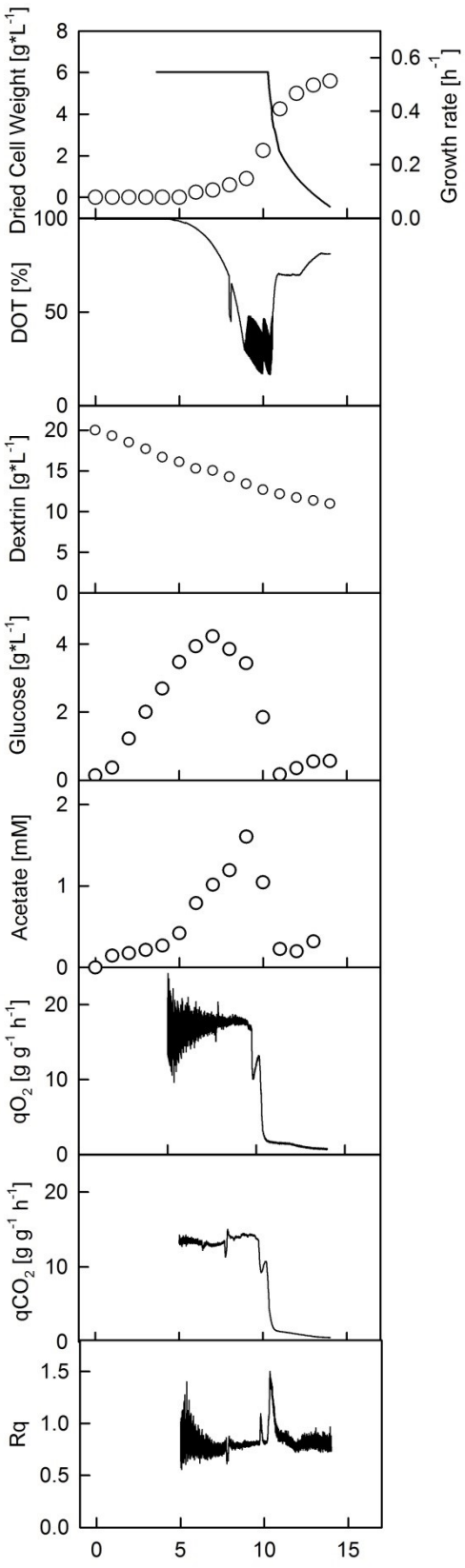

Figure 3.1.1: General parameters of phase 1 cultivation with Enbase internal fed-batch.

E. coli was cultivated in EnBase medium with 20 g L^{-1} initial dextrin concentration. The DOT was set to minimum 30% and controlled by stirrer speed. Samples were taken every hour and exhaust gas was measured online. Due to the low dried cell weight in the beginning the shown exhaust data start at 5 h. DOT: dissolved oxygen tension. qO_2: specific oxygen uptake rate. qCO_2: specific carbon dioxide production rate. Rq: Respiratory quotient of qCO_2 to qO_2.

Additional to the general cultivation parameters mentioned above, also the extracellular concentration of key organic acids were measured (figure 3.1.2). These are acetate, lactate, formate, succinate, fumarate and malate. Acetate was already shown in the former figure and serves as reference regarding the cultivation time.

The concentration of lactate increases with a delay of around 1 h compared to acetate up to 0.19 mM at 10 h cultivation time, when the acetate concentration dropped again. The lactate concentration also dropped to 0.05 mM at 11 h and stayed at 0.9 mM until 14 h. The concentration of formate started to increase at 9 h, which is the time of highest acetate concentration and start of decreasing glucose concentration. It finally increases to 0.9 mM until 14 h of cultivation. For succinate a background was measured from the beginning of the cultivation. Its concentration increased continuously from 0.074 to 0.09 mM. Fumarate shows a sudden peak at 9h with 0.09 mM which drops to 0.05 mM again, while malate concentration increases at 8 h to 0.08 mM. One of the following datapoints might be an outlier, but which one is not determinable.

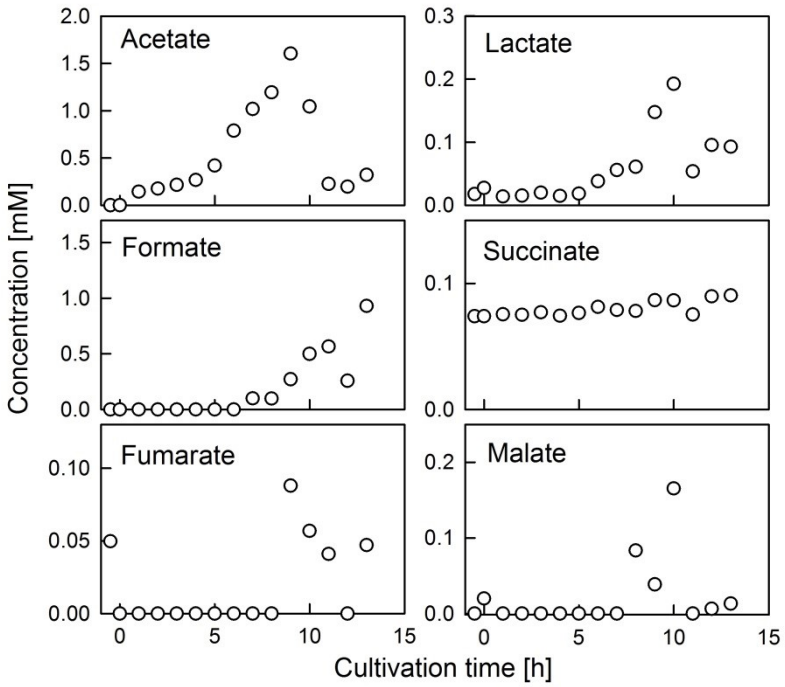

Figure 3.1.2: Extracellular accumulation of key volatile fatty acids of the central carbon metabolism during phase 1 cultivation.

For further characterization of the phase 1 cultivation, also the extracellular amino acid concentrations were measured (figure 3.1.3). The concentrations of glycolysis

deriving serine, glycine and alanine, and TCA deriving aspartate, glutamate and glutamine started to increase at 7 h of cultivation. This is the time of the highest glucose concentration and when formate also starts to accumulate. After around 3 h the accumulation decreases. This is the same time when glucose becomes limiting and the concentration of acetate and lactate drops. The concentration of extracellular serine stayed afterwards around 0.002 mM and of glycine around 0.007 mM. Also the concentration of extracellular alanine and aspartate stayed around 0.0035 mM and 0.007 mM until the end of cultivation, respectively. While the concentration of leucine increased 5 h after those of the amino acids mentioned before, no increase of isoleucine was observed. The concentration of glutamate and glutamine were on similar levels at around 0.04 at the end of the cultivation, though glutamine dropped from prior 0.06 at 12 h.

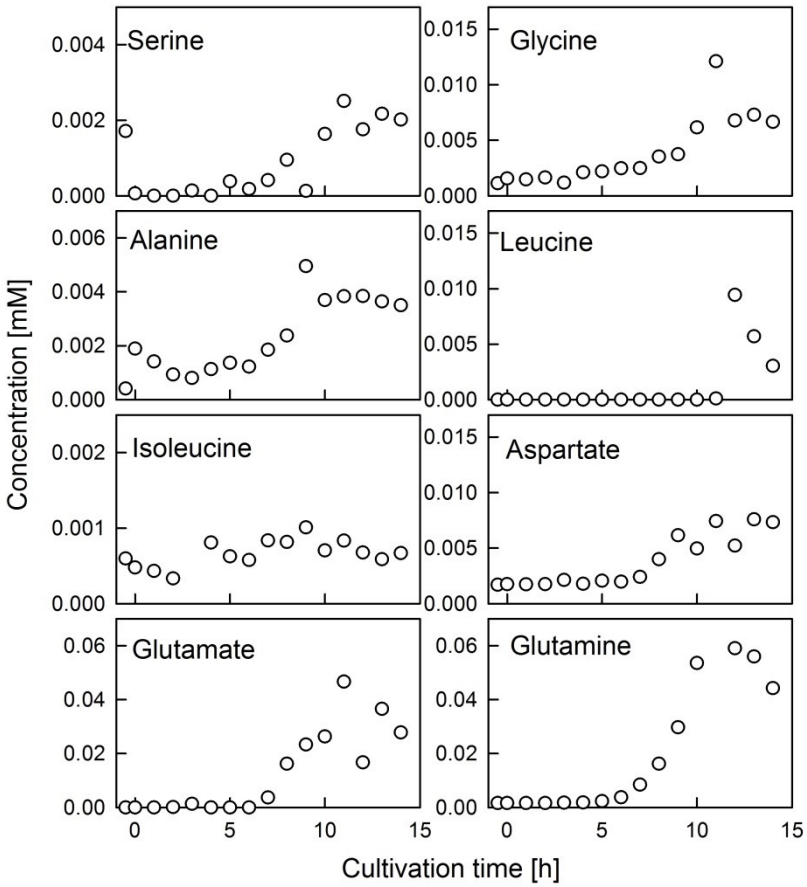

Figure 3.1.3: Extracellular concentration of amino acids deriving from glycolysis and TCA during phase 1 cultivation.

3.1.2 Phase 2 cultivation – experimental scale down fed-batch cultivation with exponentially increasing feed rate

The aim of phase 2 cultivation was to study the effect of glucose pulses on the central carbon metabolism with respect to the branched chain amino acid pathway and chain elongation towards non-canonical amino acids. Therefore, two reference fed-batch cultivations were performed, where the PFR module was not connected to the STR. Instead, the feed was applied at the top of the fermenter. A DOT above 30% and stirrer speed of at least 800 rpm guaranteed a homogeneous aerobic environment for the cells. The pH was kept at 7 by addition of ammonia throughout the complete cultivation. Two more cultivations were performed, where the PFR was connected to the STR to generate oscillating glucose conditions. Therefore, the feed was applied at the entrance of the PFR and the cells experienced repeatedly glucose pulses at anaerobic conditions. The feed rate was adapted to the OD_{600} measured before mechanical fed-batch and increased exponentially by $F(t) = 0.008 \times V_L \times e^{0.2 \times t}$ [L h^{-1}]. In the following section, general cultivation parameters and metabolome are compared of two scale-down cultivations and two reference cultivations.

All red data shown in this section are data from STR cultivation, with dots for STR1 and triangles for STR2, respectively. The same counts for the blue data from TCR cultivations, where dots represent TCR1 cultivation and triangles TCR2 cultivation. Due to a faulty dextrin charge the glucose concentration in TCR2 was not determinable. The exhaust gas data for STR1 start around 3 h after mechanical feed start.

After phase 1 cultivation, the CDW measured for each cultivation shown in figure 3.1.4 was between 4 and 5 g L^{-1}. Though the measured CDW for TCR1 was 3.25 g L^{-1}, it is supposed to be an outlier regarding the measured OD (data not shown). The biomass concentration after 6.5 h mechanical fed-batch cultivation was between 20 g L^{-1} for STR2 and 27 g L^{-1} for TCR2. Hence, no reduced biomass yield was observed for TCR cultivation. The specific growth rate was around 0.36 h^{-1} at the beginning for all cultivations except TCR1 (0.46 h^{-1}) and decreased to 0.27 h^{-1} for all cultivations after 2 h. After 6 h of cultivation the specific growth rate ranged from

0.16 h^{-1} for TCR1 to 0.2 h^{-1} for TCR2. The DOT was kept at minimum 30% for all cultivation in the STR and regulated by increase of the stirrer speed and/or increase of the aeration rate. The data to calculate the specific feed rate right after feed start was available for STR1 and TCR1 with 0.78 g $gCDW^{-1}$ h^{-1} and 0.7 g $gCDW^{-1}$ h^{-1}, respectively. After 2 h the specific feed rate dropped to 0.51 g $gCDW^{-1}$ h^{-1} for STR1 to 0.55 g $gCDW^{-1}$ h^{-1} for TCR2. At 6 h of cultivation time the specific feed rate ranged from 0.43 g $gCDW^{-1}$ h^{-1} for STR2 to 0.5 g $gCDW^{-1}$ h^{-1} for STR1. The glucose concentration was 10 times higher in the STR cultivation compared to TCR1 at the beginning of mechanical feed start and 5 times higher after 6 h. The specific OUR at the beginning of mechanical feed start range from 5.3 g g^{-1} h^{-1} for STR2 and TCR2 to 6.5 g g^{-1} h^{-1} for TCR1. A peak arises for TCR2 at 0.5 h of cultivation, and for TCR1 at 0.4 h of cultivation. For the specific CPR the values at the beginning of mechanical feed start range from 3.2 g g^{-1} h^{-1} for TCR2 to 4.4 g g^{-1} h^{-1} for TCR1. Also here a peak can be observed for both TCR cultivations at the same time as for the specific OUR. After two to three hours of oscillating glucose conditions the specific OUR and CPR of both TCR cultivations dropped to a continuous value until the end of cultivation. Generally, the specific OUR and CPR were similar for STR cultivations and TCR cultivations. The respiratory quotient stayed between 0.85 and 0.95 (TCR1) from 1 h until the end of phase 2 cultivation.

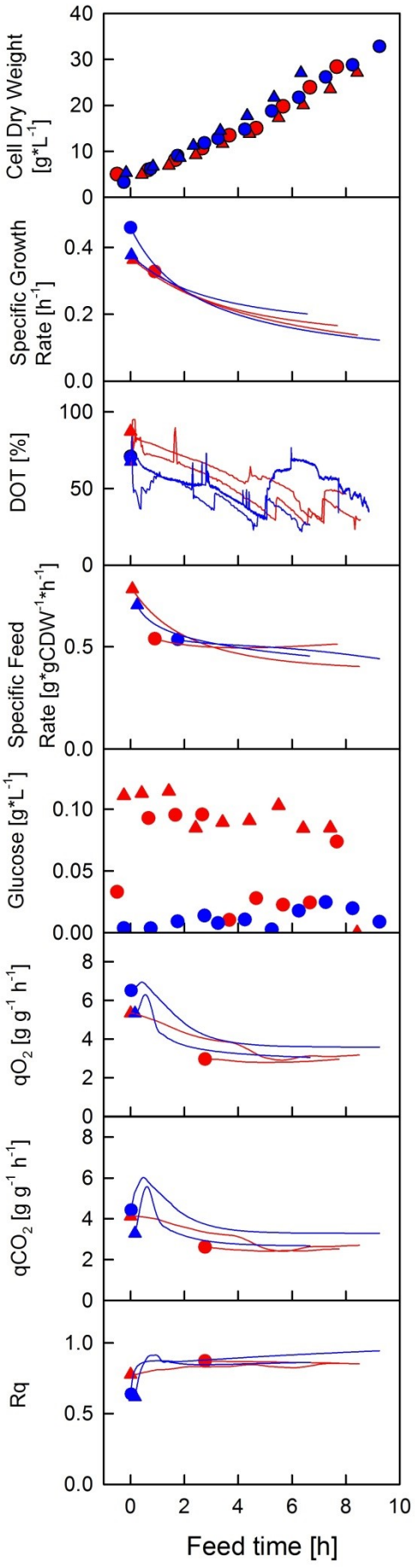

Figure 3.1.4: General parameters of phase 2 cultivations with mechanical fed-batch in TCR and STR as reference. Blue data were generated from TCR cultivations and red date from STR cultivations. Dots and triangles represent one cultivation each, of each setup two cultivations are shown. DOT: dissolved oxygen tension. qO_2: specific oxygen uptake rate. qCO_2: specific carbon dioxide production rate. Rq: quotient of qCO_2 to qO_2.

Like for phase 1 cultivation, the same key compounds of the central carbon metabolism were measured for all phase 2 cultivations. Generally, the accumulation of all compounds is higher for TCR cultivation than for STR cultivation. For acetate, an accumulation could be observed only for TCR1 of up to 0.28 mM. Lactate accumulation was observed for all cultivations with around 0.1 mM at 7 h of cultivation for STR and up to 0.4 mM for TCR cultivations. After an initial increase of formate concentration in the STR cultivations it stayed at maximal 0.7 mM until the end of mechanical feeding. For the TCR cultivations the formate concentration increased continuously up to 2 mM until the end of cultivation. A similar tendency can be observed for succinate, though its concentration doubles during STR cultivation from initial 0.08 mM to 0.16 mM. The increase is four times for TCR1 cultivation. The concentration of fumarate even decreases during mechanical feeding for STR cultivations from around 0.05 mM to 0.04 mM, while it increases up to 0.15 mM for TRC1 cultivation. Malate accumulated in the STR1 cultivation only at the end, while no malate was detected for STR2. A strong accumulation up to 0.28 mM was observed for TCR cultivation.

The accumulation patterns of key compounds of central carbon metabolism show a good reproducibility and all compounds showed higher concentration in the TCR cultivation than in the STR cultivations.

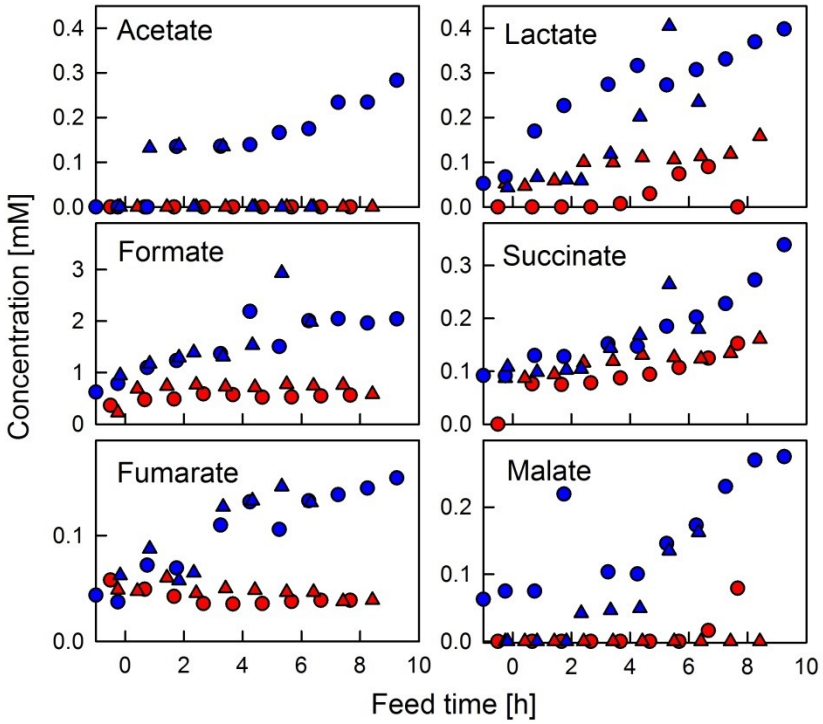

Figure 3.1.5: Extracellular accumulation pattern of central carbon metabolism key compounds of STR and TCR cultivations. Blue data were generated from TCR cultivations and red date from STR cultivations. Dots and triangles represent one cultivation each, of each setup two cultivations are shown.

During phase 1 cultivation, some amino acids deriving from glycolysis and TCA were found to show concentration dynamics for STR and TCR cultivation. While for serine a slight increasing tendency was observed for all cultivation (0.001 mM to 0.007 mM), the concentration of extracellular glycine increased stronger for TCR than for STR cultivations with up to 0.014 and 0.003, respectively. Alanine showed a similar, but stronger increase for all cultivations compared to serine. For the branched chain amino acids leucine and isoleucine a stronger increase at TCR cultivations could be observed compared to STR cultivations, though the difference is only around two-fold with maximal 0.11 mM and 0.06 mM, respectively. Also norvaline could be detected for TCR1 cultivation to a concentration up to 0.0006 mM with an accumulation starting after 6 h of mechanical feeding. The TCA deriving amino acids aspartate and glutamate show a sudden peak at 1h after mechanical feed start of 0.04 and 0.7 mM, that decreases again to the former value of 0.01 and 0.02 mM, respectively. While all the former mentioned amino acids

increase during mechanical feeding, only glutamine shows a decreasing dynamic for all cultivations, with slightly higher concentrations in the TCR cultivations than in the STR cultivations.

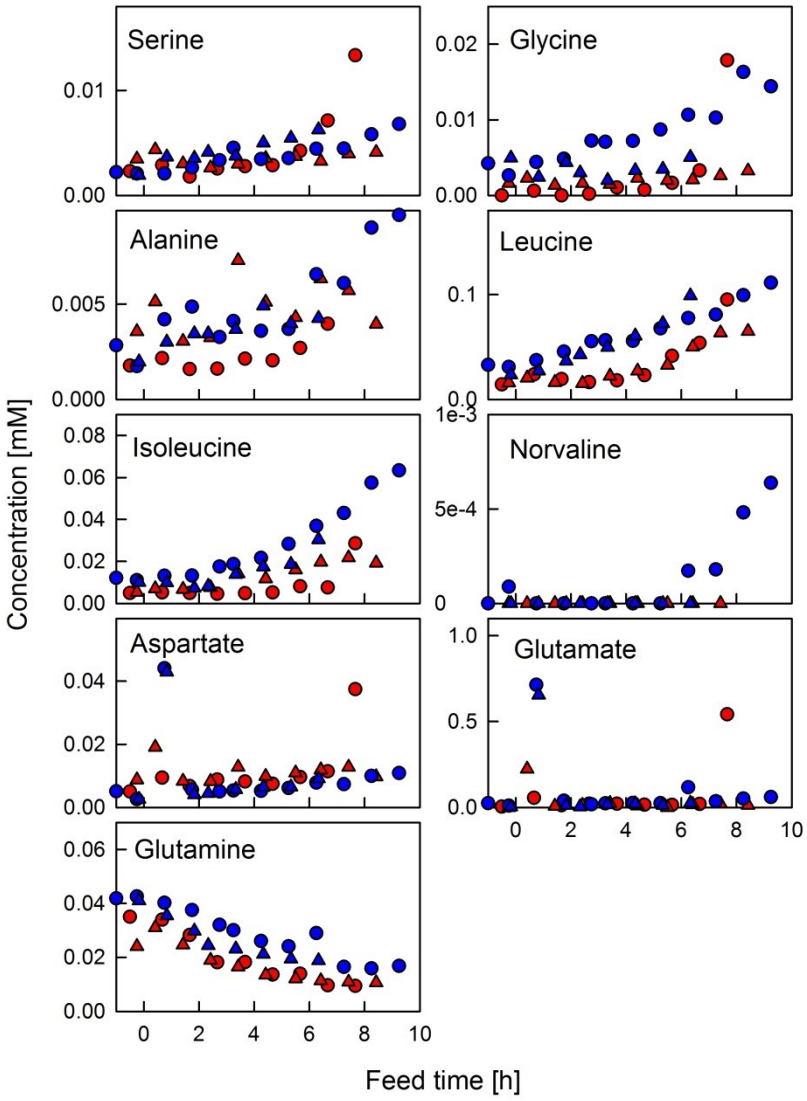

Figure 3.1.6: Extracellular accumulation pattern of glycolysis and TCA deriving amino acids of STR and TCR cultivations. Blue data were generated from TCR cultivations and red date from STR cultivations. Dots and triangles represent one cultivation, respectively. Of each setup two cultivations are shown.

For both TCR cultivations samples for extracellular key compounds of the central carbon metabolism were also taken along the PFR shown in figure 3.1.7. For better visualization, the set taken first after start of oscillating glucose conditions is depicted in yellow circles, and the last set in green diamonds. Here it is important to note, that the feed time and the according symbol differ between both cultivations, with the last sample set for TCR1 at 8.25 h and for TCR2 at 6.33 h.

For acetate an increase in extracellular concentration along the PFR was observed for both TCR cultivations with a higher tendency for TCR1. Here, after 0.75 h the acetate concentration increases from 0 mM to 0.15 mM within the first 30 s after the glucose pulse and further up to 0.21 mM after 68 s. At 8.25 h of TCR1 cultivation the acetate concentration increases from 0.23 mM in the STR to 0.42 mM within 30 s and further up to 0.56 until the last port of the PFR. Though the concentrations are lower in the TCR2 cultivation, a tendency of increasing concentration was observed along the PFR. The same increasing dynamic along the PFR war found for lactate. While 0.75 h after start of oscillating glucose conditions the concentration in TCR1 increases from 0.17 mM in the STR to 0.34 until the end of PFR, the concentration increases from 0.37 mM to 0.91 after 8.25 h of oscillating glucose conditions. Similar dynamics were observed for TCR2 cultivation. Though formate shows the highest accumulation in the STR during TCR cultivations, no accumulation pattern of extracellular formate can be observed along the PFR. For succinate, the accumulation along the PFR increases with increasing feed time. While the overall increase is from 0.13 mM to 0.14 mM at 0.75 h feed time, at 8.25 h feed time the increase is from 0.27 mM to 0.38 mM at TCR1. At the last sample set from TCR2 at 6.33 h feed time the increase was even from 0.18 mM in the STR to 0.83 mM at the last port of the PFR. For the metabolites mentioned so far the dynamics along the PFR were similar for TCR1 and TCR2. This is not the case for fumarate. In TCR1 the extracellular concentration increases for 0.04 mM to 0.1 mM from STR to the last port of the PFR, while in TCR2 the concentrations even decrease along the PFR. Another interesting observation was the decrease of malate along the PFR for both cultivations. In TCR1, the decrease was from 0.07 mM to 0.04 mM until the end of PFR at 0.75 h and from 0.27 mM to 0.15 mM at 8.25 h feed time. In TCR2, the values were slightly lower.

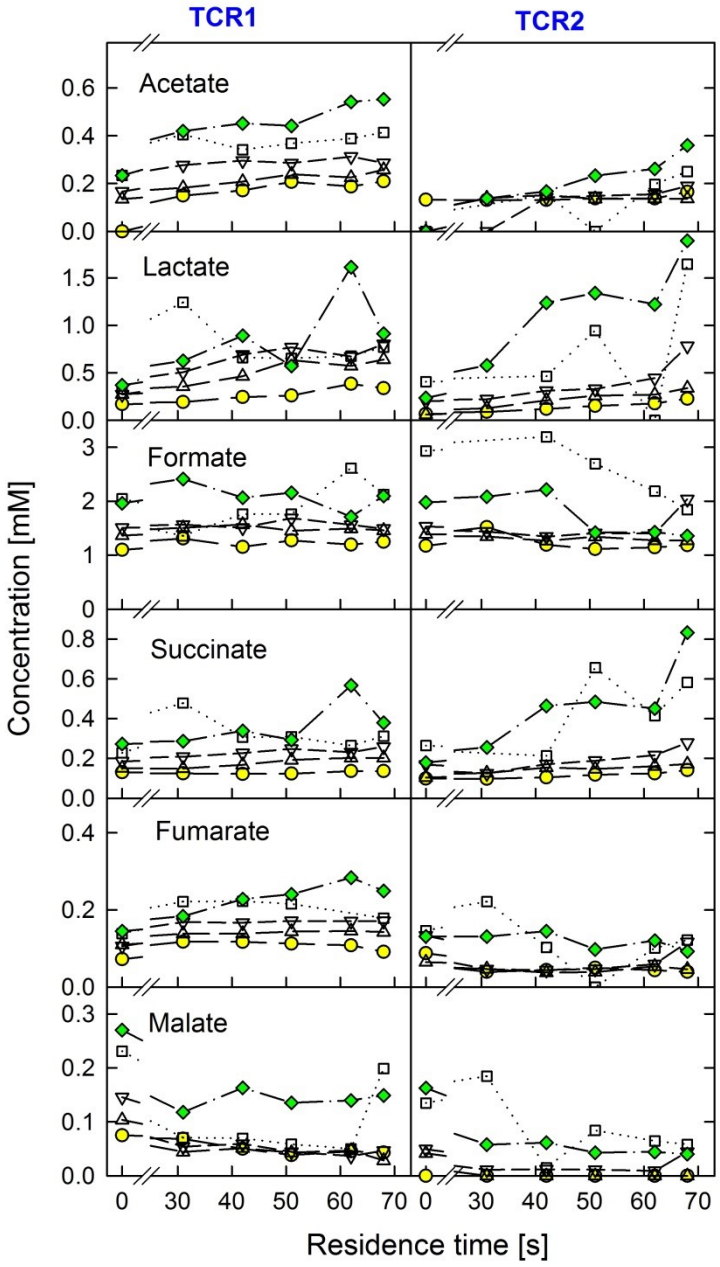

Figure 3.1.7: Extracellular accumulation pattern of central carbon metabolism key metabolites along the PFR part of two TCR cultivations. Symbols represent different feed times for each TCR cultivation: yellow circle: 0.75 h TCR1, 0.83 h TCR2; triangle up: 3.25 TCR1, 2.33 TCR2; triangle down: 5.25 h TCR1, 4.33 TCR2; square: 7.25 TCR1, 5.33 TCR2; green diamond: 8.25 h TCR1, 6.33 h TCR2.

Among all glycolysis deriving amino acids alanine is the only one showing intracellular accumulation along the PFR for both TCR cultivations. It seems the increase is not related to the feed time like for some key metabolites of the central carbon metabolism. For TCR1, the increase at 0.75 h feed time is from 0.017 mM $gDCW^{-1}$ to 0.25 mM $gDCW^{-1}$ and at 8.25 h feed time from 0.18 mM $gDCW^{-1}$ to 0.27 mM $gDCW^{-1}$. For glycine, no such tendency can be

observed. For leucine, a slight accumulation in TCR2 can be observed for the last sample set taken at the PFR at 6.33 h feed time (figure 3.1.8). Nevertheless, this accumulation was not observed for the former sample sets or the TCR1 cultivation, so the reproducibility is not given. On the other hand, an accumulation of isoleucine was observed in both TCR cultivations, though higher in TCR2 than in TCR1. Aspartate and glutamate were the amino acids which accumulated in the STR strongly within the first h of oscillating glucose conditions and decreased again to the basal value. Interestingly, this accumulation was not observed along the PFR. Glutamine is the only amino acid next to alanine showing a dynamic along the PFR reproducible for both TCR cultivations, though the concentration is decreasing instead of increasing. The decrease ranges from almost 0.01 mM $gDCW^{-1}$ to 0 mM $gDCW^{-1}$. Intracellular levels of norvaline were observed for both TCR cultivations, while no dynamics along the PFR was observed for TCR1. For TCR2, the accumulation was strongest at 0.83 h feed time with 0.00046 mM $gDCW^{-1}$ at the STR and 0.002 mM $gDCW^{-1}$ at the end of PFR, while a decrease along the PFR can be observed at 6.33 h feed time from 0.0006 mM $gDCW^{-1}$ to 0 mM $gDCW^{-1}$.

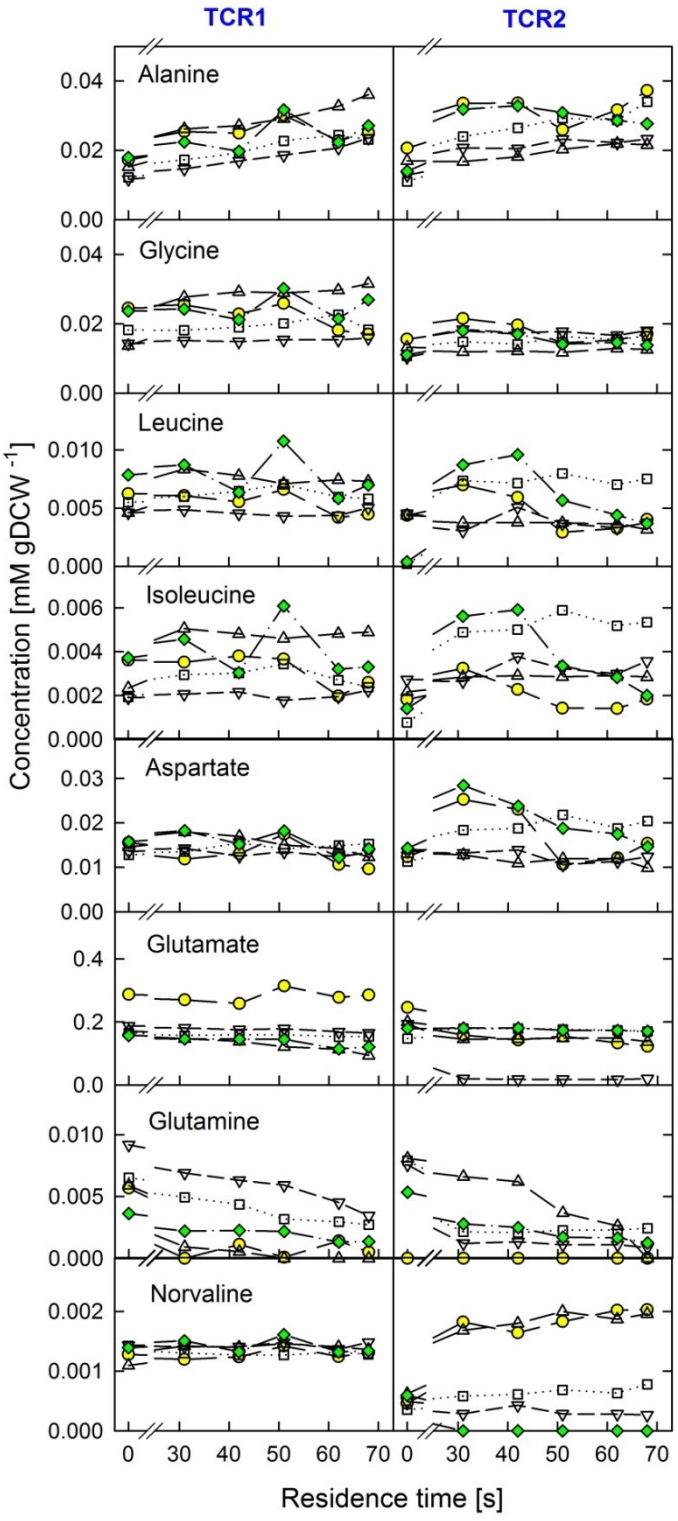

Figure 3.1.8: Intracellular accumulation pattern of central carbon metabolism deriving amino acids along the PFR part of two TCR cultivations. Symbols represent different feed times for each TCR cultivation: yellow circle: 0.75 h TCR1, 0.83 h TCR2; triangle up: 3.25 TCR1, 2.33 TCR2; triangle down: 5.25 h TCR1, 4.33 TCR2; square: 7.25 TCR1, 5.33 TCR2; green diamond: 8.25 h TCR1, 6.33 h TCR2.

3.1.3 Summary

For all cultivations aerobic conditions in the STR were realized. The phase 1 cultivation showed a typical profile of constant glucose release with a glucose accumulation in the first hours. When the cells consumed more glucose than it was released, the glucose concentration dropped and the cultivation entered fed-batch mode. The exhaust gas analysis indicates a co-utilization of glucose and acetate shortly before glucose depletion. Though organic acids and amino acids accumulated during exponential growth and transition from batch to fed-batch mode, these compounds were not re-assimilated at glucose-limited conditions.

For the experimental part, phase 2 cultivation, reproducible cultivation parameters for STR and TCR cultivations were obtained. For both TCR cultivations a peak in the exhaust gas analysis could be observed within the first 3 h of oscillating glucose conditions without influencing the respiratory quotient. Though the addition of molybdenum, selenium and nickel was supposed to prevent the accumulation of formate, its concentration increased especially in TCR cultivations with beginning of mechanical feeding. The analysis of organic acid concentrations along the PFR showed the accumulation of acetate and lactate at anaerobic, glucose-excess conditions. Nevertheless, the re-assimilation in the STR was lower than the accumulation along the PFR, so the overall concentrations increased along the cultivation. Regarding the concentrations of amino acids deriving from central carbon metabolism a higher increase for branched chain amino acids leucine and isoleucine could be observed in TCR cultivations. In TCR2, even the non-canonical amino acid norvaline accumulated extracellular. Glutamate and aspartate concentrations increased drastically 1 h after mechanical feed start in TCR cultivations, but dropped to the former level 1 h later. Glutamine is the only amino acid with decreasing concentrations during mechanical feeding. Along the PFR, only alanine and glutamine show dynamics. While the concentration of alanine (pyruvate-derived) increases, the concentration of glutamine decreases. From these results two observations are of special interest:

1. The mode of phase 1 cultivation seems to influence the reaction of E. coli towards oscillating glucose conditions regarding its central carbon metabolism.

2. Norvaline accumulated in a wild-type E. coli.

Since the synthesis of norvaline is supposed to be related to increased pyruvate levels, in the next step the influence of phase 1 cultivation mode on the reaction of the central carbon metabolism to oscillating glucose conditions was investigated. Therefore, a TCR cultivation was performed with a phase 1 batch cultivation.

3.2 Influence of batch or fed-batch phase 1 cultivation on metabolic reaction to oscillating glucose conditions

This result section was written together with Prof. Dr. Peter Neubauer.

The aim of this study was to investigate on the level of the central carbon metabolism, whether the cellular adaptation in a fed-batch process with oscillatory perturbations is dependent on how the first phase of bioprocess is performed, as batch or under glucose limited conditions, respectively. Therefore, two kinds of cultivations were performed when the first phase was either a batch (*Batch-FB*) as a control, or a fed-batch type of cultivation (*EnBase-FB*), respectively. In both cases the second phase was a fed-batch with continuous exponential feeding of a concentrated glucose solution. During this fed-batch phase a PFR was connected with the glucose feed inlet at the entrace of the PFR, to create a scale-down bioreactor with regular oscillating perturbations for the glucose.

3.2.1 Growth and glucose utilization.

In the batch phase of the *Batch-FB* control cultivation *E. coli* W3110 reached a maximum specific growth rate μ_{max} of 0.686h^{-1} with a specific maximum glucose uptake rate of q_{Smax} = 0.764 g $g^{-1}h^{-1}$ (see Fig. 1). Then, after exhaustion of the initial glucose, the feed was started with a μ_{set} of 0.20 h^{-1}. The final biomass at four hours after the feedstart was approx. 15 g L^{-1}. In contrast the first phase was much longer, approx. 15 hours, when the cultivation was performed as a glucose limited Enbase culture (*EnBase-FB)*. As this culture was started with a biocatalyst concentration

which provided a constant release rate of glucose, initially the glucose release rate was higher than the volumetric glucose consumtion rate and thus, glucose accumulated to approx. 4 g L^{-1}. Later, due to the exponential growth of the cells the volumetric glucose consumption rate increased and finally the glucose concentration decreased. Glucose limitation was obtained approx. 5 h before the feeding as started (Fig. 1B), and during this period also acetate and most of the lactate were consumed (Fig. 2A,B). μ_{max} in this case was lower compared to the *Batch-FB* control cultuvation (approx. 0.55 h^{-1}), possibly related to the lower glucose concentration. Although the initial glucose feed rate was slightly higher for the *EnBase-FB* cultures, after the feed start μ was finally the same in both cultures (μ = 0.27 h^{-1}), although there was an initial delay of biomass increase in the *EnBase-FB* cultures, and also the final biomass concentration was lower (12.75 vs. 14.75 g L^{-1} in the *Batch-FB*). This is interisting, as the specific glucose uptake rate after the feed start was different in the two culture sets. q_S was lower (0.35 g $g^{-1}h^{-1}$) in the control *Batch-FB* cultures compared to the *EnBase-FB* cultures (q_S = 0.55 g $g^{-1}h^{-1}$) (Fig. 1 D). Also the affinity for glucose was very different in the two modes of cultivation. The final glucose concentration in the stirred tank reactor was 0.28 g L^{-1} in the *Batch-FB* cultivation, but only <0.01 g L^{-1} in the *EnBase-FB* culture. The different concentration, i.e. affinity for glucose, was not related to a higher glucose uptake capacity (q_{Scap}), but q_{Scap} was the same in both culture types. This is obvious from the profiles of the glucose concentration in the PFR during different times of the cultivation.

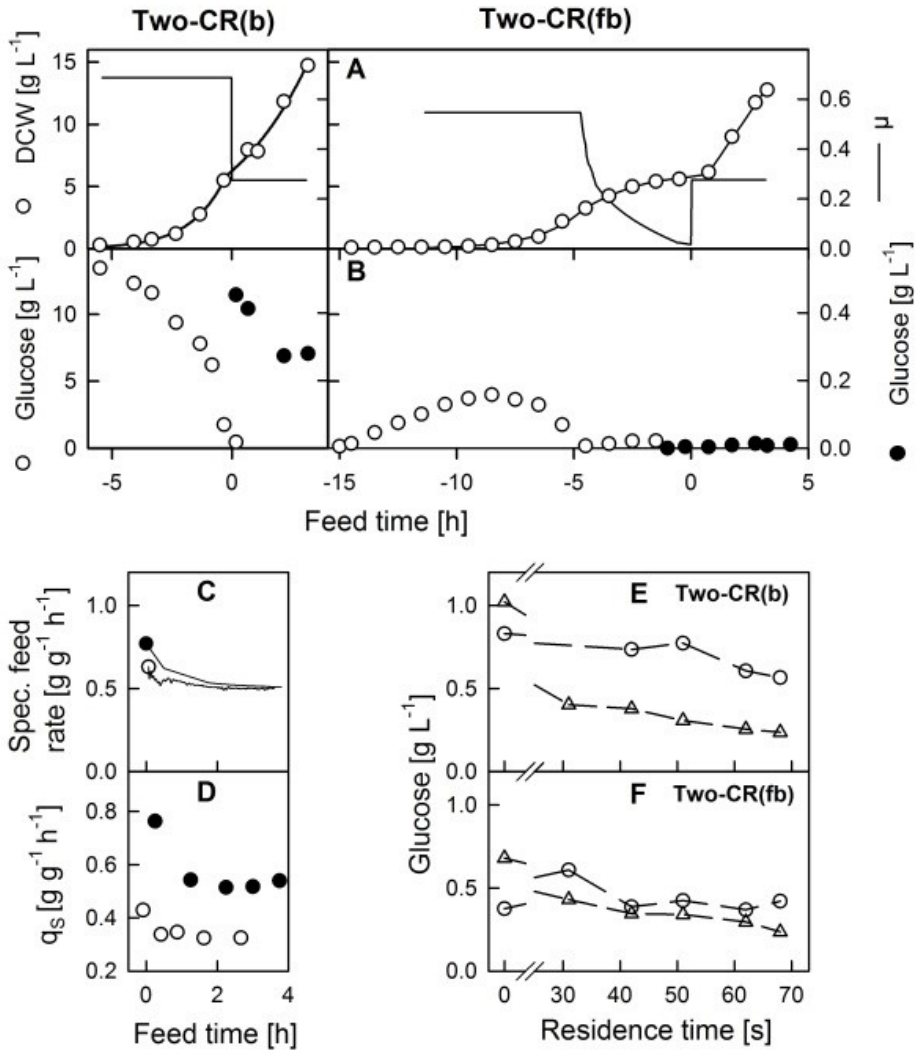

Figure 1: Comparison of DCW, specific growth rate μ and glucose utilization for two-CR fed-batch cultivations and an initial batch (*Batch-FB*) or Enbase (*EnBase-FB*) phase. A: DCW (circles) and fitted growth rate (line); **B**: Glucose (open circles left axis, closed circles right axis); **C** and **D**: Specific feed rate and specific substrate uptake rate (open circle: control culture with initial batch phase, closed circle: culture with initial glucose limited phase); E and F: Glucose profiles along the PFR of the control culture and the culture with an initial glucose limited phase, respectively. The different plots represent samples which were collected at the different ports of the PFR at 1 h (circles) or 3 h (Triangle) after the feed start. The zero value represents the concentration of the respective sample from the STR.

3.2.2 Volatile fatty acids

The glucose supply in the first cultivation phase does not only have an immediate effect on the specific glucose uptake rate itself, but also on the adaptation process to oscillating conditions in the later fed-batch feeding phase regarding the

formation of short chain fatty acids. The batch phase of the *Batch-FB* control culture showed the typical profile with an accumulation of mainly acetate and formate and to a lower level of lactate, succinate, fumarate and malate (Fig. 2A). The acetate concentration was in the *EnBase-FB* as high as in the *Batch-FB* cultivation, but it was fully consumed after the culture run into glucose limitation. Also during the feeding phase the concentrations of all volatile fatty acids remained quite low, although the distinct profiles were different between the two modes of cultivation. While acetate did not accumulate in the STR and its production was low in the PFR, lactate showed a significant accumulation over the PFR (Fig. 3A). Although lactate was fully re-assimilated under the glucose limiting conditions of the STR as already described by Xu *et al.* (1999), the cells which were primarily grown under glucose limitation (*EnBase-FB*) were not able to consume the lactate, but lactate was further accumulated (cf. graphs in Fig. 2A). Also, formate, succinate and fumarate showed a higher accumulation in this culture compared to the control cultivation. These observations indicate a much higher re-assimilation rate for volatile fatty acids when the cells were exposed to batch conditions prior to glucose pulses. On contrast, cells with fed-batch history show a higher volatile fatty acids accumulation rate.

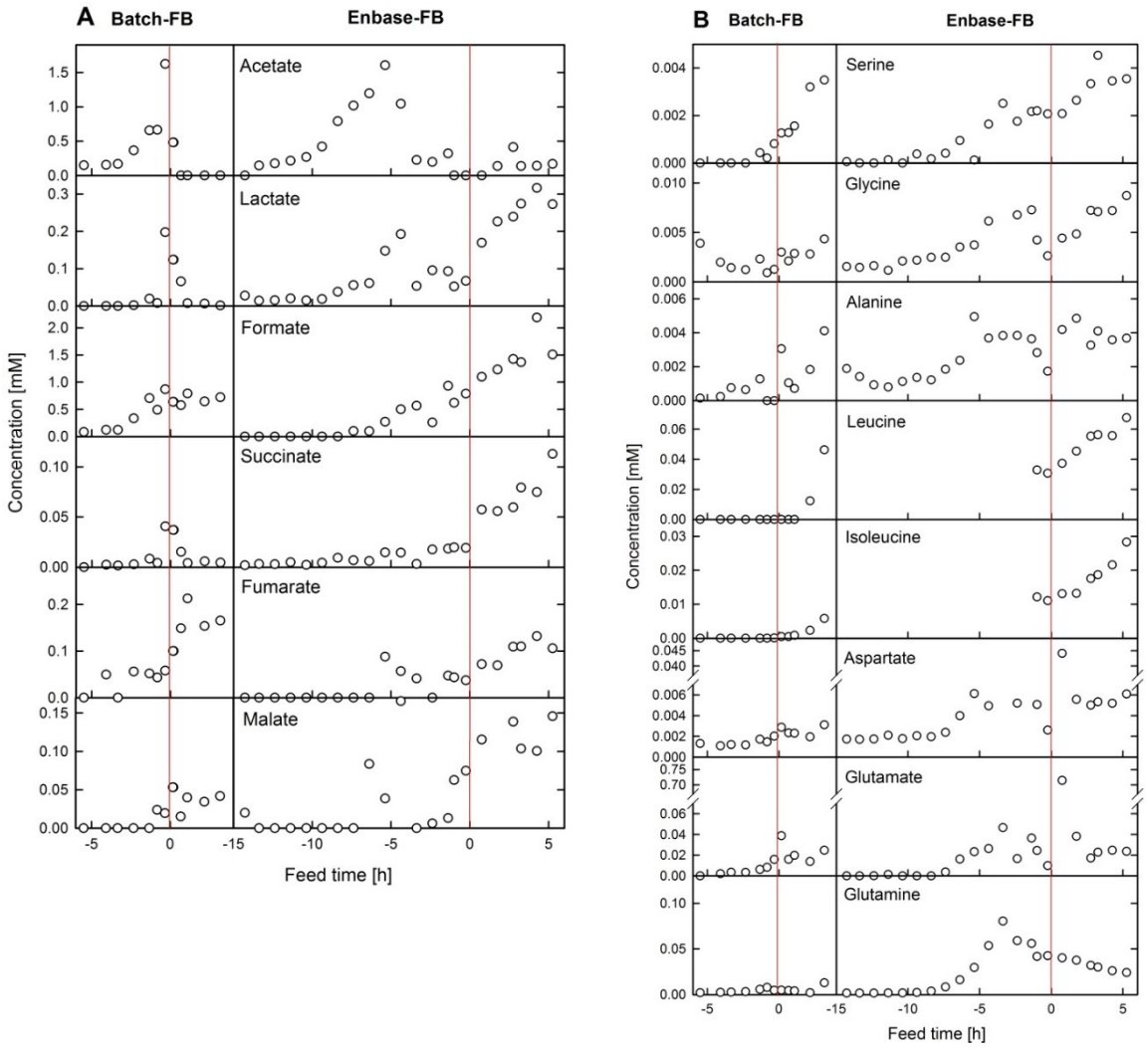

Figure 2: Extracellular short chain fatty acids (A) and amino acids (B) of the two cultivation types, *Batch-FB* and *EnBase-FB*, respectively. The vertical lines indicate the time when the PFR was connected and the feed was started.

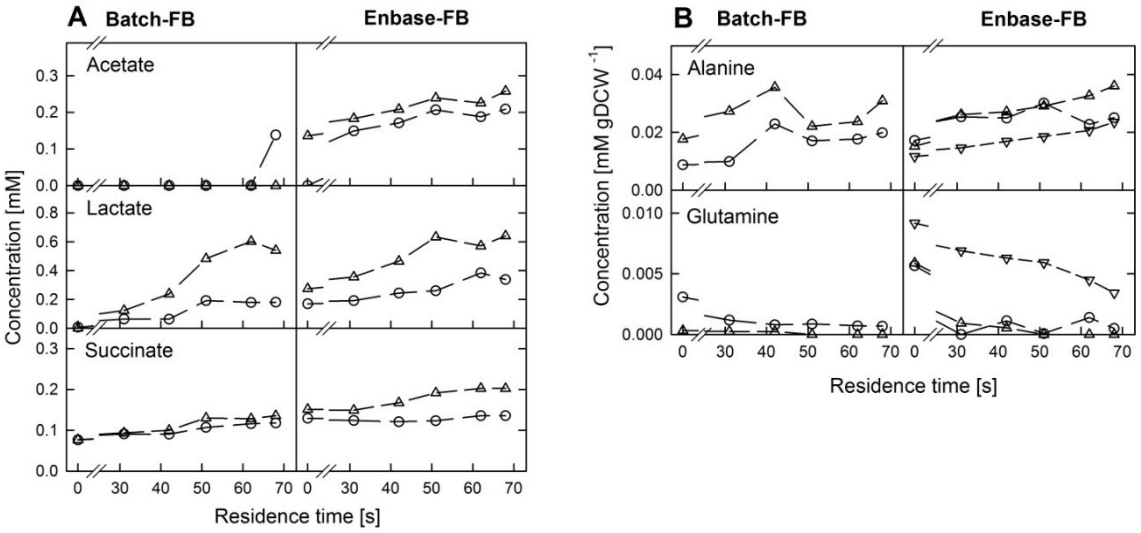

Figure 3: Comparison of profiles in the PFR of selected short chain fatty acids (A, extracellular concentration) and intracellular amino acids (A) in the two cultivation types, *Batch-FB* and *EnBase-FB*, respectively. The different plots represent samples which were collected at the different ports of the PFR at 1 h (circles), 3 h (Triangle) or 5 h (Triangle down) after the feed start. The zero value represents the concentration of the respective sample from the STR.

Also the accumulation of extracellular amino acids was generally very low (Fig. 2B). Only glutamate showed a peak directly after the start of the exponential feed, when the PFR was connected in the *Batch-FB* reference cultivation. In more detail, amino acids which are closely related to the central glucose metabolism were more accumulated in the *EnBase-FB* compared to the *Batch-FB* cultivation. However, as the accumulation stopped after the culture entered into the glucose limited phase, and even some of the amino acids were re-assimilated (glycine, alanine and glutamate), the level between both types of fermentation was not different at the time when the feed was started. Although all concentrations were still low, the accumulation of serine, glycine, leucine and isoleucine was higher after the feed start in the *EnBase-FB* cultivation. It is interesting to remark that the accumulation dynamics of leucine and isoleucine were significantly different from the *Batch-FB* reference cultivation and this was also seen in a higher intracellular accumulation of the non-canonical amino acid norvaline in the *EnBase-FB* (0.0015 mM $gDCW^{-1}$) compared to *Batch-FB* cultivation (0.00036 mM $gDCW^{-1}$) (data not shown).

For the short term response in the PFR changes of the amino acids were not detected for most of the amino acids, but for alanine and glutamine in the intracellular pools. The pool of free intracellular alanine increased along the PFR for both cultivations (Fig. 3B). In contrast glutamine decreases along the PFR, especially in the early phase of the fed-batch in the *EnBase-FB* culture.

3.2.3 Summary

The previous data show, that the cultivation mode before mechanical feed start has a major effect on the reaction of the central carbon metabolism to oscillating glucose conditions. Especially the accumulation and re-assimilation patterns of organic acids at oscillating glucose conditions differ between both cultivations, but also the glucose affinity.

To gain further insight into the behavior of *E. coli* global proteome and selected transcriptome analysis was performed for a STR and a TCR cultivation with a fed-batch phase 1 cultivation.

3.3 Proteome and Transcriptome studies on STR and TCR cultivation

In former experiments an impact of the initial feeding strategy on the reaction of *E. coli* to oscillating glucose conditions was observed. For further insights into the metabolic background global proteome and selected transcriptome analysis was performed for a STR and a TCR cultivation. For both an internal fed-batch was applied for 3 h before mechanical feeding started. In the reference cultivation the feed was applied directly in the STR, while in the TCR cultivation the feed was applied at the entrance of a PFR connected to the STR. In the TCR cultivation the cells experienced oscillating glucose pulses at anaerobic conditions and the cultivations were performed like described in chapter 3.1. Reference samples were taken directly before mechanical feed start. For better visualization, these samples

are timed -0.5 h before mechanical feed start. Further samples were taken 1, 2, 4 and 6 h after mechanical feed start and protein concentrations compared to the reference sample for clustering.

3.3.1 Proteome Clustering

916 proteins were found in all samples above threshold. Out of these, the concentration of around 25% (233 proteins) increased 1.5 times or decreased to 67% for one or both cultivations. These 233 proteins were clustered by Fuzzy-C-Means clustering into 14 clusters (optimal cluster number) and 10 outliers (figure 1). After mechanical feed start, 106 proteins (45%) show very similar dynamics for STR and TCR cultivation, 73 (31%) show the same tendency and 54 (23%) show diverging dynamics. To keep the overview simplified, the genes encoding the proteins are named.

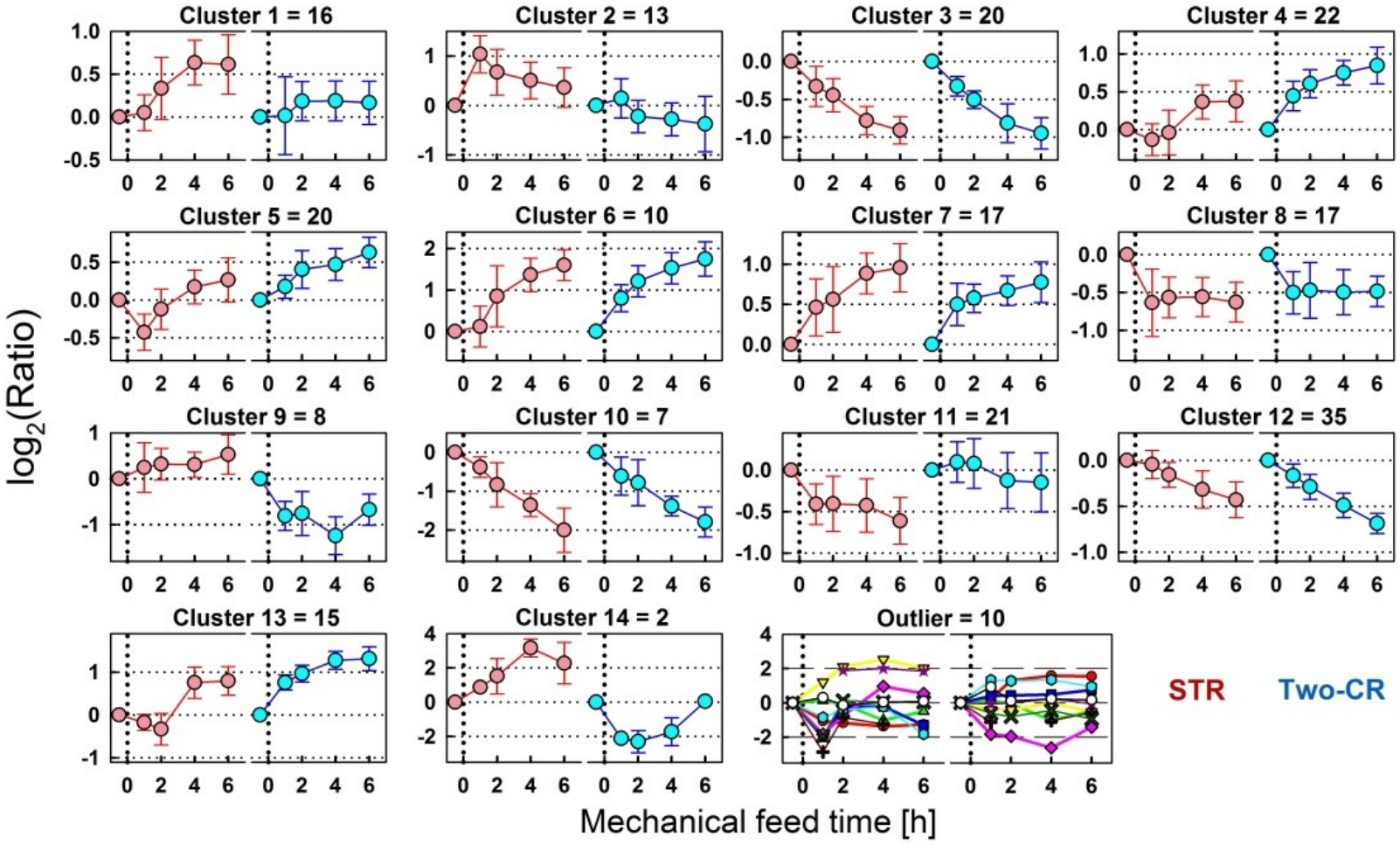

Figure 3.3.1: Fuzzy-C-Means Clustering. Out of 916 proteins 233 were found to increase 1.5 fold and/or decrease to 67% compared to the reference before mechanical feed start. The optimal cluster number is 14. Red dots: STR cultivation; Blue dots: TCR cultivation. Outliers are shown in detail in figure 3.3.2.

3.3.1.1 Outlier: Out of the 233 proteins 10 could not be sorted into a cluster. One protein encoded by *aceA* is isocitrate lyase, an enzyme of the glyoxylate shunt in the tricarboxylic acid cycle (TCA cycle). This protein decreases to less than half of the reference concentration during the STR cultivation and increases 3-fold during TCR cultivation. For a component of the maltose ABC transporter encoded by *malK* an opposite dynamic was found, while for the enzyme encoded by *cheW* (component of chemotaxis signaling complex – ribose/galactose/glucose) a more than 5-fold increase during STR cultivation and a decrease to 70% in the TCR cultivation can be observed.

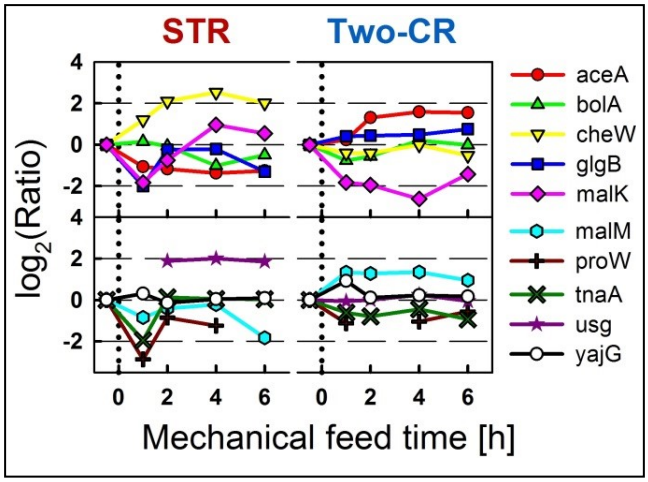

Figure 3.3.2: Outlier of proteome clustering. The ratio was calculated in relation to the protein concentration before mechanical feed start. Left side: STR cultivation; Right side: TCR cultivation

Table 3.1: Protein outliers sorted according to KEGG-pathways

Pathway or function	Protein	Pathway or function	Protein
Carbon metabolism		**Miscellaneous**	bolA
Glyoxylate and dicarboxylate metabolism	aceA		glgB
Amino acid synthesis			malM
DNA precursor and protein synthesis			tnaA
ABC-transporters and more			usg
ABC-transporters	malK		yajG
	proW		
Two-component system	cheW		

3.3.1.2 Grouped clusters with decreasing profiles: Within the 14 proteome clusters some show the same tendencies in dynamics. These clusters were grouped and the proteome data were sorted according to most relevant pathways. The membership to the pathway was evaluated with KEGG database. A complete overview of all analyzed members of chosen pathways can be found in the appendix.

In the first group all clusters with decreasing dynamics for STR and TCR cultivation were pooled. With 79 proteins this group is the biggest. Most proteins belong to synthesis pathways of amino acids like arginine, methionine, lysine and serine. In the glycolysis pathway, some enzymes catalyzing the pathway from glycerine-aldehyd-3-phosphate to pyruvate are down-regulated like *gapA*, *gpmM* and *pykF*. Also many enzymes of purine and pyrimidine precursor *de novo* synthesizing pathways are part of this cluster group, including *relA* (GDP pyrophosphokinase / GTP pyrophosphokinase), a key enzyme that catalyzes the formation of ppGpp, an alarmone involved in stringent response. In the group of miscellaneous (which are not part of the KEGG pathways listed before) interesting proteins like *bfr* (bacterioferritin for iron storage), *malP* (component of maltodextrin phosphorylase) and *pntA/pntB* (pyridine nucleotide transhydrogenase) are found. Pyridine nucleotide transhydrogenase catalyzes the equilibrium of NADPH + NAD^+ and $NADP^+$ + NADH.

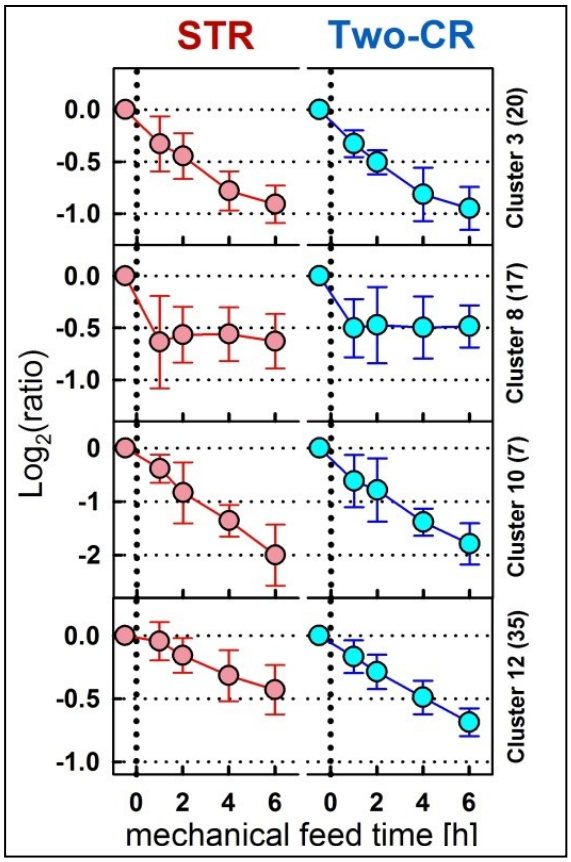

Figure 3.3.3: Grouped clusters with decreasing protein concentration for STR and Two-CR cultivation. The ratio was calculated in relation to the protein concentration before mechanical feed start. Left side: STR cultivation; Right side: TCR cultivation.

Table 3.2: Proteins with same decreasing profile for TCR and STR sorted according to KEGG-pathways

Protein	Cluster	Protein	Cluster	Protein	Cluster	Protein	Cluster
Carbon met.		*Ala, Asp and Glu met.*		**DNA prec./Ribos.**		**Miscellaneous**	
Glycolysis/Gluconeo.		argG	12	*Purine met.*		bfr	12
gapA	12	aroA	12	guaC	3	can	12
gpmM	3	aroF	8	purD	3	fadD	8
pykF	3	carA	12	purE	12	fdhE	3
yeaD	8	carB	8	purF	12	fliG	10
Pyruvate met.		gltB	3	purH	3	hdhA	12
ppc	12	gltD	3	purM	12	iscR	12
pykF	3	purF	12	purT	12	lamB	8
Glyoxy. and dicarb. met.		pyrB	3	pykF	3	malP	10
katE	12	pyrI	3	relA	12	malQ	10
Fruc. and Mann. met.		tyrA	8	*Pyrimidine met.*		moaB	12
mtlA	12	*Arg and Pro met.*		codA	3	mprA	8
mtlD	12	argG	12	pyrB	3	ompX	12
Methane met.		argD	12	carA	12	osmE	12
gpmM	3	codA	3	carB	8	pntA	12
serA	3	puuC	3	pyrD	3	pntB	12

serC	12	speD	12	pyrI	3	proP	3
ppc	12	*Cys and Met met.*		*Ribosomes*		rbbA	8
Additional		metA	3	rpmE	10	rmf	10
gcvP	12	metB	10	**ABC-transp. and more**		sra	8
gcvT	8	metC	8	*ABC-transporters*		stpA	12
metF	8	metE	8	livG	12	tgt	8
purH	3	metK	3	malF	10	uspD	8
purT	12	metL	3	metI	12	yahK	12
talA	12	speD	12	metN	8	ybdL	3
Amino Acid synt.		*2-Oxocarb. acid met.*		*Bacterial chemotaxis*		ycaO	12
Gly, Ser and Thr met.		argD	12	malE	8	ydjN	12
gcvP	12	*Additional*		*Sulfur met.*		yeaG	3
gcvT	8	gapA	12	metA	3	yffS	12
gpmM	3	pykF	3	metB	10	ygaU	12
metL	3	talA	12	*Selenocompund met.*			
serA	3			metB	10		
serC	12			metC	8		
				metE	8		

3.3.1.3 Grouped clusters with increasing profiles: In the next step, all clusters with increasing protein concentrations for STR and TCR cultivation were grouped. Among the 8 proteins of the carbon metabolism are *pfkB* (phospho-fructokinase 2), *ptsG* (component of glucose permease) and the subunits of galactitol PTS permease. An increase in protein concentration can be observed also for the enzymes catalyzing the reaction from α-keto-isovalerate to leucine (*leuA/C/D*) and from α-keto-glutarate to glutamate (*gdhA*) as well as for the subunits of sulfate adenylyl-transferase as part of the sulfur anabolism and *infA*, a translation initiation factor.

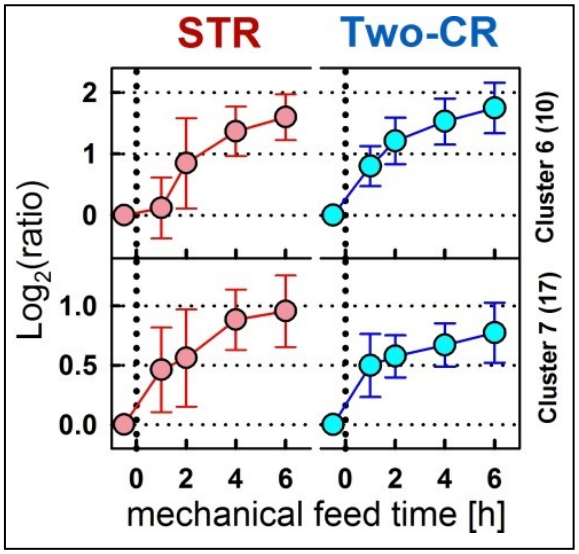

Figure 3.3.4: Grouped clusters with similar increasing protein concentration for STR and Two-CR cultivation. The ratio was calculated in relation to the protein concentration before mechanical feed start. Left side: STR cultivation; Right side: TCR cultivation.

Table 3.3: Proteins with same increasing profile for TCR and STR sorted according to KEGG-pathway.

Protein	Cluster	Protein	Cluster	Protein	Cluster	Protein	Cluster
Carbon metabolism		*Fruc. and Mann. Met.*		**DNA prec./Ribos.**		*Sulfur met.*	
Phosphotransf. system		manX	7	*Purine met.*		cysH	6
gatA	6	manZ	7	cysD	7	cysP	7
gatB	6	pfkB	7	cysN	7	cysD	7
gatC	7	*Methane met.*		*Additional*		cysN	7
manX	7	pfkB	7	pfkB	7	*Selenocompund met.*	
manZ	7	**Amino Acid synthesis**		**ABC-transp and more**		cysD	7
ptsG	7	*Val., Leu., Iso. Biosyn.*		*ABC-transporters*		cysN	7
Glycolysis / Gluconeog.		leuA	7	glnH	6	**Miscellaneous**	
pfkB	7	leuC	7	modA	7	erpA	7
ptsG	7	leuD	7	oppB	7	glcG	6
Pyruvate metabolism		*Ala., Asp. and Glu. met.*		znuA	6	infA	7
leuA	7	dadA	6	*Bacterial chemotaxis*		rlmN	7
Galactose metabolism		gdhA	6	rbsB	6	yjbR	7
gatA	6	*Arg. and Pro. Met.*					
gatB	6	gdhA	6				
gatC	7	*2-Oxocarb. acid met.*					
gatZ	6	leuA	7				
pfkB	7	leuC	7				
		leuD	7				

3.3.1.4 Grouped clusters with similar increasing profiles: In the following grouped clusters the protein levels are also increasing, though with different dynamics for STR and TCR cultivation. This group is the second biggest with 73 proteins. While for

cluster 1 the levels in STR increase stronger than in TCR cultivation, in clusters 4, 5 and 13 the dynamics show the opposite with a temporarily decrease for STR cultivation after mechanical feed start. In this group are *pck* as part of the gluconeogenesis, *acs* of the acetate node and *acnB* of the TCA cycle located. Also 3 ribosome subunits and two components of glucose ABC transporter (*glnQ and gltI*) show a stronger increase at TCR than at STR cultivation. Of those proteins of two-component system *cydA* is to name, since it is a subunit of cytochrome *bd*-I terminal oxidase. Of the proteins not sorted into a pathway four are to be mentioned: *crl*, which stimulates RpoS (RNAse polymerase subunit) activity during stationary phase, *cstA*, a peptide transporter induced by carbon starvation, *dhaK* (component of dihydroxyacetone kinase/PTS) and *ndh*, which is NADH dehydrogenase II.

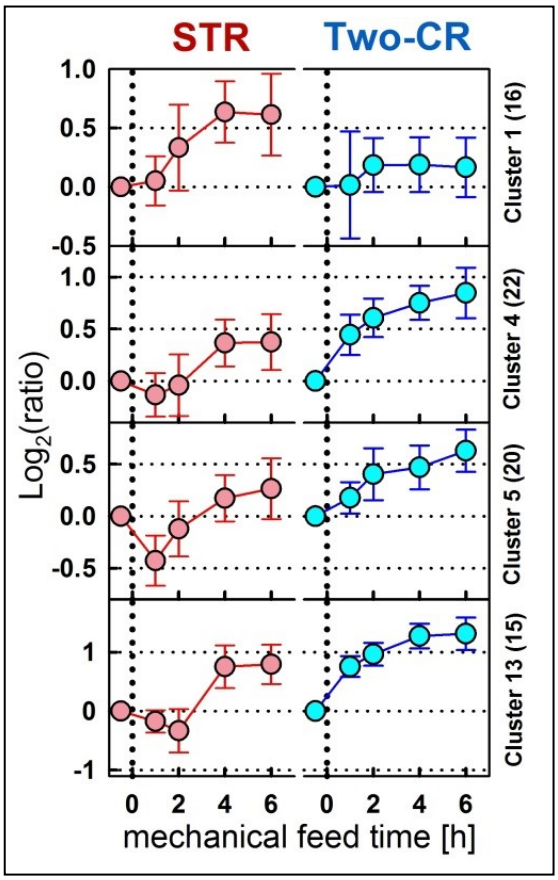

Figure 3.3.5: Grouped clusters with differently increasing protein concentration for STR and Two-CR cultivation. The ratio was calculated in relation to the protein concentration before mechanical feed start. Left side: STR cultivation; Right side: TCR cultivation.

Table 3.4: Proteins with tendency of increasing profile for TCR and STR sorted according to KEGG-pathway.

Protein	Cluster	Protein	Cluster	Protein	Cluster	Protein	Cluster
Carbon met.		**Amino acid synt.**		*Bacterial chemotaxis*		minE	5
P-Transf. system		*General*		dppA	5	mlaC	5
ptsH	13	acnB	1	mglB	5	msrB	4
Glycol. / Gluconeog.		argF	1	*Two-comp. system*		nagA	1
acs	5	*Arg. and Pro. met.*		rcsF	1	ndh	4
agp	13	argF	1	cheY	5	ppiC	13
pck	5	*2-Oxocarb. acid met.*		gltI	5	rimM	4
Pyruvate met.		acnB	1	cydA	13	slyA	4
acs	5	**DNA prec./Ribos.**		**Miscellaneous**		sstT	1
glcB	5	*Purine met.*		acpP	13	trxA	4
pck	5	adk	5	azoR	1	yajQ	4
ppsA	4	*Ribosomes*		clpA	1	ybaY	1
Glyoxy. and dicarb. met.		rpmD	13	crl	4	ybeD	13
acnB	1	rpmF	13	cspC	13	ycaR	1
fdoG	1	rpmG	4	cstA	5	yccU	4
fdoH	1	**ABC-transp. and more**		dhaK	4	ydeN	4
glcB	5	*ABC-transporters*		dsbA	4	ydhR	5
Galactose met.		argT	4	fkpB	4	yfgD	13
gatY	4	artI	4	fliC	4	yggX	13
Methane met.		fliY	4	fre	5	yibT	5
acs	5	glnQ	4	frr	5	yifE	13
fdoG	1	gsiB	4	glpK	1	yihX	5
fdoH	1	mppA	5	grxC	13	yjdM	4
ppsA	4	oppD	1	hpf	13	yqhD	5
Additional		oppF	1	iraP	5	ysgA	5
sdhD	1			lipA	13		

3.3.1.5 Grouped clusters with similar decreasing profiles: Clusters 2 and 11 have slightly decreasing dynamics for TCR cultivation in common. While in cluster 2 the protein levels in STR cultivation increase for 1h after mechanical feed start and afterwards decrease, they decrease throughout the whole STR cultivation for cluster 11. In this group *argE* can be found as the only protein of the arginine synthesis pathway with decreasing dynamics. For ribosomal subunits, *rpmH* decreases stronger in STR than in TCR cultivation, similar to *rpmE* of cluster 10 and opposite to *rpmD/F/G* of cluster 4 and 13. In "Miscellaneous" three proteins of iron uptake and storage can be found (*cirA*, *fhuA* and *ftnA*) and also three proteins of thiamin biosynthesis. With *hchA* and *uspG* two heat shock proteins can be found,

while *uspG* is induced in stationary phase. Also a component of glycogen phosphorylase, *glgP*, and superoxide dismutase (Mn), *sodA*, are parts of these clusters.

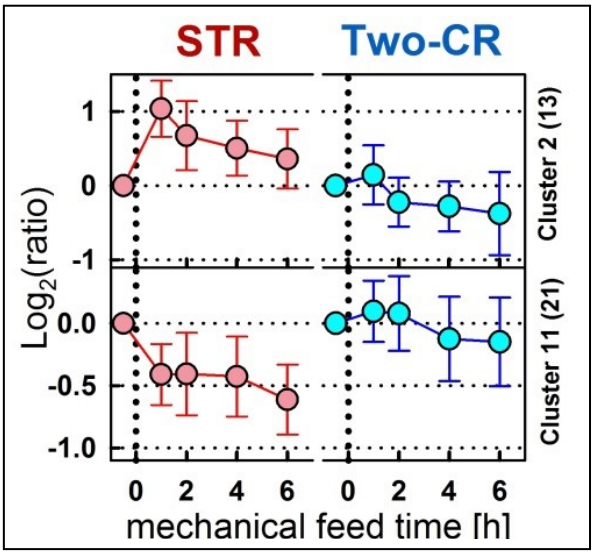

Figure 3.3.6: Grouped clusters with differently decreasing protein concentration for STR and Two-CR cultivation. The ratio was calculated in relation to the protein concentration before mechanical feed start. Left side: STR cultivation; Right side: TCR cultivation.

Table 3.5: Proteins with tendency of decreasing profile for TCR and STR sorted according to KEGG-pathway.

Protein	Cluster	Protein	Cluster	Protein	Cluster	Protein	Cluster
Carbon met.		**DNA prec./Ribos.**		**Miscellaneous**			
Pyruvate met.		*Pyrimidine met.*		cirA	2	thiI	11
lldD	11	dcd	11	dkgA	11	uspG	11
Glyoxy. and dicarb. met.		*Ribosomes*		elaB	11	uxaC	2
gcvH	11	rpmH	11	fhuA	2	yceI	11
Additional		**ABC-transp.and more**		ftnA	11	ydcL	2
fadB	11	*ABC-transporters*		glgP	11	yecD	2
Amino acid synt.		proV	11	gss	11	yecJ	2
Val., Leu. and Iso. degr.		*Two-comp. system*		hchA	11	yjiA	2
fadB	11	cheA	2	mscL	11	yncE	2
Ala., Asp. and Glu. Met.		tar	2	msrA	11	yrdA	11
fadB	11			osmY	2		
Arg. and Pro. Met.				raiA	11		
argE	11			sodA	2		
2-Oxocarb. acid met.				thiC	2		
argE	11			thiG	11		

3.3.1.5 Grouped clusters with diverging profiles: The grouped clusters 9 and 14 have protein dynamics increasing for STR and decreasing for TCR in common. *PflB* is a component of pyruvate formate-lyase and belongs to cluster 9 like aldehyde dehydrogenase A (*aldA*). Acetate permease (*actP*) shows high increase for STR cultivation while its concentration drops for TCR cultivation within the first 4 h after mechanical feed start.

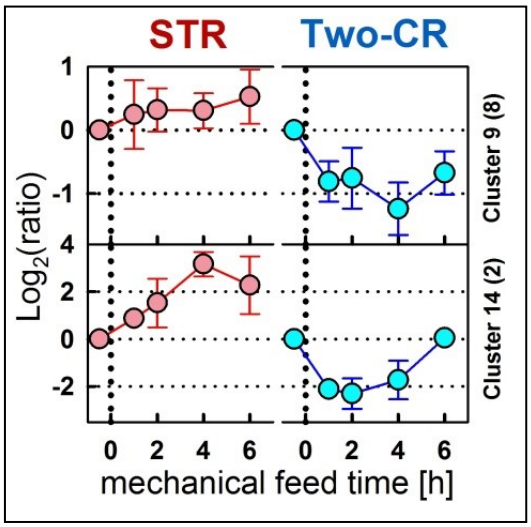

Figure 3.3.7: Grouped clusters with protein concentrations increasing for STR and decreasing for Two-CR cultivation. The ratio was calculated in relation to the protein concentration before mechanical feed start. Left side: STR cultivation; Right side: TCR cultivation. All proteins of the grouped clusters are listed according to KEGG-pathways on the right side.

Table 3.6: Proteins with profiles increasing for STR and decreasing for TCR sorted according to KEGG-pathway.

Protein	Cluster	Protein	Cluster	Protein	Cluster
Carbon met.		**DNA prec./Ribos.**		**Miscellaneous**	
Pyruvate met.		**ABC-transp. and more**		actP	14
aldA	9	*ABC-transporters*		glnK	9
pflB	9	proX	9	miaB	9
Glyoxy. and dicarb. met.		*Bacterial chemotaxis*		ycgR	14
aldA	9	cheZ	9		
Amino acid synt.		*Two-comp. system*			
Val., Leu. and Iso. Degr.		tsr	9		
fadA	9				

3.3.2 Transcriptome profiles

For a further insight into the regulatory background at oscillating glucose conditions, transcriptome profiles of selected genes were analyzed. Therefore, samples for transcriptome analysis were taken parallel to the samples for proteome analysis. Additionally samples were taken from the STR of STR and TCR cultivation to analyze the transcriptome every hour after mechanical feed start. For 1 h, 2 h and 4 h after mechanical feed start also samples along the PFR were taken and analyzed. The genes selected belong to the acetate node, TCA cycle, glyoxylate shunt, amino acid synthesis and anaerobic metabolism. The cDNA of the samples was mixed with further compounds of the real-time PCR reaction except the primers. The genes analyzed with the according mix are listed in table 3.1.

Table 3.7: cDNA Mix used for transcriptome analysis of specific genes.

cDNA-Mix	Analyzed genes
1	*pflB, leuA, aceA*
2	*acs, ackA, poxB*
3	*ilvB, ilvI, fumA, mdh, sucA, ace, pflD*
4	*sucC, fumB, frdA, gltB*

Acetate node: The genes of focus for transcriptome analysis around the acetate node were *aceE*, acs, *ackA* and *poxB*. The gene product of *aceE* is a component of pyruvate dehydrogenase, which catalyzes the conversion from pyruvate to acetyl-CoA. The transcription of this gene increases after onset of mechanical feeding for STR and TCR cultivation 6- and 8-fold, respectively. While in the STR cultivation this increase ends after 2 h of mechanical feeding, in the TCR cultivation already 1 h after start of oscillating glucose conditions the increase is realized. Afterwards, the transcriptome levels stay rather constant, with a small decrease to 5-fold compared to the reference sample after 7 h of mechanical feeding at the STR cultivation. The gene *acs* encodes for acetyl-CoA synthetase, an enzyme which converts acetate to acetyl-CoA by the use of one ATP. The transcription of *acs* increases at STR cultivation 3-fold, the increase again within the first 2 h after start of oscillating

glucose conditions. Interestingly, the increase in the TCR cultivation does not exceed 2-fold also along the PFR. The enzyme acetate kinase, converting acetate at the use of one ATP to acetyl phosphate, is encoded by the gene *ackA*. The transcription level of this gene increases with 6-fold stronger in the TCR than in the STR with 4-fold. While nearly no increase along the PFR can be observed at 1 h and 2 h of repeated glucose pulses, the profile at 4 h shows a 2.5-fold increase after 40 s of glucose pulse, which decreases again to 1.5-fold after 68 s. The fourth gene, *poxB*, encodes pyruvate oxidase, which converts pyruvate to acetate. The transcription of this gene decreases for both cultivations to around 50%. Nevertheless, the levels measured along the PFR are inconclusive, since they increase to 1.5-fold after 1 h and decrease to 50% 2 h of oscillating glucose conditions, while after 4 h an increase of up to 10-fold was measured.

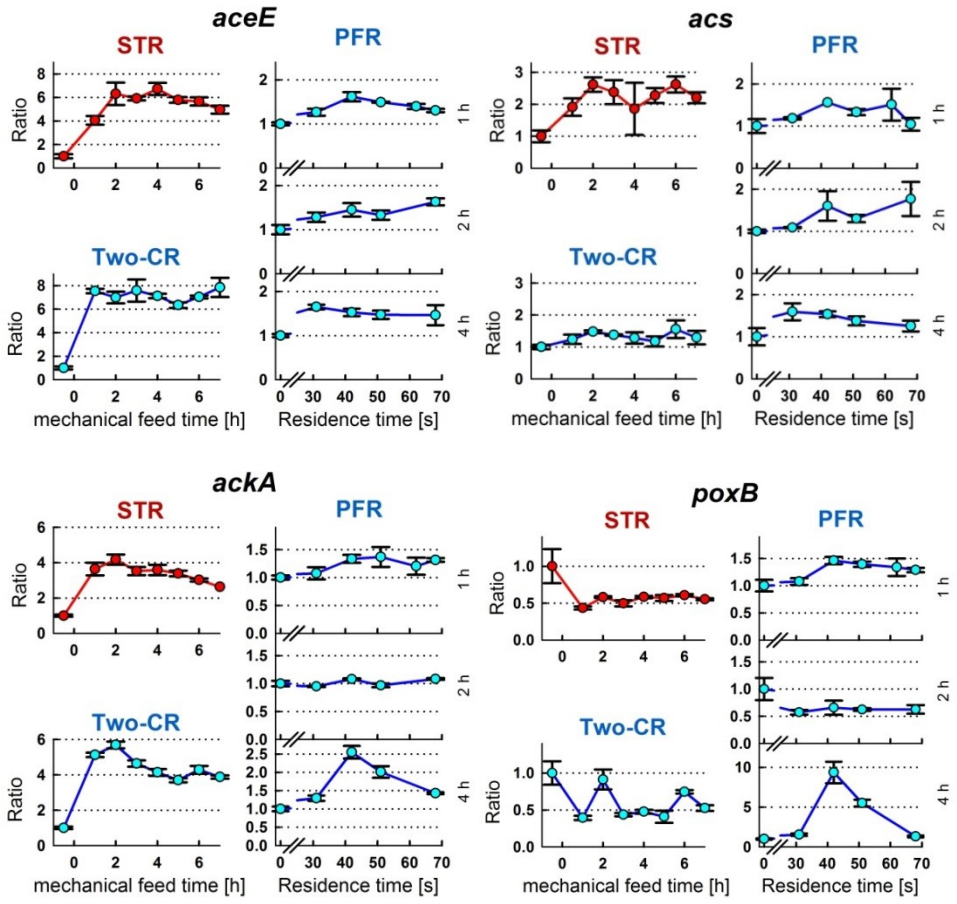

Figure 3.3.8: Transcriptome profiles of genes related to acetate node for reference cultivation in stirred tank reactor (STR) and in scale-down reactor (Two-CR). Samples taken before mechanical feed start are the reference for the transcriptome profile during cultivation. For the transcriptome profiles along the plug flow reactor (PFR) the reference is always the sample taken at the STR part of the scale-down reactor.

TCA cycle: Of the TCA cycle the genes *fumA*, *mdh*, *sucA* and *sucC* were selected for transcriptome analysis. The gene *fumA* encodes for fumarase A, an enzyme catalyzing the conversion of fumarate to malate, while the gene *mdh* encodes for malate dehydrogenase, which catalyzes the conversion from malate to oxaloacetate. The transcription of both genes increases around 4-fold in both cultivations, while nearly no increase can be observed at the last port of the PFR. The gene *sucA* encodes for 2-oxoglutarate decarboxylase (α-ketoglutarate decarboxylase), which participates in the α-ketoglutarate decarboxylation to succinyl-CoA. The gene product of *sucC*, succinyl-CoA synthetase, participates in the further reaction to succinate. For both genes the transcription rate increases 6-fold in the TCR cultivation, but only 4-fold like *fumA* and *mdh* in the STR cultivation. Like for *fumA* and *mdh* there was nearly no change in transcriptome level along the PFR observed.

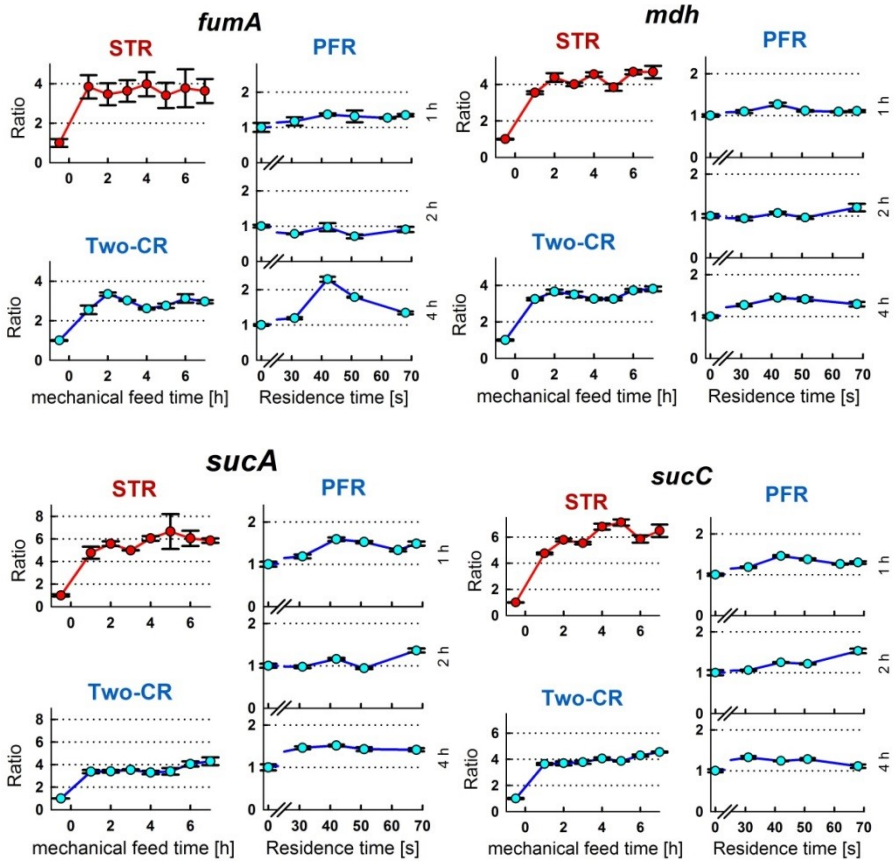

Figure 3.3.9: Transcriptome profiles of genes related to amino acid synthesis for reference cultivation in stirred tank reactor (STR) and in scale-down reactor (Two-CR). Samples taken before mechanical feed start are the reference for the transcriptome

profile during cultivation. For the transcriptome profiles along the plug flow reactor (PFR) the reference is always the sample taken at the STR part of the scale-down reactor.

Glyoxylate shunt: The enzymes of the glyoxylate shunt are encoded by the *aceBAK* operon, where *aceA* encodes for isocitrate lyase, which catalyzes the cleavage of isocitrate to succinate and glyoxylate. For this gene, the transcription was found to be higher in the STR cultivation (nearly 3-fold) than in the TCR (2-fold), though it always increases about 1.5-fold along the PFR.

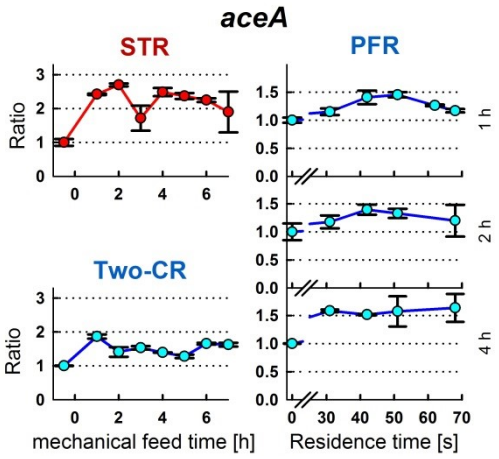

Figure 3.3.10: Transcriptome profiles of gene related to glyoxylate shunt for reference cultivation in stirred tank reactor (STR) and in scale-down reactor (Two-CR). Samples taken before mechanical feed start are the reference for the transcriptome profile during cultivation. For the transcriptome profiles along the plug flow reactor (PFR) the reference is always the sample taken at the STR part of the scale-down reactor.

Amino acid synthesis: The transcriptome of genes involved in branched chain amino acid synthesis (*leuA*, *ilvB* and *ilvI*) and one involved in glutamate synthesis (*gltB*) was analyzed. While the increase was up to 4-fold for *ilvI* and *gltB* and up to 3-fold for *leuA* for both cultivations, *ilvB* showed a very different pattern. Here, the transcription increased within 2 h after mechanical feed start to 2-fold in the STR cultivation, while nearly no increase can be observed for the TCR cultivation. The increase in the mRNA concentration along the PFR was always below 2-fold to the end of PFR for all analyzed genes.

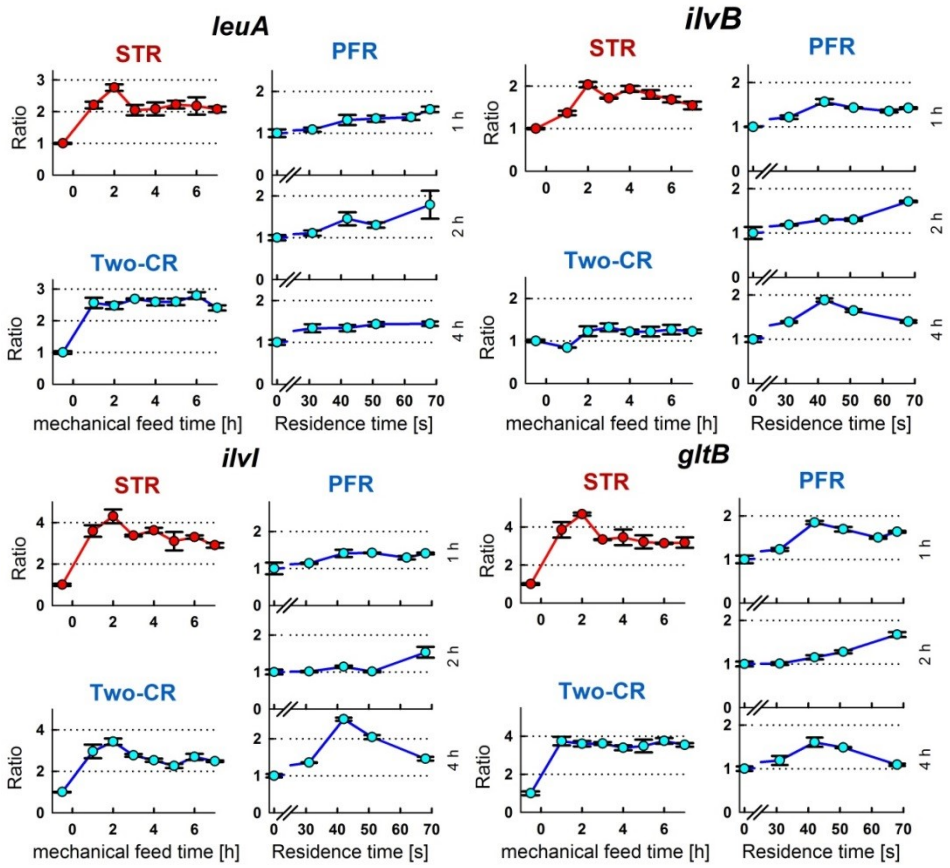

Figure 3.3.11: Transcriptome profiles of genes related to amino acid synthesis for reference cultivation in stirred tank reactor (STR) and in scale-down reactor (Two-CR). Samples taken before mechanical feed start are the reference for the transcriptome profile during cultivation. For the transcriptome profiles along the plug flow reactor (PFR) the reference is always the sample taken at the STR part of the scale-down reactor.

Oxygen limitation: In order to understand the regulatory mechanism at oscillating glucose pulses also the expression of genes related to oxygen limitation were analyzed. These genes are *pflB*, *pflD*, *frdA* and *fumB*. The gene *pflB* encodes for pyruvate formate-lyase. The enzyme catalyzes the conversion of pyruvate and CoA to formate and acetyl-CoA and is active at mixed acid fermentation. Interestingly, the transcription level of this gene increased after mechanical feed start for both cultivations, while with 3-fold in the STR cultivation even slightly higher than with 2.5-fold in the TCR cultivation. A drastic increase along the PFR could not be observed, only an increase of up to 1.7-fold. A similar pattern can be observed for the gene *frdA*, encoding a component of the fumarate reductase which catalyzes the reaction from fumarate to succinate at mixed acid fermentation. Nevertheless, the increase of transcription is stronger in the TCR cultivation (nearly 6-fold) compared to the STR cultivation (4-fold). The final levels were reached after 2 h of

oscillating glucose conditions. Though along the PFR no increase can be observed to the last port (68 s residence time), a 3-fold increase 42 s after the glucose pulse was measured. The cDNA mix used for this sample set was the same like for *sucC*, where no increase along the PFR at this sample set could be observed. Thus, this profile is unlikely to be based on a mistake in sample handling. A second pyruvate formate-lyase is encoded by *pflD*. The expression of this gene is increased 1.6-fold in the STR and about 3-fold at TCR cultivation with a high peak up to 8-fold for 2 h after start of mechanical feeding. Since the expression level along the PFR is half compared to the STR 2 h after mechanical feed start it is likely that the increased value in the STR is based on a mistake in sample handling. For the sample set taken 4 h after mechanical feed start a similar pattern can be observed like for *frdA*, though the increase is more than 20-fold 42 s after the glucose pulse. Since the samples were placed at the edge of the sample field of the microtitre plate, enhanced evaporation during real-time PCR might be a source of handling mistake. Nevertheless, for the samples of the last port (68 s) of the last PFR set (4 h) no special outliers are observed, though these were placed at the edge of the microtitre plate as well. A similar pattern like *frdA* but with higher increased outliers was observed for the gene *fumB*, encoding for fumarase B. This enzyme catalyzes the formation of malate by fumarate at anaerobic conditions.

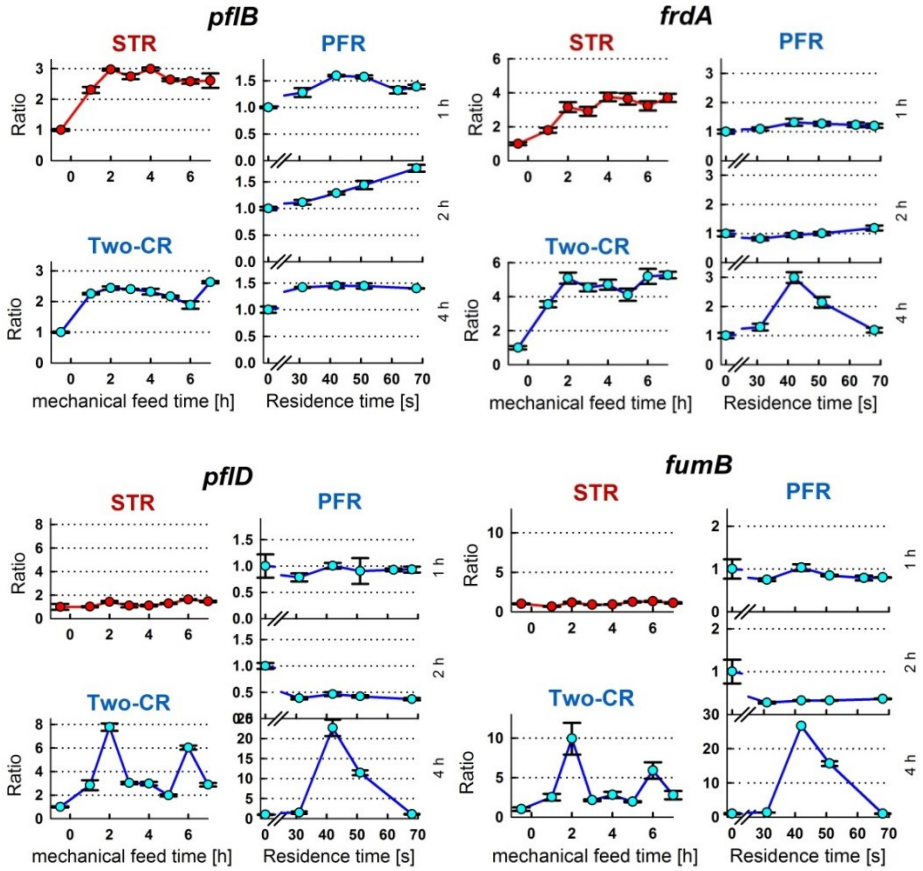

Figure 3.3.12: Transcriptome profiles of genes related to amino acid synthesis for reference cultivation in stirred tank reactor (STR) and in scale-down reactor (Two-CR). Samples taken before mechanical feed start are the reference for the transcriptome profile during cultivation. For the transcriptome profiles along the plug flow reactor (PFR) the reference is always the sample taken at the STR part of the scale-down reactor.

3.3.3 Combined proteome and transcriptome profiles of the central carbon metabolism, amino acid and nucleotide precursor synthesis

Additional to proteome data, also transcriptome data of 17 chosen genes were analyzed. Their profiles are depicted with all proteome profiles of the central carbon metabolism, amino acid synthesis pathway and purine/pyrimidine precursor pathway in figure 3.3.13.

3.3.2.1 Proteome profiles: Two proteins of gluconeogenesis were analyzed, of which *pck* shows an increase to 1.5-fold in TCR cultivation compared to STR cultivation. In the glycolysis pathway, a switch can be observed at

glycerinealdehyde-3-phosphate. While the concentration of some proteins increases in the pathway from glucose to glycerinealdehyde-3-phosphate similar for both cultivations, the concentration of some proteins drops afterwards towards the reactions to pyruvate. Proteins catalyzing the reactions from glucose-6-phosphate to ribose-5-phosphate do not show significant dynamics. Within the PPP, only *talA* decreases similar for STR and TCR cultivation. In the acetate node, only *acs* drops in STR cultivation after mechanical feed start to 60% but increases again. In TCR cultivation it increases up to 1.5-fold within 4 h after mechanical feed start. For TCA cycle, only *acnB* and *sdhD* show concentration dynamics increasing similar for both cultivations. For *sdhD*, also a small drop after mechanical feed start can be observed. The biggest difference for STR and TCR cultivation proteome profile can be found in the glyoxylate shunt, where the concentration of the key enzyme, *aceA*, decreases for STR cultivation decreases to 40% and increases 3-fold for TCR cultivation. For the formation of anaerobic side products lactate, formate and ethanol, only the protein profile for *plfB* shows dynamics, which are increasing to 1.4-fold for STR and decreasing to 50% for TCR cultivation. For amino acid synthesis pathways, all protein concentrations either are constant or decrease, with two exceptions: the pathway from α-keto-isovalerate to leucine and from α-keto-glutarate to glutamate. While in the leucine pathway the proteins leuA/C/D increase up to 2-fold, *gdhA* for glutamate synthesis increases up to 3-fold for both cultivations. The protein levels for the synthesis pathways for purine/pyrimidine precursors inosine monophosphate and uridine monophosphate either stay constant or decrease. All global regulators, which could be analyzed, did not show significant dynamics except *relA*. *relA* shows an increase for STR cultivation 4 h after mechanical feed start, but finally decreases like for TCR cultivation below the reference sample before mechanical feed start. For proteins involved in respiration an increase in the TCR cultivation was found for *cydA* and *ndh* to 3- and 2-fold, respectively. No change could be observed for *cydBCD*, *cyoABD* and *nuoA-J*.

3.3.2.2 Transcriptome profiles: For 14 genes, of which the transcriptome was analyzed, the according proteome data exist and are depicted in figure 8. Only for one gene, *leuA*, the dynamic of the transcriptome correlates to the proteome. For both cultivations the trancriptome levels increase up to 3-fold, while the proteome level increases up to 1.7-fold for STR and 1.5-fold for TCR cultivation. The transcriptome profiles for *ilvB*, *ilvI*, *ackA*, *acs*, aceE, *sucA*, sucC, *fumA* and *mdh* increase up to 8-fold, while the according protein levels do not change significantly. For *gltB*, even a drop in protein level can be observed while the transcriptome level increases. For *poxB*, the opposite can be observed with a drop in the transcriptome profiles while the protein levels stay constant. For *gltB* even an increase in transcriptome levels can be observed while the protein levels drop for both cultivations. For the key enzyme of the glyoxylate shunt, *aceA*, a higher increase in the transcriptome profile can be observed for STR cultivation than for TCR cultivation, while in the proteome profiles the dynamic decreases for STR and increases for TCR cultivation. Furthermore, the transcription profile of three genes for anaerobic respiration was measured. For *frdA* (fumarate reductase) the transcriptome profile increases in both cultivations, though around 50% higher in TCR. A great difference can be observed for *pflD* (pyruvate formate lyase II) and *fumB* (fumarase B) for both cultivations. A peak can be observed 2 h after mechanical feed start in TCR cultivation with an increase of up to 10-fold, while in the STR cultivation increase up to 1.7-fold.

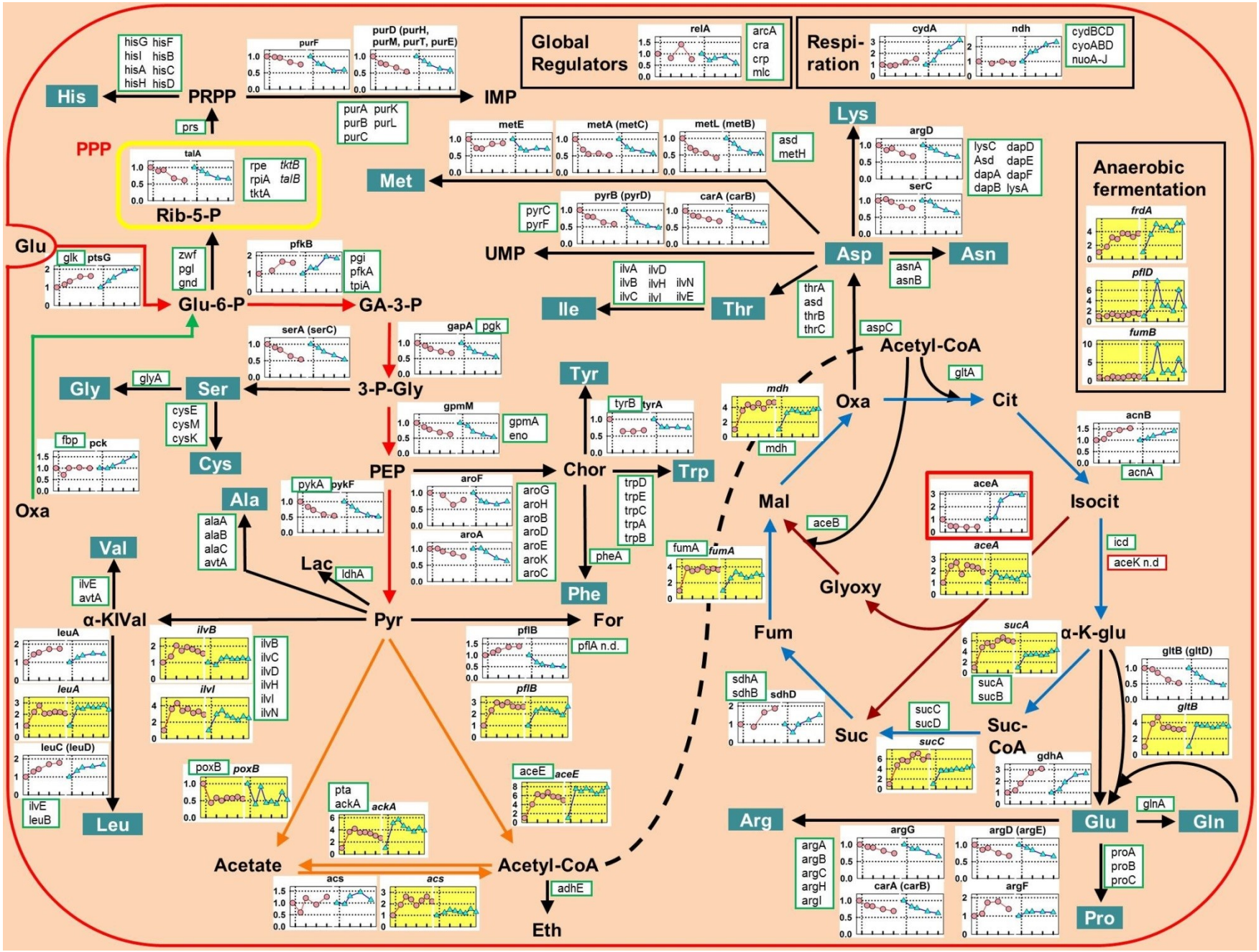
Global Regulators
relA
arcA cra crp mlc
Respi-ration
cydA
ndh
cydBCD cyoABD nuoA-J
His
PRPP
hisG hisF hisI hisB hisA hisC hisH hisD
purF
purD (purH, purM, purT, purE)
IMP
purA purK purB purL purC
prs
PPP
talA
rpe tktB rpiA talB tktA
Rib-5-P
Met
metE
metA (metC)
metL (metB)
asd metH
Lys
argD
lysC dapD Asd dapE dapA dapF dapB lysA
serC
Anaerobic fermentation
frdA
pflD
fumB
Glu
glk ptsG
zwf pgl gnd
pfkB
pgi pfkA tpiA
Glu-6-P
GA-3-P
pyrC pyrF
pyrB (pyrD)
carA (carB)
UMP
Asp
Asn
asnA asnB
ilvA ilvD ilvB ilvH ilvN ilvC ilvI ilvE
Ile
Thr
thrA asd thrB thrC
aspC
Acetyl-CoA
serA (serC)
gapA
pgk
Gly
glyA
Ser
3-P-Gly
Tyr
gltA
mdh
Oxa
Cit
acnB
acnA
cysE cysM cysK
Cys
gpmM
gpmA eno
tyrB tyrA
fbp
pck
PEP
Chor
Trp
aceA
Isocit
pykA
pykF
aroF
aroG aroH aroB aroD aroE aroK aroC
aroA
Ala
alaA alaB alaC avtA
Mal
aceB
trpD trpE trpC trpA trpB
pheA
fumA
fumA
Lac
ldhA
Glyoxy
icd
aceK n.d
Val
ilvE avtA
Phe
α-KIVal
Pyr
For
Fum
α-K-glu
leuA
ilvB
ilvB ilvC ilvD ilvH ilvI ilvN
ilvI
pflB
pflA n.d.
sucA
gltB (gltD)
gltB
leuA
leuC (leuD)
sdhA sdhB
sdhD
sucC sucD
Suc
Suc-CoA
sucA sucB
gdhA
ilvE leuB
Leu
poxB
poxB
aceE
aceE
pta ackA
ackA
Arg
Glu
glnA
Gln
argA argB argC argH argI
argG
argD (argE)
carA (carB)
argF
proA proB proC
Pro
Acetate
Acetyl-CoA
acs
acs
adhE
Eth

Figure 3.3.13: Proteome and transcriptome profiles of central carbon metabolism, amino acid synthesis pathway and purine/pyrimidine precursor for STR and Two-CR cultivation. All proteins analyzed along the pathways are depicted. Proteome profiles are marked as graphs with black titles (with gene names encoding the proteins), trancriptome profiles have a yellow background. Y-axis: Ratio to proten concentration before mechanical feed start (vertical dotted line). X-axis: mechanical feed time with 2 h increments. Proteins with profiles with less than 1.5 fold increase or decrease to 67% are framed green. Green arrow: Gluconeogenesis; Red arrows: Glycolysis; Yellow frame: Pentose-phosphate pathway; Orange arrows: Acetate node; Blue arrows: TCA cycle; Brown arrows: Glyoxylate shunt.

3.3.4 Summary

To study the effect of oscillating glucose conditions on the central carbon metabolism of *E. coli* with primarily reduced growth rate a global proteome analysis and selected transcriptome analysis was performed. For all genes except *leuA* a transcriptional dynamic can be observed which does not agree with the proteome levels. The most profound difference between a homogeneous cultivation and a cultivation with oscillating glucose conditions regarding the central carbon metabolism proteome profile can be seen for the increase of glyoxylate shunt enzyme isocitrate lyase and respiration related proteins in the TCR cultivation. For most of the synthesis pathways for amino acids and nucleotide precursors a decrease after mechanical feed start was found for both cultivations with the exception of *leuA/C/D* and *gdh*. For the central carbon metabolism an increase in enzyme level was observed for the upper glycolysis until glycerinealdehyde-3-phosphate. Afterwards the enzyme levels decreased. Also in the TCA cycle the enzyme concentrations either were constant or increased just slightly.

4. Discussion

The focus of this doctoral thesis lies on the influence of growth rate on the effect of oscillating glucose conditions on the central carbon metabolism of *E. coli*. Therefore, a scale-down cultivation system was established comprised of an STR and a PFR. A phase 1 cultivation was performed, where *E. coli* W 3110 wild-type cells were grown in EnBase mineral salt medium containing the glucose polymer dextrin and its degrading enzyme, α-amylase. In the beginning the cell growth was unlimited, when the glucose release rate was higher than the glucose uptake rate of the cells. Finally the cells entered the fed-batch phase several hours before the mechanical feed was applied. So the cells were in fed-batch mode at a reproducible physiological state and amount at the beginning of phase 2 cultivation, the experimental part.

For establishment two cultivations with only the STR used were performed and two more cultivations as TCR. The general parameters were reproducible, though differences in the accumulation pattern of organic acids and amino acids were found which were not described like that in literature so far. To gain further information, a TCR cultivation was performed with the same phase 2 cultivation settings but with a batch cultivation before mechanical feed start. Additionally, global proteome and selected transcriptome analysis were performed for STR and TCR cultivation with phase 1 cultivation as fed-batch. The results gained from these experiments are discussed in the following sections.

4.1 Accumulation and re-assimilation of organic acids and non-canonical amino acid norvaline at oscillating glucose conditions

For this study, a scale-down TCR cultivation was established with an EnBase fed-batch strategy as phase 1 cultivation before the start of mechanical feeding and oscillating glucose conditions. As reference, the same mechanical feeding strategy was applied to a STR cultivation with the same phase 1 cultivation conditions. The comparison of both cultivation modes showed, that in the TCR cultivation the

organic acids acetate, lactate, formate, succinate, fumarate and malate accumulated during oscillating glucose conditions while they partly did not accumulate in the STR cultivation. The analysis of organic acid profiles along the PFR showed and accumulation of extracellular acetate, lactate and succinate at glucose excess and oxygen limited conditions in the PFR, while they were re-assimilated in the STR compartment.

When a batch cultivation was applied as phase 1 cultivation with following oscillating glucose conditions (*Batch-FB* cultivation), it was found that acetate, lactate and succinate accumulated during the transition from batch to fed-batch, but were completely re-assimilated within the first 2 h of oscillating glucose conditions. Though also lactate and succinate accumulated along the PFR after 3 h of oscillating glucose conditions, too, no accumulation could be observed for acetate. Though formate was present in the STR at the beginning of mechanical feed start, no further accumulation was observed at oscillating glucose conditions for *Batch-FB* cultivation

The accumulation of acetate, lactate and formate at large scale and scale-down cultivations was described earlier by Xu *et al.* (1999) and Enfors *et al.* (2001). They found, that the organic acids accumulate at conditions of glucose excess and oxygen limitation along the PFR and are re-assimilated at the aerobic, glucose limited area of the STR. Nevertheless, they further found that the re-assimilation of acetate and lactate is complete, so these organic acids were not found in the STR part of the TCR, while formate accumulated due to lower re-assimilation rates compared to acetate and lactate. *E. coli* can use three isozymes of formate dehydrogenase to catalyze the conversion of formate to carbon dioxide and hydrogen (Sawers, 1994; Sawers *et al.*, 1991). Two of these need molybdenum and selenium for proper function, the third nickel. It was found, that the addition of these compounds during a TCR cultivation of *E. coli* W3110 decreases the accumulation of formate at oscillating glucose conditions (Soini et al., 2008). Interestingly, while the accumulation of formate was not observable anymore and also previously accumulated acetate was re-assimilated faster at oscillating glucose conditions, the organic acids lactate and succinate accumulated. These acids did not accumulate at

the reference cultivation without the addition of molybdenum, selenium and nickel, which might indicate a bottleneck in respiration or other flux related issues. As preparing experiment the effect of a permanent oxygen downshift at a fed-batch cultivation was performed. The accumulated lactate was analyzed and found to consist of exclusively D-lactate, so an alternative lactate synthesis by methylglyoxyl pathway starting from dihydroxyacetone phosphate (glycolysis intermediate) (Weber *et al.*, 2005a) was excluded. In this study, the same concentration of molybdenum, selenium and nickel was added to the medium. Nevertheless, formate accumulation was observed for the TCR cultivations (chapter 3.1). Both studies, the one by Soini *et al.* (2008) and this, share the same *E. coli* strain, the same mineral salt medium composition and the same bioreactor setup. The main differences in the experimental setup are the feeding strategy at mechanical feeding and the growth rate before start of oscillating glucose conditions. Soini *et al.* (2008) applied a constant feeding of 76 g glucose · h^{-1}. Reitz performed TCR cultivations also with similar setup (data not published yet). Though the specific feed rate with an exponential increase of e=0.4 h^{-1} was higher than used here, no accumulation of formate was observed. In contrary to this study, he performed a batch cultivation before the start of oscillating glucose conditions. Hence, it seems very likely that the cultivation mode and the growth rate going hand in hand with it, to which the cells are adapted before the start of oscillating glucose conditions, have a major impact on the reaction of the central carbon metabolism to glucose pulses.

An interesting finding is also the accumulation of norvaline during the TCR cultivation. Norvaline belongs to a group of non-canonical amino acids which can be synthesized by the same set of enzymes synthesizing the branched chain amino acids (Kisumi *et al.*, 1976). The precursor is α-ketobutyrate. Non-canonical amino acids were found especially in connection with the expression of leucine rich, recombinant proteins (Apostol *et al.*, 1997; Lu *et al.*, 1988; Muramatsu *et al.*, 2002). The expression imbalances the branched chain amino acid synthesis pathway in a way, that α-ketobutyrate is further processed by chain elongation to the precursors of these non-canonical amino acids (Andersen *et al.*, 2001; Sycheva *et al.*, 2007). In wild-type *E. coli* at normal growth conditions, α-ketobutyrate is supposed to be

generated by degradation of threonine as precursor for isoleucine synthesis. Nevertheless, in more recent studies it was found, that the chain elongation of pyruvate to α-ketobutyrate is supposed to be triggered by elevated pyruvate concentrations due to glucose pulses (Lu, 2016; Soini, 2011). Also the addition of molybdenum, selenium and nickel was found to reduce the accumulation of norvaline to 1 µM at glucose excess and oxygen limitation (Biermann *et al.*, 2013), which is very similar to these results.

The findings in this study are in accordance with the recent studies regarding glucose pulses as source of non-canonical amino acid precursor α-ketobutyrate. Nevertheless, they are in disagreement regarding the accumulation and re-assimilation pattern of organic acids. The comparison with existing literature indicates, that the reduced growth rate before the start of oscillating glucose conditions lead to the differences. This will be discussed with a closer look to the proteome data gained in this study in the next section.

4.2 Adaptation of the central carbon metabolism and biosynthesis proteome to increasing growth rate.

A STR and a TCR cultivation were performed and analyzed regarding the proteome profile shortly before and until 6 h after start of mechanical feeding. 916 proteins were detectable in all samples, of which 233 proteins showed a 1.5-fold change for at least one cultivation. More than 75% of these proteins showed the same or similar tendency for both cultivations after mechanical feed start. For the central carbon metabolism, all amino acids synthesis pathways and nucleotide precursor pathways the analyzed proteins were sorted regardless if a change occurred or not. It was found, that with some exceptions all protein levels of these pathways either stayed constant of decreased to around the half. An increase was only found for the protein encoded by *ptsG,* one protein of the upper glycolysis until glycerinealdehyde-3-phosphate (*pfkB*), proteins encoded by the *leuABCD* operon of the branched chain synthesis pathway, two proteins of the TCA cycle (*acnB* and *sdhD*) and one proteins of glutamate synthesis (*gdhA*). The increases were 1.5 to

3-fold. Though not directly coupled to glucose utilization, an increase of proteins of galactitol and mannose PTS transporter up to 4-fold was found for both cultivations. Regarding proteins involved in respiration, that encoded by *ndh* increased for both cultivation types though stronger in the TCR cultivation. Similar results were found for *cydA* encoded protein, and no change for both cultivations could be observed for the proteins encoded by the *cyo* operon and the *nuo* operon. Trancriptome analysis of selected genes showed, that changed transcription rates did not necessarily change the protein level.

Valgepea *et al.* measured the protein concentration in accordance to the growth rate (Valgepea *et al.*, 2013). They found, that the protein concentration of biosynthesis pathways in the cell decreases with increasing growth rate. Furthermore, they assumed the cells to be in "stand by" mode since the protein abundances are high for low growth rates. This observation is in accordance to the findings in the present study.

Yoon *et al.* performed transcriptome and proteome analysis of a HCD fed-batch cultivation (Yoon *et al.*, 2003). They used the strain W3110 and a modified R medium, which is a mineral salt medium. During transition from batch to fed-batch ($\mu = 0.14\ h^{-1}$) they found a decrease of proteins encoded *by ptsI, ilvC* and *leuC* and an increase for the TCA cycle proteins encoded by *icdA, mdh, sdhA* and *sucC*. Of these proteins, only the one encoded by *leuC* showed a change in the concentration level when the growth rate increased in STR and TCR cultivation.

Due to sequence analysis it is assumed, that the global regulator system cAMP-CRP controls the transcription of the major genes involved in substrate uptake (Shimada *et al.*, 2011). In a recent study it was also found, that the cAMP-CRP regulation controls the overall substrate uptake, not necessarily preferring glucose over other substrates (You *et al.*, 2013). When the glucose concentration in the environment decreases below 3 mM, the cAMP concentration increases and provokes the global regulation by cAMP-CRP (Notley-McRobb *et al.*, 1997). Weber *et al.* studied the effect of the transition from famine to feast in *E. coli* K-12 TG1 (Weber *et al.*, 2005b). They performed a glucose-limited continuous culture with a sudden up- and downshift in glucose concentration at dilution rate from 0.066 h^{-1} to 0.23 h^{-1} and

reverse. The level of growth rate increase is similar to that used in this study at the start of mechanical feeding. Interestingly, they found an increase of cAMP to 1 µmol·g^{-1} also for the upshift within the first 2 min. The decrease to the former level took 3 h of continuous culture. With the upshift methylglyoxal accumulated to 0.6 mg·L^{-1} within 14 min in the supernatant. After 2 – 4 h, so when cAMP reached it basal concentration, also acetate, D-lactate, L-lactate, pyruvate and formate accumulated. After 9 h of continuous cultivation with the higher feed rate the concentration of all these organic acids in the medium dropped again. From the detection of both forms of lactate and methylglyoxal they concluded the activation of the methylglyoxal bypass at the transition from famine to feast. The methylglyoxal bypass converts dihydroxyacetone-phosphate (which is converted to glyceraldehyde-3-phosphate for lower glycolysis) into pyruvate via D-lactate and L-lactate without the generation of ATP connected to lower glycolysis. Concentration analysis of fructose-1,6-bisphosphate and the cleavage products glycerinealdehyde-3-phosphate and dihydroxyacetone-phosphate revealed limitations in the upper part of the glycolysis. The observed accumulation of organic acids at oscillating glucose conditions after an increase of growth rate presented here and the increase in upper glycolysis protein *pfkB* is in accordance to the observation of Weber *et al.* (2005).

Another growth rate dependent parameter with strong influence on the central carbon metabolism is the maximal specific glucose uptake rate and the according maximal specific oxygen consumption rate. Lin *et al.* found, that with decreasing growth rate the respiration capacity decreases stronger than the glucose uptake capacities (Lin *et al.*, 2001) (for more detail see chapter 1.4.1). When applying a closer look to the proteome data achieved in this study, it is obvious that the substrate uptake capacities with an increase of *ptsG* (1.6-fold for STR and 2-fold for TCR) also increases together with the mannose PTS permease (1.7-fold for both cultivations) and the galactitol PTS permease (up to 6-fold for both cultivations). The protein level of the NADH:ubiquinone oxidoreductase I encoded by the *nuo* operon and cytochrome o oxidase do not change after mechanical feed start for the STR and the TCR cultivation, while NADH:ubiquinone oxidoreductase II (*ndh*) increased 2.3-fold in TCR and Cytochrome d (*bd*-I) terminal oxidase subunit I was

found to increase by 1.5-fold for STR and 3-fold for TCR cultivation. NADH:ubiquinone oxidoreductase II is strongly associated to aerobic respiration and its expression is repressed during anaerobic growth mediated by FNR (Spiro *et al.*, 1989).

The proteome and trancriptome data along the branched chain amino acid pathway show a different behavior compared to most of the amino acid synthesis pathway while they show little difference between the STR and the TCR cultivation. The gene *ilvB* encoding for one of the acetohydroxy acid synthase isozymes of *E. coli* is known to be positively regulated by cAMP (Sutton and Freundlich, 1980). This would be in accordance to the results presented here assuming an increased cAMP concentration during transition from famine to feast. A cAMP independent regulation was found for the remaining genes involved in branched chain amino acid synthesis pathway (Freundlich, 1977). The transcriptome data show an increase in expression also for *ilvI* and *leuA*. The expression of the genes *ilvIH* and *gltBD* are both regulated by leucine-responsive regulatory protein (Lrp) (Calvo and Matthews, 1994). While the proteome levels for the acetohydroxy acid synthase isozymes stayed constant for both cultivations, the levels of the proteins encoded by the *leuABCD* operon increased according to increased transcriptional activity. The *leuABCD* operon was found to be not regulated by the global amino acid starvation regulator Lrp (Landgraf *et al.*, 1999).

4.3 Adaptation to oscillating glucose conditions at increasing growth rate.

In order to study the effect of oscillating glucose conditions on the central carbon metabolism scale-down cultivations with a TCR were compared to reference cultivations with a STR regarding general cultivation parameters, metabolome, proteome and transcriptome. The greatest differences were found in the accumulation of organic acids and norvaline, which are already discussed. Furthermore, differences were observed for the exhaust gas analysis with increased OUR and carbon dioxide production rate in the first 3 h of oscillating glucose

conditions compared to the reference cultivation. The respiratory quotient was not affected. The greatest change in the proteome of the central carbon metabolism was found in the increased levels of *aceA* encoded isocitrate lyase of the glyoxylate shunt. While the concentration decreased to less than a half of the level before mechanical feeding in the STR, it increased nearly 3-fold in the TCR cultivation. Additionally, proteins of the cytochrome d (*bd*-I) terminal oxidase subunit I and NADH:ubiquinone oxidoreductase II (*ndh*) were found increased (stronger) for the TCR cultivation.

An increased OUR and carbon dioxide production rate is coupled to higher metabolic activity. In the case of TCR cultivation the higher metabolic activity can be seen in the secretion and re-assimilation of organic acids. When the cells oscillate in the TCR system, the broth is pumped through the PFR with 1.2 L min^{-1}. With a cultivation volume of 10 L, the whole cultivation broth was theoretically at least once exposed to conditions of oxygen limitation and glucose excess. After 1 h more than 7 volumes of the cultivation broth were pumped through. For the increase of protein level of *aceA* it took more than 2 h of oscillating glucose conditions, indicating that even after several exposures to glucose pulses the cells adapt only slowly to these conditions. This is also in accordance to the exhaust data, where a peak for the specific oxygen uptake rate and the specific carbon dioxide production rate was observed for the first 3 h of oscillating glucose conditions in the TCR. This is the same time scale Wick *et al.* found for *E. coli*, when it was transferred from glucose excess to glucose limitation. It took 3 h of continuous cultivation for the glucose concentration in the medium to drop to a constant level (Wick *et al.*, 2001). Also the adaptation to increased growth rate on the proteome level takes in the present study several hours until they reach a new constant level.

The glyoxylate shunt is active in *E. coli* when acetate is utilized and serves as bypass of the TCA cycle to replenish its metabolite pools (Kornberg, 1966). When the high level acetate producing *E. coli* K-12 strain was compared to the low acetate producer BL 21 strain, it was found that a flux through glyoxylate shunt (22% of the complete TCA cycle flux) was connected to the low acetate production of BL 21, while no glyoxylate shunt flux was found for K-12 strain (Noronha *et al.*, 2000). In

the present study, the acetate secreted along the PFR in the TCR cultivation was mostly, though not completely, re-assimilated in the STR part. The increased protein level of the isocitrate lyase is in accordance to the role of the glyoxylate shunt during acetate utilization.

5. Conclusions and Outlook

In this thesis the influence of the metabolic state of *E. coli* before exposed to challenging environmental conditions was investigated. It was shown, that the cultivation mode with the corresponding growth rate and glucose availability has a huge effect on the reaction of the central carbon metabolism to oscillating glucose conditions, how they occur at large-scale HCDC. In recent years a great progress regarding genetic engineering and analysis of proteomic and transcriptomic reactions was achieved. With this study the influence and importance also of bioprocess control was once more set in focus and it is clear, that both aspects are relevant for successful production processes.

Especially when considering how *E. coli* adapts its proteome to face a sudden increase of substrate availability by increased levels of enzymes involved in the central carbon metabolism and biosynthesis pathways bears possibilities to investigate more productive cultivation processes of recombinant protein production. The possible advantages of fitting the metabolic state of the cell before using it for producing the desired compound can also be estimated by being aware of the time scale of adaptation processes, which can take several hours of cultivation.

Finally, to the writer of this thesis the obtained results show, that E. coli evolved to a successful organism by good reasons: the main focus lies in survival and growth by very effective use of resources. This also implies the utilization of the present enzymes of the metabolic pathways in a very flexible way and that adaptation to changed environmental conditions can also happen on different levels involved in the final fluxes, maybe even resulting in different immediate answers to the changed conditions. A further exploration in this field seems intriguing.

6. Theses

1. The growth rate and glucose availability before oscillating glucose conditions influences the accumulation of organic acids in the mechanical fed-batch phase of a scale-down cultivation. It does not influence the accumulation of amino acids, though those close to central carbon metabolism accumulated in phase 1 EnBase cultivation during transition from batch to fed-batch conditions.
2. Acetate does not accumulate along the PFR in *Batch-FB* cultivation, while it does in *EnBase-FB* cultivation. In both cultivations accumulate lactate and succinate along the PFR in a similar way, while the re-assimilation in the STR part is incomplete for *EnBase-FB* and complete for *Batch-FB*.
3. In *EnBase-FB* and *Batch-FB* cultivation glutamine levels decreased and alanine levels increased along the PFR.
4. Within the first 3 h of oscillating glucose conditions the respiratory activity was increased for TCR compared to STR. Afterwards, it decreased to the same level like in STR cultivation.
5. The extracellular glutamate and aspartate concentrations were strongly increased 1 h after start of oscillating glucose conditions and decreased to the former level after 2 h of oscillating glucose conditions.
6. Comparing TCR and STR cultivation, 25% of detected proteins showed an increase of 1.5-fold or decrease to 66% for at least one cultivation from before mechanical feed start until 6 h of mechanical feeding. 77% of these proteins showed the same or similar dynamic for both cultivations.
7. The decrease of growth rate has a bigger influence on protein levels than the presence of oscillating glucose conditions.
8. Protein levels of the central carbon metabolism and amino acid and nucleotide precursor biosynthesis pathway decreased for both cultivations. Exceptions are glucose uptake (*ptsG*), branched chain amino acid pathway (proteins encoded by the *leuABCD* operon), glutamate synthesis (*gdhA*) and upper glycolysis (*pfkB*).
9. The main difference of STR and TCR cultivation regarding the proteome of the central carbon metabolism is the activation of the glyoxylate shunt and increased respiration.

10. Changes in the proteome are not directly linked to changes in the transcriptome.

7. Literature

Alvarez, A.F., Georgellis, D., 2010. Chapter 12 - In Vitro and In Vivo Analysis of the ArcB/A Redox Signaling Pathway, Methods in Enzymology. Academic Press, pp. 205-228.

Andersen, D.C., Swartz, J., Ryll, T., Lin, N., Snedecor, B., 2001. Metabolic oscillations in an E. coli fermentation. Biotechnology and Bioengineering 75, 212-218.

Apostol, I., Levine, J., Lippincott, J., Leach, J., Hess, E., Glascock, C.B., Weickert, M.J., Blackmore, R., 1997. Incorporation of norvaline at leucine positions in recombinant human hemoglobin expressed in Escherichia coli. The Journal of biological chemistry 272, 28980-28988.

Babu, K.R., Swaminathan, S., Marten, S., Khanna, N., Rinas, U., 2000. Production of interferon-α in high cell density cultures of recombinant Escherichia coli and its single step purification from refolded inclusion body proteins. Appl Microbiol Biotechnol 53, 655-660.

Bachmann, B.J., 1972. Pedigrees of some mutant strains of Escherichia coli K-12. Bacteriol Rev 36, 525-557.

Bezdek, J.C., Hathaway, R.J., 1992. Numerical convergence and interpretation of the fuzzy c-shells clustering algorithm. IEEE Trans Neural Netw 3, 787-793.

Biermann, M., Linnemann, J., Knüpfer, U., Vollstädt, S., Bardl, B., Seidel, G., Horn, U., 2013. Trace element associated reduction of norleucine and norvaline accumulation during oxygen limitation in a recombinant Escherichia coli fermentation. Microbial Cell Factories 12, 116.

Blankenhorn, D., Phillips, J., Slonczewski, J.L., 1999. Acid- and base-induced proteins during aerobic and anaerobic growth of Escherichia coli revealed by two-dimensional gel electrophoresis. Journal of Bacteriology 181, 2209-2216.

Brand, E., Ralla, K., Neubauer, P., 2012. Strategies for Plasmid DNA Production in Escherichia coli, Biopharmaceutical Production Technology. Wiley-VCH Verlag GmbH & Co. KGaA, pp. 1-41.

Brinkmann, U., Mattes, R.E., Buckel, P., 1989. High-level expression of recombinant genes in Escherichia coli is dependent on the availability of the dnaY gene product. Gene 85, 109-114.

Bylund, F., Collet, E., Enfors, S.-O., Larsson, G., 1998. Substrate gradient formation in the large-scale bioreactor lowers cell yield and increases by-product formation. Bioprocess Engineering 18, 171-180.

Calvo, J.M., Matthews, R.G., 1994. The leucine-responsive regulatory protein, a global regulator of metabolism in Escherichia coli. Microbiological Reviews 58, 466-490.

Choi, V.W., Asokan, A., Haberman, R.A., McCown, T.J., Samulski, R.J., 2006. Production of recombinant adeno-associated viral vectors and use for in vitro and in vivo administration. Curr Protoc Neurosci Chapter 4, Unit 4 17.

Cunningham, L., Gruer, M.J., Guest, J.R., 1997. Transcriptional regulation of the aconitase genes (acnA and acnB) of Escherichia coli. Microbiology 143 (Pt 12), 3795-3805.

Deutscher, J., 2008. The mechanisms of carbon catabolite repression in bacteria. Curr Opin Microbiol 11, 87-93.

El-Mansi, E.M., Holms, W.H., 1989. Control of carbon flux to acetate excretion during growth of Escherichia coli in batch and continuous cultures. J Gen Microbiol 135, 2875-2883.

Enfors, S.O., Jahic, M., Rozkov, A., Xu, B., Hecker, M., Jürgen, B., Krüger, E., Schweder, T., Hamer, G., O'Beirne, D., Noisommit-Rizzi, N., Reuss, M., Boone, L., Hewitt, C., McFarlane, C., Nienow, A., Kovacs, T., Trägårdh, C., Fuchs, L., Revstedt, J., Friberg, P.C., Hjertager, B., Blomsten, G., Skogman, H., Hjort, S., Hoeks, F., Lin, H.Y., Neubauer, P., van der Lans, R., Luyben, K., Vrabel, P., Manelius, A., 2001. Physiological responses to mixing in large scale bioreactors. Journal of biotechnology 85, 175-185.

Evangelista, J.J., Katz, S., Shinnar, R., 1969. Scale-up criteria for stirred tank reactors. AIChE Journal 15, 843-853.

Farmer, W.R., Liao, J.C., 1997. Reduction of aerobic acetate production by Escherichia coli. Applied and environmental microbiology 63, 3205-3210.

Ferreira, G.N., Monteiro, G.A., Prazeres, D.M., Cabral, J.M., 2000. Downstream processing of plasmid DNA for gene therapy and DNA vaccine applications. Trends Biotechnol 18, 380-388.

Franzén, B., Becker, S., Mikkola, R., Tidblad, K., Tjernberg, A., Birnbaum, S., 1999. Characterization of periplasmic Escherichia coli protein expression at high cell densities. ELECTROPHORESIS 20, 790-797.

Freundlich, M., 1977. Cyclic AMP can replace the relA-dependent requirement for derepression of acetohydroxy acid synthase in E. coli K-12. Cell 12, 1121-1126.

George, S., Larsson, G., Enfors, S.-O., 1993. A scale-down two-compartment reactor with controlled substrate oscillations: Metabolic response of Saccharomyces cerevisiae. Bioprocess Engineering 9, 249-257.

Glazyrina, J., Materne, E.-M., Dreher, T., Storm, D., Junne, S., Adams, T., Greller, G., Neubauer, P., 2010. High cell density cultivation and recombinant protein production with Escherichia coli in a rocking-motion-type bioreactor. Microb Cell Fact 9, 42.

Grunzel, P., Pilarek, M., Steinbrück, D., Neubauer, A., Brand, E., Kumke, M.U., Neubauer, P., Krause, M., 2014. Mini-scale cultivation method enables expeditious plasmid production in Escherichia coli. Biotechnol J 9, 128-136.

Han, M.-J., Lee, S.Y., 2006. The Escherichia coli Proteome: Past, Present, and Future Prospects. Microbiology and Molecular Biology Reviews 70, 362-439.

Hanahan, D., 1983. Studies on transformation of Escherichia coli with plasmids. J Mol Biol 166, 557-580.

Hardiman, T., 2009. Dynamics and Regulation of the Central Carbon Metabolism in Escherichia coli During Fed-Batch Cultivations. Universität Stuttgart.

Hayashi, K., Morooka, N., Yamamoto, Y., Fujita, K., Isono, K., Choi, S., Ohtsubo, E., Baba, T., Wanner, B.L., Mori, H., Horiuchi, T., 2006. Highly accurate genome sequences of Escherichia coli K-12 strains MG1655 and W3110. Mol Syst Biol 2, 2006 0007.

Herendeen, S.L., VanBogelen, R.A., Neidhardt, F.C., 1979. Levels of major proteins of Escherichia coli during growth at different temperatures. Journal of Bacteriology 139, 185-194.

Hermsen, R., Okano, H., You, C., Werner, N., Hwa, T., 2015. A growth-rate composition formula for the growth of E. coli on co-utilized carbon substrates. Molecular Systems Biology 11.

Hershey, A.D., 1939. Factors Limiting Bacterial Growth: IV. The Age of the Parent Culture and the Rate of Growth of Transplants of Escherichia coli. J Bacteriol 37, 285-299.

Hewitt, C.J., Nienow, A.W., 2007. The scale-up of microbial batch and fed-batch fermentation processes. Adv Appl Microbiol 62, 105-135.

Hollinshead, W.D., Rodriguez, S., Martin, H.G., Wang, G., Baidoo, E.E.K., Sale, K.L., Keasling, J.D., Mukhopadhyay, A., Tang, Y.J., 2016. Examining Escherichia coli glycolytic pathways, catabolite repression, and metabolite channeling using Δpfk mutants. Biotechnology for Biofuels 9, 212.

Holms, H., 1996. Flux analysis and control of the central metabolic pathways in Escherichia coli. FEMS Microbiol Rev 19, 85-116.

Holms, W.H., 1986. The central metabolic pathways of Escherichia coli: relationship between flux and control at a branch point, efficiency of conversion to biomass, and excretion of acetate. Curr Top Cell Regul 28, 69-105.

Hunter, I.S., Kornberg, H.L., 1979. Glucose transport of Escherichia coli growing in glucose-limited continuous culture. Biochem J 178, 97-101.

Huntington, E., Winslow, C.E., 1937. Cell Size and Metabolic Activity at Various Phases of the Bacterial Culture Cycle. J Bacteriol 33, 123-144.

Ingram, L.O., Conway, T., Clark, D.P., Sewell, G.W., Preston, J.F., 1987. Genetic engineering of ethanol production in Escherichia coli. Appl Environ Microbiol 53, 2420-2425.

Iuchi, S., Chepuri, V., Fu, H.A., Gennis, R.B., Lin, E.C., 1990. Requirement for terminal cytochromes in generation of the aerobic signal for the arc regulatory system in Escherichia coli: study utilizing deletions and lac fusions of cyo and cyd. Journal of Bacteriology 172, 6020-6025.

Iuchi, S., Lin, E.C., 1993. Adaptation of Escherichia coli to redox environments by gene expression. Molecular Microbiology 9, 9-15.

Jantama, K., Haupt, M.J., Svoronos, S.A., Zhang, X., Moore, J.C., Shanmugam, K.T., Ingram, L.O., 2008. Combining metabolic engineering and metabolic evolution to

develop nonrecombinant strains of Escherichia coli C that produce succinate and malate. Biotechnol Bioeng 99, 1140-1153.

Jensen, E.B., Carlsen, S., 1990. Production of recombinant human growth hormone in Escherichia coli: expression of different precursors and physiological effects of glucose, acetate, and salts. Biotechnology and Bioengineering 36, 1-11.

Junne, S., Klingner, A., Kabisch, J., Schweder, T., Neubauer, P., 2011. A two-compartment bioreactor system made of commercial parts for bioprocess scale-down studies: Impact of oscillations on Bacillus subtilis fed-batch cultivations. Biotechnology Journal 6, 1009-1017.

Kalscheuer, R., Stolting, T., Steinbüchel, A., 2006. Microdiesel: Escherichia coli engineered for fuel production. Microbiology 152, 2529-2536.

Kang, Y., Weber, K.D., Qiu, Y., Kiley, P.J., Blattner, F.R., 2005. Genome-wide expression analysis indicates that FNR of Escherichia coli K-12 regulates a large number of genes of unknown function. Journal of bacteriology 187, 1135-1160.

Käß, F., Junne, S., Neubauer, P., Wiechert, W., Oldiges, M., 2014. Process inhomogeneity leads to rapid side product turnover in cultivation of Corynebacterium glutamicum. Microbial Cell Factories 13, 6.

Khankal, R., Chin, J.W., Ghosh, D., Cirino, P.C., 2009. Transcriptional effects of CRP* expression in Escherichia coli. Journal of Biological Engineering 3, 13.

Kisumi, M., Sugiura, M., Chibata, I., 1976. Biosynthesis of norvaline, norleucine, and homoisoleucine in Serratia marcescens. J Biochem 80, 333-339.

Kleman, G.L., Strohl, W.R., 1994. Acetate metabolism by Escherichia coli in high-cell-density fermentation. Applied and environmental microbiology 60, 3952-3958.

Kornberg, H.L., 1966. The role and control of the glyoxylate cycle in Escherichia coli. Biochem J 99, 1-11.

Körner, H., Sofia, H.J., Zumft, W.G., 2003. Phylogeny of the bacterial superfamily of Crp-Fnr transcription regulators: exploiting the metabolic spectrum by controlling alternative gene programs. FEMS Microbiol Rev 27, 559-592.

Krause, M., Ukkonen, K., Haataja, T., Ruottinen, M., Glumoff, T., Neubauer, A., Neubauer, P., Vasala, A., 2010. A novel fed-batch based cultivation method provides high cell-density and improves yield of soluble recombinant proteins in shaken cultures. Microb Cell Fact 9, 11.

Krömer, J.O., 2006. Systembiotechnologische Studien an Corynebacterium glutamicum zur Charakterisierung der Methioninsynthese. Universität des Saarlandes.

Lambden, P.R., Guest, J.R., 1976. Mutants of Escherichia coli K12 unable to use fumarate as an anaerobic electron acceptor. J Gen Microbiol 97, 145-160.

Landgraf, J.R., Boxer, J.A., Calvo, J.M., 1999. Escherichia coli Lrp (Leucine-Responsive Regulatory Protein) Does Not Directly Regulate Expression of the leu Operon Promoter. Journal of Bacteriology 181, 6547-6551.

Lapin, A., Schmid, J., Reuss, M., 2006. Modeling the dynamics of E. coli populations in the three-dimensional turbulent field of a stirred-tank bioreactor—A structured–segregated approach. Chemical Engineering Science 61, 4783-4797.

Lara, A.R., Leal, L., Flores, N., Gosset, G., Bolivar, F., Ramirez, O.T., 2006. Transcriptional and metabolic response of recombinant Escherichia coli to spatial dissolved oxygen tension gradients simulated in a scale-down system. Biotechnology and Bioengineering 93, 372-385.

Lara, A.R., Taymaz-Nikerel, H., Mashego, M.R., van Gulik, W.M., Heijnen, J.J., Ramírez, O.T., van Winden, W.A., 2009. Fast dynamic response of the fermentative metabolism of Escherichia coli to aerobic and anaerobic glucose pulses. Biotechnology and Bioengineering 104, 1153-1161.

Larsson, G., Törnkvist, M., Wernersson, E.S., Trägårdh, C., Noorman, H., Enfors, S.-O., 1996. Substrate gradients in bioreactors: origin and consequences. Bioprocess Engineering 14, 281-289.

Lederberg, J., 1947. Gene Recombination and Linked Segregations in Escherichia Coli. Genetics 32, 505-525.

Lemaux, P.G., Herendeen, S.L., Bloch, P.L., Neidhardt, F.C., 1978. Transient rates of synthesis of individual polypeptides in E. coli following temperature shifts. Cell 13, 427-434.

Lemoine, A., Maya Martínez-Iturralde, N., Spann, R., Neubauer, P., Junne, S., 2015. Response of Corynebacterium glutamicum exposed to oscillating cultivation conditions in a two- and a novel three-compartment scale-down bioreactor. Biotechnology and Bioengineering 112, 1220-1231.

Limberg, M.H., Pooth, V., Wiechert, W., Oldiges, M., 2016. Plug flow versus stirred tank reactor flow characteristics in two-compartment scale-down bioreactor: Setup-specific influence on the metabolic phenotype and bioprocess performance of Corynebacterium glutamicum. Engineering in Life Sciences 16, 610-619.

Lin, H., Bennett, G.N., San, K.Y., 2005. Fed-batch culture of a metabolically engineered Escherichia coli strain designed for high-level succinate production and yield under aerobic conditions. Biotechnol Bioeng 90, 775-779.

Lin, H.Y., Mathiszik, B., Xu, B., Enfors, S.O., Neubauer, P., 2001. Determination of the maximum specific uptake capacities for glucose and oxygen in glucose-limited fed-batch cultivations of Escherichia coli. Biotechnology and Bioengineering 73, 347-357.

Liu, H., Valdehuesa, K.N., Nisola, G.M., Ramos, K.R., Chung, W.J., 2012. High yield production of D-xylonic acid from D-xylose using engineered Escherichia coli. Bioresour Technol 115, 244-248.

Liu, M., Yao, L., Xian, M., Ding, Y., Liu, H., Zhao, G., 2016. Deletion of arcA increased the production of acetyl-CoA-derived chemicals in recombinant Escherichia coli. Biotechnology Letters 38, 97-101.

Löffler, M., Simen, J.D., Jager, G., Schäferhoff, K., Freund, A., Takors, R., 2016. Engineering E. coli for large-scale production - Strategies considering ATP expenses and transcriptional responses. Metabolic engineering 38, 73-85.

Lu, H.S., Tsai, L.B., Kenney, W.C., Lai, P.H., 1988. Identification of unusual replacement of methionine by norleucine in recombinant interleukin-2 produced by E. coli. Biochem Biophys Res Commun 156, 807-813.

Lu, P., 2016. Response of Escherichia coli Processes for the Production of Heterologous Inclusion Bodies by Oscillating Cultivation Conditions in a Scale-Down Bioreactor, Department of Bioprocess Engineering. Technische Universität Berlin, Berlin.

Luli, G.W., Strohl, W.R., 1990. Comparison of growth, acetate production, and acetate inhibition of Escherichia coli strains in batch and fed-batch fermentations. Applied and environmental microbiology 56, 1004-1011.

Lynch, A.S., Lin, E.C., 1996. Transcriptional control mediated by the ArcA two-component response regulator protein of Escherichia coli: characterization of DNA binding at target promoters. Journal of Bacteriology 178, 6238-6249.

Majewski, R.A., Domach, M.M., 1990. Chemostat-cultivated Escherichia coli at high dilution rate: multiple steady states and drift. Biotechnology and Bioengineering 36, 179-190.

Manfredini, R., Cavallera, V., Marini, L., Donati, G., 1983. Mixing and oxygen transfer in conventional stirred fermentors. Biotechnology and Bioengineering 25, 3115-3131.

Martin, D.S., 1932. The Oxygen Consumption of Escherichia Coli during the Lag and Logarithmic Phases of Growth. J Gen Physiol 15, 691-708.

Martinez-Antonio, A., Collado-Vides, J., 2003. Identifying global regulators in transcriptional regulatory networks in bacteria. Curr Opin Microbiol 6, 482-489.

Meagher, R.B., Tait, R.C., Betlach, M., Boyer, H.W., 1977. Protein expression in E. coli minicells by recombinant plasmids. Cell 10, 521-536.

Molenaar, D., van Berlo, R., de Ridder, D., Teusink, B., 2009. Shifts in growth strategies reflect tradeoffs in cellular economics. Molecular Systems Biology 5.

Muramatsu, R., Negishi, T., Mimoto, T., Miura, A., Misawa, S., Hayashi, H., 2002. Existence of beta-methylnorleucine in recombinant hirudin produced by Escherichia coli. Journal of biotechnology 93, 131-142.

Neidhardt, F.C., VanBogelen, R.A., 1981. Positive regulatory gene for temperature-controlled proteins in Escherichia coli. Biochem Biophys Res Commun 100, 894-900.

Neijssel, O.M., Hardy, G.P.M.A., Lansbergen, J.C., Tempest, D.W., O'Brien, R.W., 1980. Influence of growth environment on the phosphoenolpyruvate: Glucose phosphotransferase activities of Escherichia coli and Klebsiella aerogenes: A comparative study. Archives of Microbiology 125, 175-179.

Neijssel, O.M., Hueting, S., Tempest, D.W., 1977. Glucose transport capacity is not the rate-limiting step in the growth of some wild-type strains of Escherichia coli and Klebsiella aerogenes in chemostat culture. FEMS Microbiology Letters 2, 1-3.

Neubauer, P., Åhman, M., Tornkvist, M., Larsson, G., Enfors, S.O., 1995a. Response of guanosine tetraphosphate to glucose fluctuations in fed-batch cultivations of Escherichia coli. Journal of biotechnology 43, 195-204.

Neubauer, P., Hägström, L., Enfors, S.O., 1995b. Influence of substrate oscillations on acetate formation and growth yield in Escherichia coli glucose limited fed-batch cultivations. Biotechnology and Bioengineering 47, 139-146.

Neubauer, P., Junne, S., 2010. Scale-down simulators for metabolic analysis of large-scale bioprocesses. Current Opinion in Biotechnology 21, 114-121.

Neubauer, P., Lin, H.Y., Mathiszik, B., 2003. Metabolic load of recombinant protein production: Inhibition of cellular capacities for glucose uptake and respiration after induction of a heterologous gene in Escherichia coli. Biotechnology and Bioengineering 83, 53-64.

Nienow, A.W., Flickinger, M.C., 2009. Scale-Up, Stirred Tank Reactors, Encyclopedia of Industrial Biotechnology. John Wiley & Sons, Inc.

Nikam, P.S., Ansari, H.R., Hasan, M., 2000. Density and viscosity studies of glucose and fructose solutions in aqueous and 0.5 mol dm3 aqueous NH 4Cl. Journal of Molecular Liquids 87, 97-105.

Noronha, S.B., Yeh, H.J., Spande, T.F., Shiloach, J., 2000. Investigation of the TCA cycle and the glyoxylate shunt in Escherichia coli BL21 and JM109 using (13)C-NMR/MS. Biotechnology and Bioengineering 68, 316-327.

Notley-McRobb, L., Death, A., Ferenci, T., 1997. The relationship between external glucose concentration and cAMP levels inside Escherichia coli: implications for models of phosphotransferase-mediated regulation of adenylate cyclase. Microbiology 143 (Pt 6), 1909-1918.

Ong, S.E., Blagoev, B., Kratchmarova, I., Kristensen, D.B., Steen, H., Pandey, A., Mann, M., 2002. Stable isotope labeling by amino acids in cell culture, SILAC, as a simple and accurate approach to expression proteomics. Mol Cell Proteomics 1, 376-386.

Oosterhuis, N.M., Kossen, N.W., 1984. Dissolved oxygen concentration profiles in a production-scale bioreactor. Biotechnology and Bioengineering 26, 546-550.

Oosterhuis, N.M.G., Kossen, N.W.F., Olivier, A.P.C., Schenk, E.S., 1985. Scale-down and optimization studies of the gluconic acid fermentation by Gluconobacter oxydans. Biotechnology and Bioengineering 27, 711-720.

Paalme, T., Elken, R., Kahru, A., Vanatalu, K., Vilu, R., 1997. The growth rate control in Escherichia coli at near to maximum growth rates: the A-stat approach. Antonie van Leeuwenhoek 71, 217-230.

Park, S.J., Cotter, P.A., Gunsalus, R.P., 1995. Regulation of malate dehydrogenase (mdh) gene expression in Escherichia coli in response to oxygen, carbon, and heme availability. Journal of bacteriology 177, 6652-6656.

Park, S.J., McCabe, J., Turna, J., Gunsalus, R.P., 1994. Regulation of the citrate synthase (gltA) gene of Escherichia coli in response to anaerobiosis and carbon supply: role of the arcA gene product. Journal of bacteriology 176, 5086-5092.

Peebo, K., Valgepea, K., Nahku, R., Riis, G., Oun, M., Adamberg, K., Vilu, R., 2014. Coordinated activation of PTA-ACS and TCA cycles strongly reduces overflow metabolism of acetate in Escherichia coli. Appl Microbiol Biotechnol 98, 5131-5143.

Perrenoud, A., Sauer, U., 2005. Impact of global transcriptional regulation by ArcA, ArcB, Cra, Crp, Cya, Fnr, and Mlc on glucose catabolism in Escherichia coli. Journal of bacteriology 187, 3171-3179.

Phue, J.N., Lee, S.J., Kaufman, J.B., Negrete, A., Shiloach, J., 2010. Acetate accumulation through alternative metabolic pathways in ackA (-) pta (-) poxB (-) triple mutant in E. coli B (BL21). Biotechnology Letters 32, 1897-1903.

Postma, P.W., Lengeler, J.W., Jacobson, G.R., 1993. Phosphoenolpyruvate:carbohydrate phosphotransferase systems of bacteria. Microbiological Reviews 57, 543-594.

Roe, A.J., O'Byrne, C., McLaggan, D., Booth, I.R., 2002. Inhibition of Escherichia coli growth by acetic acid: a problem with methionine biosynthesis and homocysteine toxicity. Microbiology 148, 2215-2222.

Romano, A.H., Conway, T., 1996. Evolution of carbohydrate metabolic pathways. Research in microbiology 147, 448-455.

Rowley, D.L., Fawcett, W.P., Wolf, R.E., 1992. Molecular characterization of mutations affecting expression level and growth rate-dependent regulation of the Escherichia coli zwf gene. Journal of Bacteriology 174, 623-626.

Salmon, K., Hung, S.P., Mekjian, K., Baldi, P., Hatfield, G.W., Gunsalus, R.P., 2003. Global gene expression profiling in Escherichia coli K12. The effects of oxygen availability and FNR. The Journal of biological chemistry 278, 29837-29855.

Sandoval-Basurto, E.A., Gosset, G., Bolivar, F., Ramirez, O.T., 2005. Culture of Escherichia coli under dissolved oxygen gradients simulated in a two-compartment scale-down system: metabolic response and production of recombinant protein. Biotechnology and Bioengineering 89, 453-463.

Sawers, G., 1994. The hydrogenases and formate dehydrogenases ofEscherichia coli. Antonie van Leeuwenhoek 66, 57-88.

Sawers, G., Heider, J., Zehelein, E., Böck, A., 1991. Expression and operon structure of the sel genes of Escherichia coli and identification of a third selenium-containing formate dehydrogenase isoenzyme. Journal of Bacteriology 173, 4983-4993.

Schweder, T., Krüger, E., Xu, B., Jürgen, B., Blomsten, G., Enfors, S.O., Hecker, M., 1999. Monitoring of genes that respond to process-related stress in large-scale bioprocesses. Biotechnology and Bioengineering 65, 151-159.

Shiloach, J., Fass, R., 2005. Growing E. coli to high cell density--a historical perspective on method development. Biotechnology advances 23, 345-357.

Shimada, T., Fujita, N., Yamamoto, K., Ishihama, A., 2011. Novel roles of cAMP receptor protein (CRP) in regulation of transport and metabolism of carbon sources. PLoS One 6, e20081.

Shimizu, K., 2013. Regulation Systems of Bacteria such as Escherichia coli in Response to Nutrient Limitation and Environmental Stresses. Metabolites 4, 1-35.

Šiurkus, J., Panula-Perälä, J., Horn, U., Kraft, M., Rimšeliene, R., Neubauer, P., 2010. Novel approach of high cell density recombinant bioprocess development: Optimisation and scale-up from microlitre to pilot scales while maintaining the fed-batch cultivation mode of E. coli cultures. Microbial Cell Factories 9, 35.

Smith, M.W., Neidhardt, F.C., 1983. Proteins induced by anaerobiosis in Escherichia coli. Journal of Bacteriology 154, 336-343.

Soini, J., Ukkonen, K., Neubauer, P., 2008. High cell density media for Escherichia coli are generally designed for aerobic cultivations – consequences for large-scale bioprocesses and shake flask cultures. Microbial Cell Factories 7, 26.

Soini, J.U., K.; Neubauer, P., 2011. Accumulation of amino acids deriving from pyruvate in Escherichia coli W3110 during fed-batch cultivation in a two-compartment scale-down bioreactor. Advances in Bioscience and Biotechnology 2, 336-339.

Song, X.Y., Chen, Q.H., Ruan, H., He, G.Q., Xu, Q., 2006. Synthesis and paste properties of octenyl succinic anhydride modified early Indica rice starch. J Zhejiang Univ Sci B 7, 800-805.

Spiro, S., Roberts, R.E., Guest, J.R., 1989. FNR-dependent repression of the ndh gene of Escherichia coli and metal ion requirement for FNR-regulated gene expression. Molecular Microbiology 3, 601-608.

Steel, R., Maxon, W.D., 1966. Dissolved oxygen measurements in pilot- and production-scale novobiocin fermentations. Biotechnology and Bioengineering 8, 97-108.

Sutton, A., Freundlich, M., 1980. Regulation by cyclic AMP of the ilvB-encoded biosynthetic acetohydroxy acid synthase in Escherichia coli K-12. Molecular and General Genetics MGG 178, 179-183.

Sutton, V.R., Mettert, E.L., Beinert, H., Kiley, P.J., 2004. Kinetic Analysis of the Oxidative Conversion of the [4Fe-4S]2+ Cluster of FNR to a [2Fe-2S]2+ Cluster. Journal of Bacteriology 186, 8018-8025.

Swartz, J.R., 2001. Advances in Escherichia coli production of therapeutic proteins. Curr Opin Biotechnol 12, 195-201.

Sweere, A.P.J., Luyben, K.C.A.M., Kossen, N.W.F., 1987. Regime analysis and scale-down: Tools to investigate the performance of bioreactors. Enzyme and Microbial Technology 9, 386-398.

Sycheva, E.V., Yampol'skaya, T.A., Preobrazhenskaia, E.S., Novikova, A.E., Matrosov, N.G., Stoinova, N.V., 2007. [Overproduction of noncanonical amino acids by Escherichia coli cells]. Mikrobiologiia 76, 805-812.

Taymaz-Nikerel, H., De Mey, M., Baart, G., Maertens, J., Heijnen, J.J., van Gulik, W., 2013. Changes in substrate availability in Escherichia coli lead to rapid metabolite, flux and growth rate responses. Metabolic engineering 16, 115-129.

Tseng, C.P., Albrecht, J., Gunsalus, R.P., 1996. Effect of microaerophilic cell growth conditions on expression of the aerobic (cyoABCDE and cydAB) and anaerobic (narGHJI, frdABCD, and dmsABC) respiratory pathway genes in Escherichia coli. Journal of Bacteriology 178, 1094-1098.

Unden, G., Trageser, M., 1991. Oxygen regulated gene expression in Escherichia coli: Control of anaerobic respiration by the FNR protein. Antonie van Leeuwenhoek 59, 65-76.

Valgepea, K., Adamberg, K., Nahku, R., Lahtvee, P.J., Arike, L., Vilu, R., 2010. Systems biology approach reveals that overflow metabolism of acetate in Escherichia coli is triggered by carbon catabolite repression of acetyl-CoA synthetase. BMC Syst Biol 4, 166.

Valgepea, K., Adamberg, K., Seiman, A., Vilu, R., 2013. Escherichia coli achieves faster growth by increasing catalytic and translation rates of proteins. Molecular BioSystems 9, 2344-2358.

van Beilen, J.W.A., Hellingwerf, K.J., 2016. All Three Endogenous Quinone Species of Escherichia coli Are Involved in Controlling the Activity of the Aerobic/Anaerobic Response Regulator ArcA. Frontiers in Microbiology 7, 1339.

VanBogelen, R.A., Neidhardt, F.C., 1990. Ribosomes as sensors of heat and cold shock in Escherichia coli. Proc Natl Acad Sci U S A 87, 5589-5593.

VanBogelen, R.A., Olson, E.R., Wanner, B.L., Neidhardt, F.C., 1996. Global analysis of proteins synthesized during phosphorus restriction in Escherichia coli. Journal of Bacteriology 178, 4344-4366.

Vemuri, G.N., Eiteman, M.A., Altman, E., 2006. Increased recombinant protein production in Escherichia coli strains with overexpressed water-forming NADH oxidase and a deleted ArcA regulatory protein. Biotechnology and Bioengineering 94, 538-542.

Villadsen, J., Nielsen, J., Lidén, G., 2011. Scale-Up of Bioprocesses, Bioreaction Engineering Principles. Springer US, Boston, MA, pp. 497-546.

Vogel, C., Marcotte, E.M., 2012. Insights into the regulation of protein abundance from proteomic and transcriptomic analyses. Nat Rev Genet 13, 227-232.

Watanabe, K., Hotta, K., Praseuth, A.P., Koketsu, K., Migita, A., Boddy, C.N., Wang, C.C., Oguri, H., Oikawa, H., 2006. Total biosynthesis of antitumor nonribosomal peptides in Escherichia coli. Nat Chem Biol 2, 423-428.

Weber, J., Kayser, A., Rinas, U., 2005a. Metabolic flux analysis of Escherichia coli in glucose-limited continuous culture. II. Dynamic response to famine and feast, activation of the methylglyoxal pathway and oscillatory behaviour. Microbiology 151, 707-716.

Weber, J., Kayser, A., Rinas, U., 2005b. Metabolic flux analysis of Escherichia coli in glucose-limited continuous culture. II. Dynamic response to famine and feast,

activation of the methylglyoxal pathway and oscillatory behaviour. Microbiology 151, 707-716.

Wick, L.M., Quadroni, M., Egli, T., 2001. Short- and long-term changes in proteome composition and kinetic properties in a culture of Escherichia coli during transition from glucose-excess to glucose-limited growth conditions in continuous culture and vice versa. Environmental microbiology 3, 588-599.

Williams, J.A., Luke, J., Langtry, S., Anderson, S., Hodgson, C.P., Carnes, A.E., 2009. Generic plasmid DNA production platform incorporating low metabolic burden seed-stock and fed-batch fermentation processes. Biotechnology and Bioengineering 103, 1129-1143.

Wood, E.J., 1983. Molecular cloning. A laboratory manual by T Maniatis, E F Fritsch and J Sambrook. pp 545. Cold Spring Harbor Laboratory, New York. 1982. $48 ISBN 0-87969-136-0. Biochemical Education 11, 82-82.

Xu, B., Jahic, M., Blomsten, G., Enfors, S.O., 1999. Glucose overflow metabolism and mixed-acid fermentation in aerobic large-scale fed-batch processes with Escherichia coli. Applied Microbiology and Biotechnology 51, 564-571.

Yan, J.X., Devenish, A.T., Wait, R., Stone, T., Lewis, S., Fowler, S., 2002. Fluorescence two-dimensional difference gel electrophoresis and mass spectrometry based proteomic analysis of Escherichia coli. Proteomics 2, 1682-1698.

Yau, S.Y., Keshavarz-Moore, E., Ward, J., 2008. Host strain influences on supercoiled plasmid DNA production in Escherichia coli: Implications for efficient design of large-scale processes. Biotechnology and Bioengineering 101, 529-544.

Yohannes, E., Barnhart, D.M., Slonczewski, J.L., 2004. pH-dependent catabolic protein expression during anaerobic growth of Escherichia coli K-12. Journal of Bacteriology 186, 192-199.

Yoon, S.H., Han, M.J., Lee, S.Y., Jeong, K.J., Yoo, J.S., 2003. Combined transcriptome and proteome analysis of Escherichia coli during high cell density culture. Biotechnology and Bioengineering 81, 753-767.

You, C., Okano, H., Hui, S., Zhang, Z., Kim, M., Gunderson, C.W., Wang, Y.-P., Lenz, P., Yan, D., Hwa, T., 2013. Coordination of bacterial proteome with metabolism by cyclic AMP signalling. Nature 500, 301-306.

Yu, C., Cao, Y., Zou, H., Xian, M., 2011. Metabolic engineering of Escherichia coli for biotechnological production of high-value organic acids and alcohols. Appl Microbiol Biotechnol 89, 573-583.

Zheng, D., Constantinidou, C., Hobman, J.L., Minchin, S.D., 2004. Identification of the CRP regulon using in vitro and in vivo transcriptional profiling. Nucleic Acids Research 32, 5874-5893.

8. Appendix

8.1 Table of chemicals

α-aminobutyric acid	Sigma Aldrich, Taufkirchen
Agar	Carl Roth, Karlsruhe
Antifoam 204	Sigma Aldrich, Taufkirchen
$CaCl_2 \cdot 2H_2O$	Carl Roth, Karlsruhe
$CoCl_2 \cdot 6H_2O$	Fluka, Buchs (Switzerland)
$CuSO_4 \cdot 5H_2O$	VWR, Bruchsal
Dextrin	Sigma Aldrich, Taufkirchen
$FeCl_3 \cdot H_2O$	Carl Roth, Karlsruhe
Glucose	Komplet, Germany
Glycerole	Carl Roth, Karlsruhe
HCl (70%)	VWR, Bruchsal
H_3PO_4	Carl Roth, Karlsruhe
H_2SO_4	VWR, Bruchsal
K_2CO_3	Carl Roth, Karlsruhe
K_2HPO_4	Carl Roth, Karlsruhe
KOH	Carl Roth, Karlsruhe
MeOH	VWR, Bruchsal
$MgSO_4 \cdot 7H_2O$	Carl Roth, Karlsruhe
$MnSO_4 \cdot H_2O$	Merck, Darmstadt
NaCl	VWR, Bruchsal
Na_2-EDTA	Fluka, Buchs (Switzerland)
$Na_2MoO_4 \cdot 2H_2O$	Merck, Darmstadt
$Na_2SeO_3 \cdot 5H_2O$	Ferak, Berlin
Na_2SO_4	Carl Roth, Karlsruhe
NH_4^+	VWR, Bruchsal
NH_4Cl	Carl Roth, Karlsruhe
$(NH_4)_2$-H-citrate	Carl Roth, Karlsruhe
$NaH_2PO_4 \cdot H_2O$	Carl Roth, Karlsruhe
NaOH	Carl Roth, Karlsruhe
$(NH_4)_2SO_4$	VWR, Bruchsal
$Ni(NO_3)_2 \cdot 6H_2O$	Fluka, Buchs (Switzerland)
pH calibration buffer	VWR, Bruchsal
Thiamine-HCl	Carl Roth, Karlsruhe
Tris-HCl	Carl Roth, Karlsruhe
Tryptone	Carl Roth, Karlsruhe
Yeast extract	DHW, Nürnberg
$ZnSO_4 \cdot 7H_2O$	Merck, Darmstadt

8.2 List of electronic supplements

Online access: http://dx.doi.org/10.14279/depositonce-6618

- **Folder: Cultivations**
  - **1_Phase 1 Cultivation**
    - **General Parameters1:** DCW, OD / O_2, CO_2 / pH, DOT / qO_2, qCO_2, µ
    - **Metabolites1:** Extracellular organic acids / extracellular amino acids / Dextrin, glucose
  - **2_STR1**
    - **General Parameters2:** DCW, OD / federate / O_2, CO_2 / pH, DOT / qO_2, qCO_2, µ
    - **Metabolites2:** Organic acids / Amino acids / Dextrin, glucose
  - **3-STR2**
    - **General Parameters3:** DCW, OD / federate / O_2, CO_2 / pH, DOT / qO_2, qCO_2, µ
    - **Metabolites3:** Organic acids / Amino acids / Dextrin, glucose
  - **4_TCR1**
    - **General Parameters4:** DCW, OD / federate / O2, CO2 / pH, DOT / qO2, qCO2, µ / PFR DOT & pH
    - **Metabolites4:** Organic acids STR / Organic acids PFR / Amino acids / Dextrin, glucose STR / Dextrin, glucose PFR
  - **5_TCR2**
    - **General Parameters5:** DCW, OD / federate / O2, CO2 / pH, DOT / qO2, qCO2, µ / PFR DOT & pH
    - **Metabolites5:** Organic acids STR / Organic acids PFR / Amino acids
  - **6_Batch-FB**
    - **General Parameters6:** DCW, OD / federate / O2, CO2 / pH, DOT / qO2, qCO2, µ / PFR DOT & pH
    - **Metabolites6:** Organic acids STR / Organic acids PFR / Amino acids / Dextrin, glucose STR / Dextrin, glucose PFR
  - **7_STR Proteome**
    - **General Parameters 7:** DCW, OD / federate / O2, CO2 / pH, DOT / qO2, qCO2, µ
    - **Metabolites7:** Organic acids / Amino acids / Dextrin, glucose
  - **8_TCR Proteome**
    - **General Parameters8:** DCW, OD / federate / O2, CO2 / pH, DOT / qO2, qCO2, µ / PFR DOT & pH
    - **Metabolites8:** Organic acids STR / Organic acids PFR / Amino acids
- **Folder: Proteome data**
  - **Proteomics-appendix:** Ratios of protein concentrations
  - **Fuzzy-c-Means-Cluster-eColiProtein:** Clustered proteins
  - **Fuzzy_Cluster_Coli-STR_TCR:** Power point with clustering and KEGG-pathways
- **Folder: Transcriptome data**
  - **Separate calculations for each gene:** Measured value and change calculations

Publications

Neubauer, P., Lemoine, A., Trippel, S., **Brand, E.**, Spann, R., Runge, D., Lu, P., El Kady, B., Reitz, C., Junne, S.. 2014. “Microorganisms Respond in Different Ways to Oscillations in Large-Scale Bioreactors: Conclusions from Scaledown Approaches.” New Biotechnology, Abstracts of the 16th European Congress on Biotechnology, 31, Supple (July): S87. doi:10.1016/j.nbt.2014.05.1812

Grunzel, P., Pilarek, M., Steinbrück, D., Neubauer, A., **Brand, E.**, Kumke, M. U., Neubauer, P., Krause, M.. 2014. “Mini-scale cultivation method enables expeditious plasmid production in Escherichia coli.” Biotechnology Journal 9 (1): 128-136.

Palela, M., Bahrim, G. E., Glazyrina, J., **Brand, E.**, Neubauer, P.. 2013. “Enzyme-based glucose delivery: a possible tool for biosorbent preparation for heavy metal removal from polluted environments.” Bioprocess and Biosystems Engineering 36 (11): 1601-1611.

Pilarek, M., **Brand, E.**, Hillig, F., Krause, M., Neubauer, P.. 2013. “Enhanced plasmid production in miniaturized high-cell-density cultures of Escherichia coli supported with perfluorinated oxygen carrier.” Bioprocess and Biosystems Engineering 36 (8): 1079-1086.

Junne, S., Klingner, A., Itzeck, D., **Brand, E.**, Neubauer, P.. 2012. “Consistency of Scale-Up from Bioprocess Development to Production.” Biopharmaceutical Production Technology, Volume 1 & Volume 2: 511-543.

Brand, E., Ralla, K., Neubauer, P.. 2012. “Strategies for plasmid DNA production in Escherichia coli.” Biopharmaceutical Production Technology, Volume 1 & Volume 2: 1-41.

Brand, E., Junne, S., Neubauer, P.. 2010. “Divalent ion composition and demand for E. coli in high cell density cultivations.” Journal of Biotechnology 150 (402).

Brand, E., Neubauer, A., Neubauer, P.. 2010. “EnBase®-high plasmid yield in micro-scale cultures.” Journal of Biotechnology 150 (402).